INFORMATION TO USERS

This manuscript has been reproduced from the microfilm master. UMI films the text directly from the original or copy submitted. Thus, some thesis and dissertation copies are in typewriter face, while others may be from any type of computer printer.

The quality of this reproduction is dependent upon the quality of the copy submitted. Broken or indistinct print, colored or poor quality illustrations and photographs, print bleedthrough, substandard margins, and improper alignment can adversely affect reproduction.

In the unlikely event that the author did not send UMI a complete manuscript and there are missing pages, these will be noted. Also, if unauthorized copyright material had to be removed, a note will indicate the deletion.

Oversize materials (e.g., maps, drawings, charts) are reproduced by sectioning the original, beginning at the upper left-hand corner and continuing from left to right in equal sections with small overlaps.

ProQuest Information and Learning
300 North Zeeb Road, Ann Arbor, MI 48106-1346 USA
800-521-0600

University of Alberta

Efficient Synthesis of 4,6-*bis*(alkylamino) and -*bis*(arylimino)dibenzofurans. Pre-organized Sterically Bulky Ligand Systems for Bimetallic Coordination.

by

Nolan C. Erickson ©

A thesis submitted to the Faculty of Graduate Studies and Research in partial fulfillment of the requirements for the degree of Master of Science.

Department of Chemistry

Edmonton, Alberta

Spring 2005

Dedication

To My Father

At times I haven't always been able to learn the way I was taught but you never ever gave up teaching me in ways I could learn. Your unwavering support was a large part this work's success. This work is dedicated to you, Dad.

Abstract

The development of hindered, rigid ligand systems for the construction of bimetallic coordination compounds is reported as models for putative bimetallic active sites of heterogeneous Ziegler-Natta catalyst systems. Our focus has been to make available efficient methodology for the synthesis of well-defined, sterically hindered organic templates to facilitate a more detailed investigation of novel supported bimetallic or polymetallic catalysts for olefin polymerization.

The efficient synthesis of *bis*(amido) and *bis*(imino) ligands based on a dibenzofuranyl template is reported. By making use of directed *ortho*-lithiation and electrophilic azide quench strategies as previously demonstrated, we have been able to develop a novel *in situ* Staudinger reaction for the formation of hindered 4,6-*bis*(amido) and 4,6-*bis*(imino) organic templates appropriate for bridging two interacting metal centres.

Acknowledgements

Special thanks to Dr. Bob McDonald and Dr. Mike Ferguson at the University of Alberta for the X-ray crystallographic studies and to the staff of the Spectral Services and MSPEC labs for all their assistance.

Great thanks to Jeff - Your unyielding patience and constant encouragement has made my time in your group the most rewarding experience of my life.

Thanks to Drs. Rik Tykwinski, Dennis Hall, Joe Takats, Neil Branda and Lois Brown for your kindness and patience over the years.

Thanks to the Bullies for all your help - Paul T., Megumi, Guizhong, Anne, Grace, Jason, Mee-Kyung, Rick, Brian, Paul, Owen and especially Ross and Dave - I will miss seeing you guys everyday.

To Uncle T-rent, Cap, Grich, and 'ole Deaner. School is *school*! I was very fortunate to have spent so much time with my very best friends in the world. Thank you for always believing in me.

Table of Contents

Tables

Page No.

Figures

Page No.

Page No.

Symbols and Nomenclature

Cp - cyclopentadienyl

dba - dibenzylideneacetone

DME - dimethoxyethane

DMG -directed metallation group

DoM - directed *ortho*-metallation

HDPE - high density polyethylene

LLPDE - linear low density polyethylene

MAO - methyl aluminoxane

$MesN_3$ - mesitylenesulfonyl azide

MNDO - modified neglect of diatomic overlap

MPLC - medium pressure liquid chromatography

Mw - weight average molecular weight

PMDETA - *N,N,N',N',N''*-pentamethyldiethylenetriamine

SM - starting material

TBME - *tert*-butyl methyl ether

TLC - thin layer chromatography

TMEDA - *N,N,N',N'*-tetramethylethylenediamine

TMSCl - trimethylsilyl chloride

Trityl - triphenylcarbonium ion

TrN_3 - Triisopropylsulfonyl azide

TsN_3 - *para*-toluenesulfonyl azide

Z/N - Ziegler-Natta

Schemes

Page No.

Page No.

Equations

Page No.

Page No.

Page No.

Chapter 1 - Introduction

1.1 - Historical design of olefin polymerization catalysts

Advances in ligand design for olefin polymerization catalysts have improved understanding of factors important for overall catalytic activity. The efficient industrial production of polyolefins began with Ziegler's[1,2] discovery that $TiCl_4$, along with aluminum alkyls, displayed high ethylene polymerization activity under relatively mild conditions. Soon after the publication of Ziegler's initial work, Natta and co-workers[3] created isotactic polypropylene using similar conditions. Ziegler and Natta's early success with these heterogeneous[4] systems was followed by a period of careful investigation until the discovery that $MgCl_2$-supported $TiCl_4$ catalysts[5] showed activities at least twice those of Ziegler's Ti(IV) system, producing linear low density polyethylene (LLDPE), high density polyethylene (HDPE), and stereoregular polypropylene. Nevertheless, control of polymer microstructure and molecular weight remained a challenge, owing in part to the unknown multi-site nature of the heterogeneous catalyst.[6]

Natta and Breslow reported the first homogeneous metallocene polymerization catalyst, Cp_2TiCl_2—$AlEt_2Cl$.[7] These single site catalysts showed promise as models of hetereogeneous systems, although low activities, susceptibility to decomposition, and the inability to polymerize higher olefins limited their commercial usage. The combination of other Group IV metallocenes and partially hydrolyzed aluminum alkyls, described initially by Meyer[8] and later by Breslow[9] renewed interest in these systems. Subsequently, Sinn and

Kaminsky discovered that Group IV metallocenes showed good activity when used in combination with methylaluminoxane (MAO) cocatalysts.[10,11,12] (ex. Figure 1.1) Activities close to those of supported $MgCl_2$-$TiCl_4$ heterogeneous systems led to exponential growth in the study of homogeneous systems.

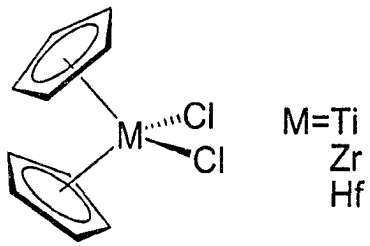

Figure 1.1 - Group IV metallocenes

The well-defined nature of the active site of metallocenes has allowed the judicious design of the catalytic system, providing access to previously unattainable polymer microstructures.[13] By varying zirconocene symmetry, (Figure 1.2) new routes to stereospecific polypropylene were attainable.[14,15,16,17]

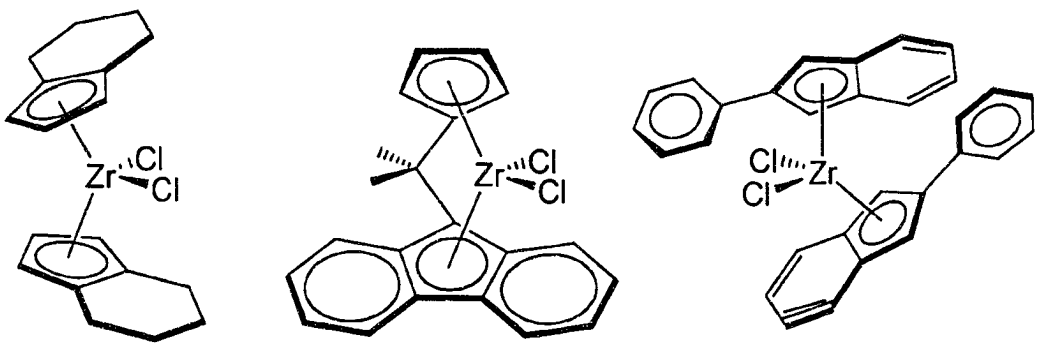

Figure 1.2 – Zirconocene catalysts for stereospecific propylene polymerization

Nevertheless, these catalysts are less thermally stable than classical Z/N systems and produce polymers of lower molecular weight under standard industrial conditions.[4] In addressing these limitations, researchers sought new coordination compounds where the Cp ligand(s) or metal centre has been replaced. For example, the 'constrained-geometry' *ansa*-monocyclopentadienyl-amido (CpA)[4] Group IV catalysts were developed coincidently by both Dow and Exxon[18,19,20,21] (Figure 1.3).

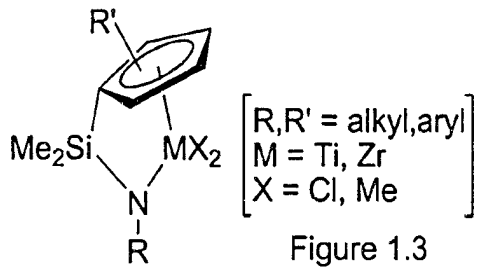

Figure 1.3

Figure 1.3 – Cyclopentadienyl catalysts

Although the synthesis of these cyclopentadienyl amido coordination compounds was based on Bercaw[22] and Okuda's[23] work, the Group IV cyclopentadienyl amido complex has unique features. The open nature of the active site allows the co-polymerization of other olefins with ethylene, increased thermal and MAO stability, and the ability to produce higher molecular weight polymers compared to Group IV metallocene analogues.[14]

Investigation into the relative metal-ligand effects on catalyst behaviour continued with the discovery of novel late metal post-metallocene systems identified by Brookhart[24,25,26] (Figure 1.4).

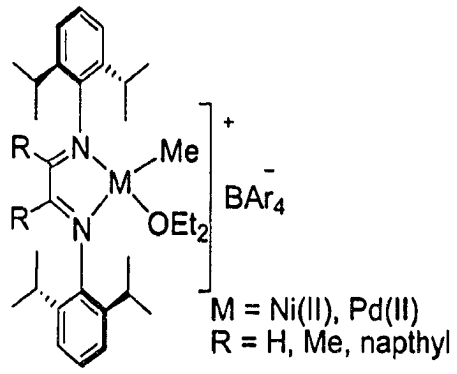

Figure 1.4 – Brookhart's post-metallocene catalysts

Brookhart's discovery was the first identified use of a hetero-atom coordinated with late metals, resulting in less competitive associative displacement and chain transfer mechanisms for ethylene polymerizations.[6,14] Building on Brookhart's work, McConville and co-workers[27,28] showed that Ti-coordinated diamido ligands (Figure 1.5 (a)) also showed high activities toward higher α-olefin polymerization. Similarly, Brookhart and Gibson[29,30] identified complexes containing pyrrolidine diimine ligands (Figure 1.5 (b)) that provided high ethylene polymerization activities. Subsequently, reports by Grubbs[31,32] (Figure 1.5 (c)) and Fujita[33] (Figure 1.5 (d)) ushered in a new era in high performance olefin polymerization catalysts, with catalyst activities equal to or exceeding Group IV metallocene catalysts. In fact, this latter class of phenoxy-imine catalysts (the FI catalysts) has shown living polymerization behaviour for α-olefins, producing branched polyethylenes without comonomers, and in some reported cases, promoting the copolymerization of ethylene or α-olefins[26,28,34] with polar olefins to produce functionalized polyolefins.[25]

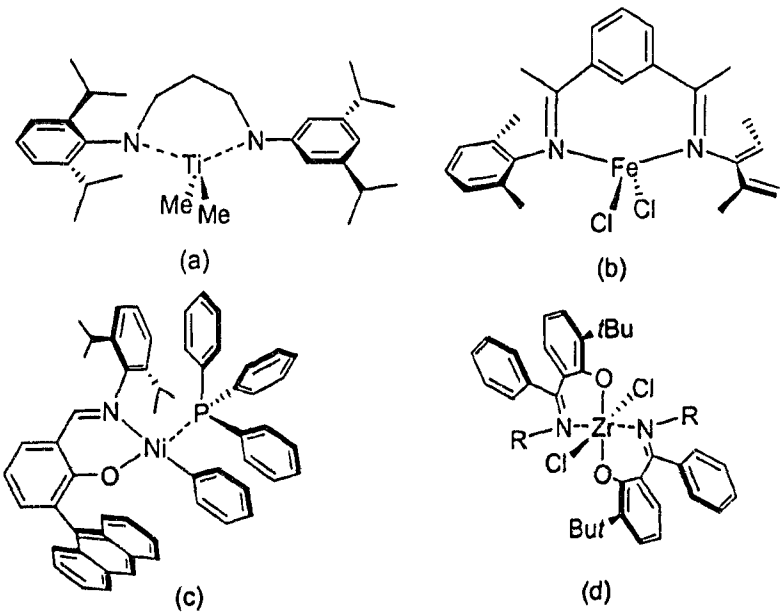

Figure 1.5 – Post-metallocene catalysts – (a) McConville's Ti-coordinated diamido ligands (b) Brookhart and Gibson's pyrrolidine diimine ligands (c) Grubbs' and (d) Fujita's ligands

Other hindered aryl-imine based late metal supported catalysts include those reported by Sugimura, in which the *bis*-imine complex has been in contact with MAO, producing polyethylene in a toluene or hexane slurry[4,35] (Figure 1.6).

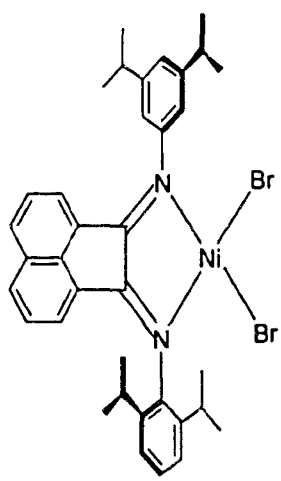

Figure 1.6 – Ni(II) 1,2-diimine complex of Sugimura

1.2 - Supported post-metallocene systems

1.2.1 - Silica Supported systems

Diimine catalysts may be supported on a wide range of inorganic oxide supports, although silica is the support of choice and generally involves the use of MAO. Following earlier work from our group[36] (allyl cationic single component Z/N systems), others reported that 'constrained-geometry' titanium dialkyls also form active heterogeneous supported catalysts when treated with alkylaluminum-treated silica containing $[HNMe_2Ph][B(C_6F_5)_4$ or $B(C_6F_5)_3$.[37] In fact, complexes such as $Me_2Si(C_5Me_4)$(N-*tert*-butyl)Ti(η^4-C_5H_8), when converted to zwitterionic complexes after treatment with $B(C_6F_5)_3$ (Equation 1.1), have shown good catalytic activities when adsorbed on silica.[38]

Equation 1.1 – Zwitterionic 'constrained geometry' amido catalyst

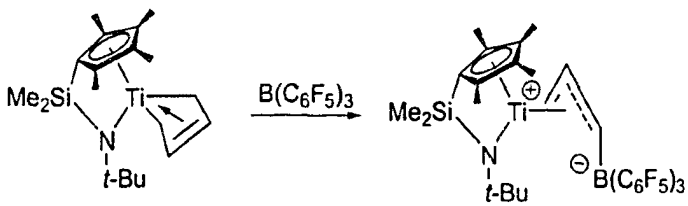

1.2.2 - Resin supported systems

In addition, ligand libraries for combinatorial screening of diimine-based Ni and Pd catalysts have been shown to form through reductive amination (Scheme

1.1). After attachment of a diketone to a Merrifield resin and condensation with various anilines in the presence of a dehydrating catalyst, complexation of the metal produces an active catalyst when exposed to ethylene.[4,39]

Scheme 1.1 – Ni(II) based diimine supported catalyst

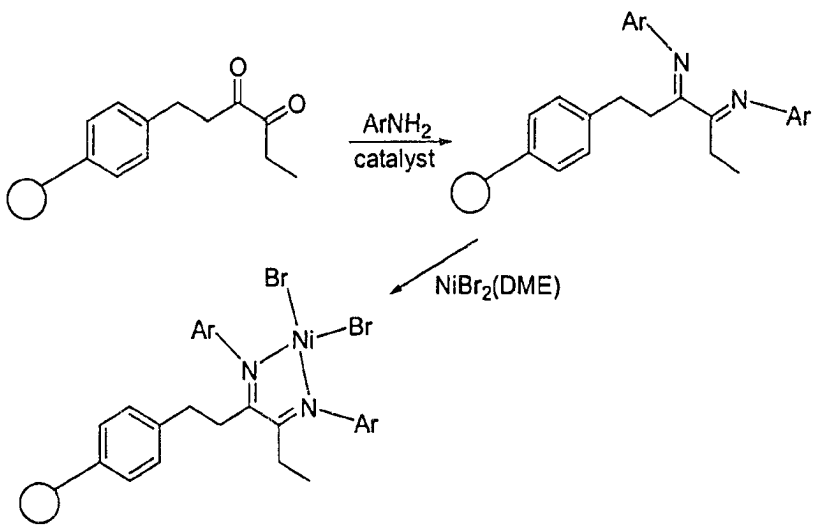

1.2.3 - Soluble vs. insoluble catalysts

Despite the interest in adapting metallocene catalysts to heterogeneous supported systems, challenges remain in generating polymers with narrow molecular weight distributions, high stereoregularities or specific melting points. Disparity in catalyst activities between supported and unsupported systems has been shown to be consistent in most cases.[4] That is, the activity of supported catalysts have been shown to be one-half to one-tenth of their soluble unsupported cousins. This has been suggested to be in large part a result of the reduced diffusion of monomer into the pores of the supported catalyst.[4] It is

reasonable to propose that there may also be fewer active catalytic centres present in the heterogeneous variant. As well, catalytic centres may be deactivated when supported or less effective as a result of reduced catalyst-cocatalyst interaction. For example, over 90% of the same zirconocene centres, although activated by MAO in solution, were near completely deactivated when supported on silica.[4]

Molecular weights of the polymers formed have been shown to be somewhat higher for supported single site catalysts. As mentioned above, Hlatky suggests[4] that the lower activity of supported catalysts may be due to a reduced number of active centres. He reasons that for propagation rates to be lower for the supported analogue, the termination rates would also have to be reduced at least proportionately for these molecular weight (MW) observations to be consistent. In fact, the expected reduction in termination rates have not been shown to follow from reduced propogation rates.[4] Jungling and co-workers[40] studied temperature effects on propylene polymerization with the use of both homogeneous and supported Me_2Si(2-Me-4,5-benzoindenyl)$_2ZrCl_2$-MAO catalysts, also finding that activity, molecular weight, isotacticity, and polymer bulk density were poorer for the supported system than the homogeneous variant.

1.3 – Polymerization Process Considerations

As mentioned, single site heterogeneous catalysts have been successfully used in large scale operations in a variety of processes, including

slurry, bulk monomer, and fluidized gas-phases. In fact, in the latter case, supported metallocenes can also be utilized within a 'condensed mode' operation, where a solvent such as isopentane is added to aid in heat transfer, improving the activity of the catalyst.[41,42,43]

In addition, single-site heterogeneous catalysts are affected by conditions differently than traditional Z/N catalysts, especially with respect to comonomer or hydrogen addition. Although $AlEt_3$ is often used as a scavenger for, and activator of Z/N catalysts, the presence of a scavenger can cause fouling of the reactor when supported metallocene catalysts are used.[4]

Nevertheless, the introduction of co-monomers may be cumbersome and lack utility with Z/N systems. For example, in fluidized-bed gas-phase processes, ethylene polymerization must be terminated by the addition of water or methanol to deactivate the catalyst irreversibly. A second catalyst may then be added by adjusting feed streams, allowing comonomer incorporation into the resultant polymer.[44,45]

1.4 – Ziegler-Natta active sites

The commonly held consensus among researchers is that the active site of polymerization catalysts is a coordinatively unsaturated, typically cationic, alkyl complex that is stabilized by several ligands[30] (Scheme 1.2). Many methods can be followed to generated such a species, including three shown below.

Scheme 1.2 – Routes to the catalytically active $[L_nMR]^+$

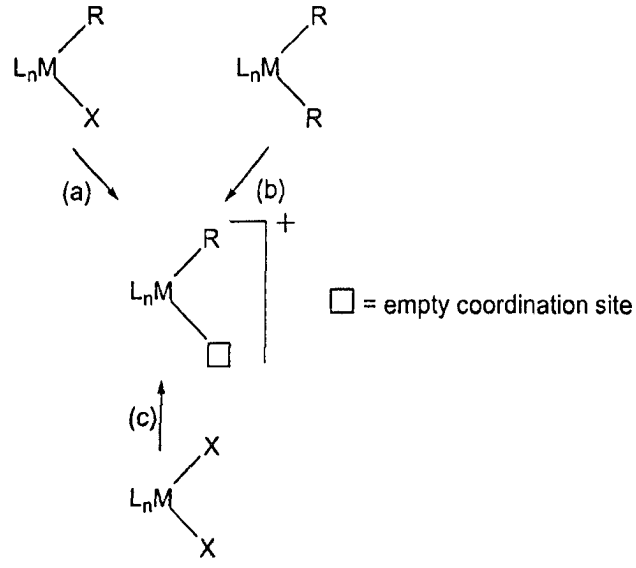

Route (a), through anionic abstraction of ligand X (ie., halide), substitutes a 'non-coordinating' anion by salt elimination. Similarly, route (b) follows an initial abstraction mechanism of ligand R (as the alkyl anion). However, route (c) is both an alkylation and abstraction process, achieved by treating a dihalide procatalyst with an alkylating species first, then followed by an alkyl-abstraction agent.[46] A fourth route for the generation of an active catalytic species involves the combined cationic and anionic parts within the same molecule, termed "zwitterionic metallocenes."[30,38]

Nevertheless, the chemistry at the active site of heterogeneous Z/N catalysts is not well understood,[47] especially with respect to stereocontrol of polypropylene polymerization by Z/N systems.[48] Historically, commercially applied systems have been modifications of the classic $TiCl_3/AlR_3$ systems.[1,2,3] The treatment of bulk $TiCl_3$ with AlR_2Cl is believed to activate surface titanium

sites. The picture in Figure 1.7 is assumed to be monoalkylated Ti(III) ion attached to the crystal by a Ti-Cl-M bridge, where 'M' is thought to be either Mg or Ti and attached alkylaluminum groups at or near the active site by Al-Cl-Ti coordination. The growing polymer chain is thought by some researchers[49,50,51,52,53,54] to attach to the coordinatively unsaturated lateral face of the crystal by a Ti-C σ-bond. A propylene monomer, coordinated to the Ti adjacent to the aforementioned Ti-C bond,[52] inserts into the growing polymer chain with consistent regularity of both head-to-tail orientation and tacticity.[48] Better understanding the nature of this crowded active site may be best served by developing rigid ligand systems which force metals to be in close proximity, producing homogeneous models of this Z/N active site to better comprehend the mechanism of polymerization.

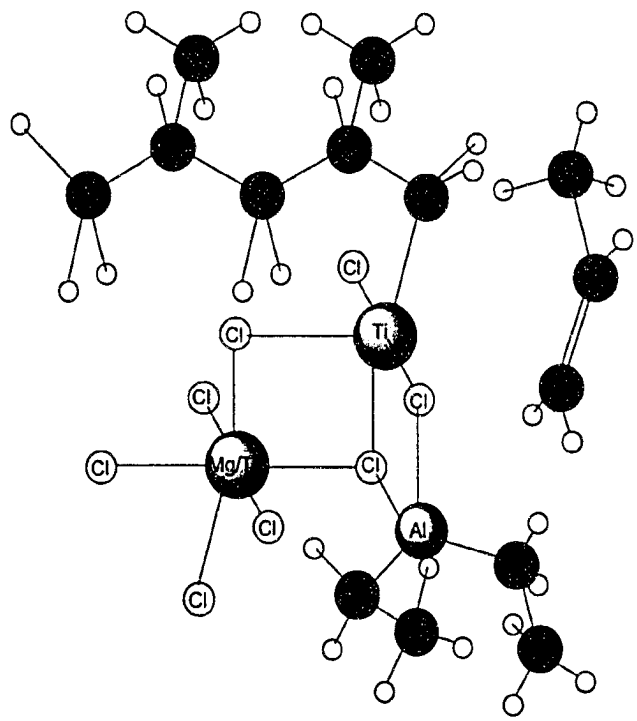

Figure 1.7 – Active site of a Z/N catalyst showing incoming propylene.

1.5 – Catalyst activities

Despite remarkable advances in the catalysis of olefin polymerization, metallocenes are still markedly different from the heterogeneous analogues. Homogeneity with the polymerization medium has led to lower polydisperities and increased incorporation of olefin comonomers than those obtained with classical heterogeneous Z/N systems. Nevertheless, such improvements have come at a significantly higher cost, so industrial acceptance has been slower than originally expected.[55] The oxophilicity of early transition metal (Ti, Zr, Cr) Z/N systems also results in poisoning by heteroatom-functionalized olefins. Although the literature[56,57,58,59,60,61,62,63] is replete with examples of copolymerizations with unusual substrates and the inclusion of Lewis acids in the polymerization system to protect polar monomer functionality through complexation,[64,65,66] early metal Z/N heterogeneous systems are less conducive to heteroatom comonomer polymerization applications, rigorous kinetic studies, and most importantly from an industrial perspective, active site characterization.

Recent research has focused on addressing the most fundamental prerequisite for olefin polymerization catalysis – high catalyst activity. Traditionally, it was thought that to achieve high activities a catalyst complex must contain a metal(s) centre, ancillary ligands(s), a growing polymer chain, and an accessible monomer coordination site[6] (Equation 1.2).

Equation 1.2 – Olefin insertion in metal-catalyzed polymerization

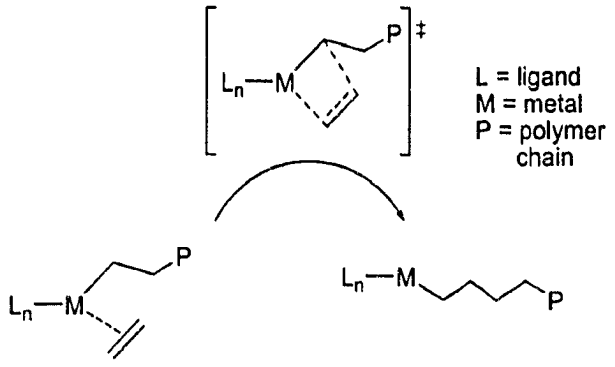

Historically, researchers have understood the metal centre to be the primary focus of the catalytic cycle, whereas the purpose of the ligands are to hold the metal in a monomeric fashion, preserve the electrophilicity and oxidation state of the metal at a suitably high level, and provide enough reaction space for incoming substrates. However, Equation 1.2 does show the impractical simplicity of the model. With the possibility of varying so many of the factors affecting this cycle (ie. stereochemistry of the monomer, ligand design, and/or metal(s)), appreciation of these complexities demands even more detailed studies of heterogeneous Z/N systems and their respective model systems.

1.6 – Heterogeneous systems from homogeneous successes

Understanding the nature of the active site of heterogeneous Z/N catalytic systems stems is necessitated by the drawbacks of homogeneous analogues in industrial applications. Although researchers have demonstrated the importance of 'post-metallocene' homogeneous systems in providing access to polymers

previously unattainable, the utility of these homogeneous systems is often limited to the laboratory as they suffer from the difficulty of separating the catalyst from the polymer product, especially in large-scale conversions within open reaction systems.[67] In slurry, bulk monomer, or gas-phase processes, the polymer is often of higher density and crystallinity, and insoluble in the reactor diluent or gas stream. To operate these processes continuously in an industrial reactor, the active site of the catalyst must be uniform in nature and must be able to be fed into the reaction medium smoothly without clumping. Single-site catalysts have been supported on many different types of carriers, producing polymers of narrow particle size distributions and high bulk densities.[4]

For example, Soga[68,69] studied supported (Al_2O_3, $MgCl_2$, CaF_2, AlF_3, silica, MgO, MgF_2, SiO_2 zirconocenes activated by simple alkyl aluminum compounds ($AlMe_3$, $AlEt_3$, Al(*i*-Bu)$_3$) or MAO. The zirconocenes were supported by way of an impregnation procedure, and these supported catalysts provided unexpected results in the polymerization of propylene. Compared to the homogeneous analogues where alkylaluminum reagents are ineffective activators for zirconocenes, the $MgCl_2$ or alumina supported variants show dramatic activity increases, although still considerably less than the homogeneous MAO-activated analogue. As well, in other studies, $CpTiCl_3$ with MAO or Al(*i*-Bu)$_3$ show little activity for olefin polymerization, but function considerably better when supported on silica, alumina, or $MgCl_2$.[70]

Single-site catalysts, activated by the addition first of MAO on supported inorganic oxides, especially silica, have historically provided the majority of

heterogeneous catalysts for olefin polymerization.[4,71] For example, the silsequioxane complex (c-$C_5H_9)_7Si_8O_{12}$-OH),[72] a model system for (1,3-$SiMe_3$—C_5H_3)$TiCl_3$ (Figure 1.8), supported on silica shows activity towards ethylene polymerization.

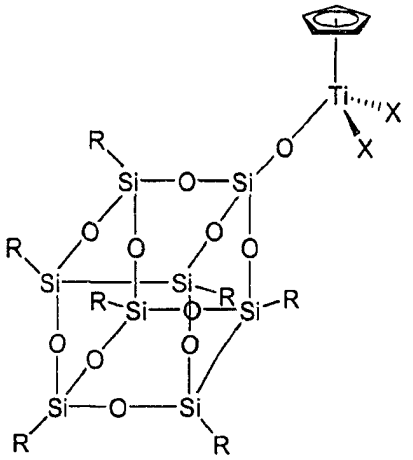

Figure 1.8 – van Tol's silica supported titanocene

As well, the activity and nature of supported catalysts often depends on the method with which they are prepared, with variables extending from the order of addition of the catalyst, to the MAO/alkylaluminum activator, and to the support.[4]

1.6.1 – Bimetallic catalytic cooperativity

Bimetallic group IV catalytic precursors,[73,74,75,76,77,78] including demonstrated cases of bimetallic cooperativity[79,80] (Figure 1.9), have been studied with an eye to achieving unique catalytic transformations. Although

these complexes do not involve metal-metal bonds, having the metals in close proximity is thought to be paramount to inducing the high activity seen in heterogeneous Z/N systems.

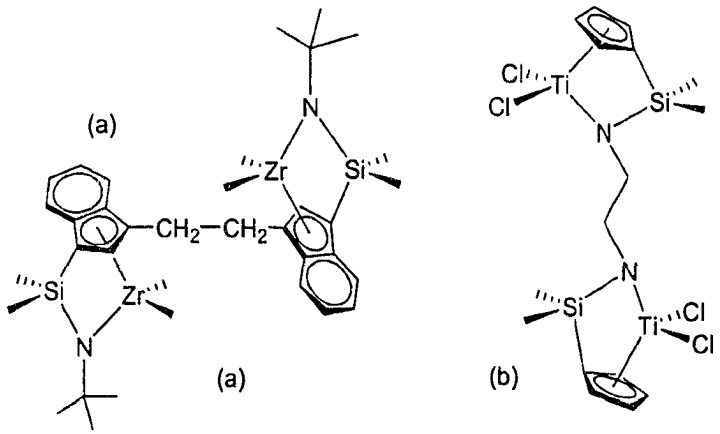

Figure 1.9 – (a) Marks' bimetallic catalyst[80] and (b) Royo's bimetallic catalyst.[81]

There have been some reports of precatalyst systems with direct metal-metal bonds[82,83,84,85,86,87] (Figure 1.10 (a), (b)) or Group IV bridged dimers (Figure 1.10 (c), (d)),[88,89] illustrating the utility of ligand design in creating a sterically encumbered bimetallic catalytic system.

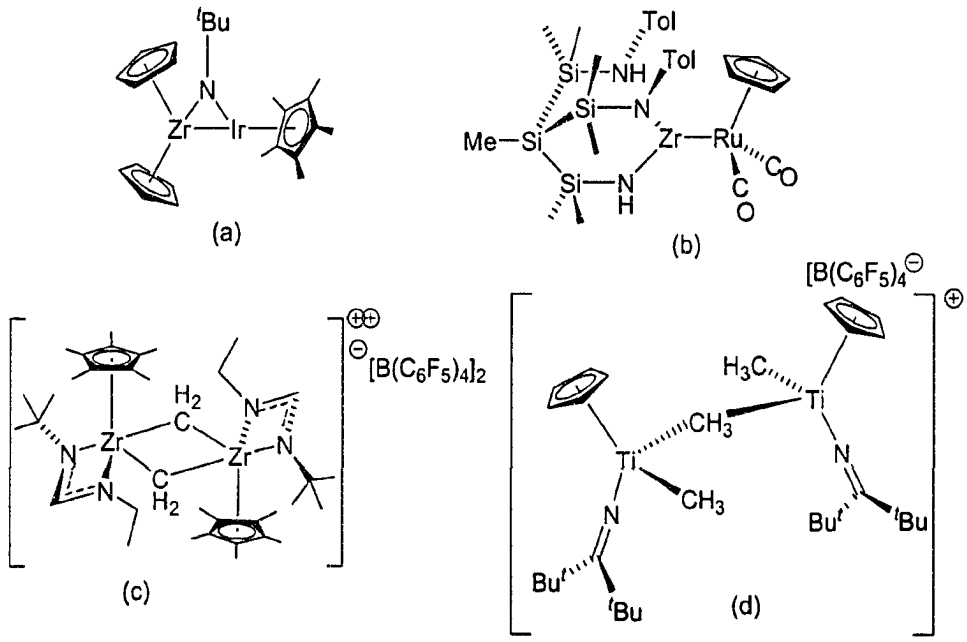

Figure 1.10 – (a) Bergman's bimetallic carbon-hetero bond cleavage catalyst[82] (b) McParlin's bimetallic oxygen transfer catalyst[83] (c) Sita's bridged Zr complex[88] (d) Piers' bridged Ti complex[89]

Much investigation remains to be completed, as many questions have arisen, including the extent to which an olefin-terminated polymer fragment, having left one metal centre, might have an enhanced probability of being captured by another proximate metal centre.[80] Brintzinger[90] and Mulhaupt[91] have suggested that such high nuclearity might very well offer new insight into the mechanism of Z/N polymerization, where the roles of the dimer or ion pairs of the propagating species may be crucial.

Efforts in our group[92,93,94] and others[95] have focused on challenging previously held assumptions on the nature of the active site of the catalytic complex. Although dimerization is thought to deactivate homogeneous catalyst systems, Fujita[95] has also examined basic strategies of ligand design, asserting

that a ligand should have: (1) moderate electron-donating properties; (2) a non-symmetric chelating structure that meets thermal stability demands; (3) an electron-count that allows the complex to remain coordinatively unsaturated; and (4) structural diversity and synthetic accessibility. This 'ligand-oriented' catalyst design approach may actually have begun with the discovery of Keim's SHOP catalyst[96] and has produced for others many active catalysts for ethylene polymerization[97,98,99,100,101,102,103,104,105] (Figure 1.11).

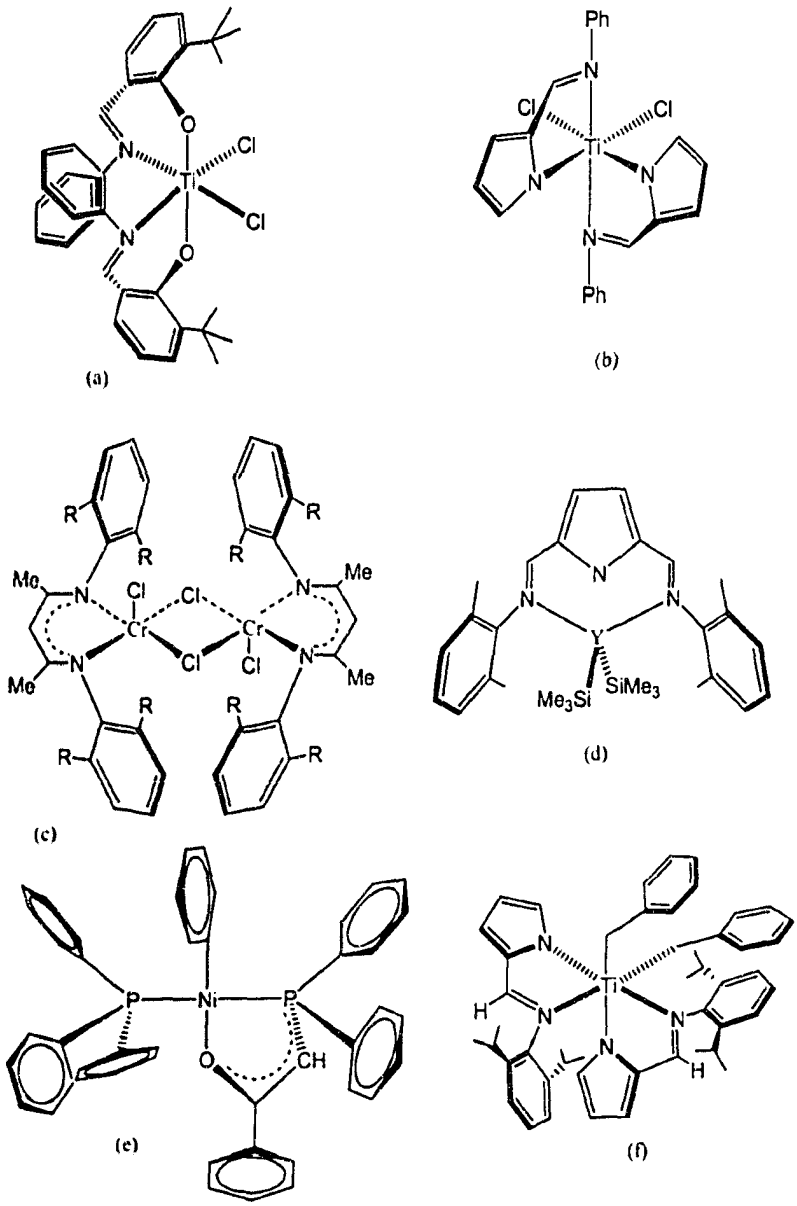

Figure 1.11 – Ligand–oriented designer catalysts – (a) Fujita's Fenokishi-Imine (FI) catalyst[106] (b) Fujita's pyrrolide-imine (PI) catalyst[98] (c) Gibson's β-diketimate catalyst[99] (d) Mashima's indolide-imine (II) catalyst[100] (e) Keim's SHOP catalyst[96] (f) Mashima's pyrrolyl-imine catalyst[107]

The 'ligand-oriented' catalyst design may also offer what has been to date unattainable: active, structural models of polymetallic heterogeneous systems,

particularly those incorporating proximal bridging transition metal(s) or bridging between a transition metal and a main group element.

Notes and References

---

[1] Ziegler, K.; Gellert, H.G.; Zoel, K.; Pfohl, W. *Angew. Chem.* **1955**, *67*, 424-426.

[2] Ziegler, K.; Holzkamp, E.; Breil, H.; Martin, H. *Angew. Chem.* **1955**, *67*, 541-543.

[3] Natta, G., *J. Am. Chem. Soc.* **1955**, *77*, 1708-1710.

[4] Hlatky, G. Chem. Rev. **2000**, 100, 1347-1376. The term "heterogeneous" refers to the insolubility of the catalyst in the polymerization medium and the multisite nature of the catalyst itself.

[5] Kashiwa, N.; Tokumizu, T.; Fujimura, H. (Mitsui Petrochemicals, Ind.), *US Patent* 3,642,746, **1967**.

[6] Fujita, T.; Haruyuki, M.; Kashiwa, N. *Adv. Synth. Catal.* **2002**, *344*, 477-493.

[7] Natta, G.; Pino, P.; Mazzanti, G.; Giannini, U.; Montica, E.; Peralto, M. *J. Polym. Sci.* **1957**, *26*, 120-123.

[8] Reichert, K.H.; Meyer, K.R. *Makromol. Chem.* **1973,** *169*, 163-176.

[9] Long, W.P.; Breslow, D.S. *Leibigs Ann. Chem.* **1975,** 464-465.

[10] Andresen, A.; Cordes, H.-G.; Herwig, J.; Kaminsky, W.; Merck, A.; Mottweiler, R.; Pein, J.; Sinn, H.; Vollmer, H.-J. *Angew. Chem., Int. Ed. Engl.* **1976,** *15*, 630-632.

[11] Sinn, H.; Kaminsky, W. *Adv. Organomet. Chem.* **1980,** *18*, 99-123.

[12] Sinn, H.; Kaminsky, W.; Vollmer, H.-J.; Woldt, R. *Angew. Chem., Int. Ed. Engl.* **1980,** *19*, 390-392.

[13] Kaminsky, W. *J. Chem. Soc. Dalton Trans.* **1998**, *9*, 1413-1418.

[14] Waymouth, R.; McKnight, A. *Chem. Rev.* **1998,** *98*, 2587-2598.

[15] Ewen, J. A. *J. Am. Chem. Soc.* **1984**, *106*, 6355-6364.

[16] Kaminsky, W.; Kulper, K.; Brintzinger, H. H.; Wild, F. *Angew. Chem., Int. Ed. Engl.* **1985**, *24*, 507-508.

[17] Coates, G. ; Waymouth, R. *Science* **1995**, *267*, 217-219.

[18] Canich, J. A. M. (Exxon). *U.S. Patent* 5,026,798, **1991**.

[19] Canich, J. A. M.; Licciardi, G. F. (Exxon). *U.S. Patent* 5,057,475, **1991**.

[20] Canich, J. A. M. (Exxon). *Eur. Pat.* 0 420 436 A1, **1991**.

[21] Stevens, J. C.; Neithamer, D. R. (Dow). *Eur. Pat.* 0 418 044 A2, **1991**.

[22] Shapiro, P.; Bunel, E.; Schaefer, W.; Bercaw, J. *Organometallics*. **1990**, *9*, 867-869.

[23] Okuda, J. *Chem. Ber.* **1990**, *123*, 1649-1655.

[24] Johnson, L.; Killian, C.; Brookhart, M. *J. Am. Chem. Soc.* **1995**, *117*, 6414-6415.

[25] Johnson, L. ; Mecking, S.; Brookhart, M. *J. Am. Chem. Soc.* **1996**, *118*, 267-268.

[26] Killian, C.; Temple, D.; Johnson, L.; Brookhart, M. *J. Am. Chem. Soc.* **1996**, *118*, 11664-11665.

[27] Scollard, J.; McConville, D.; Payne, N.; Vital, J. *Macromolecules* **1996**, *29*, 5241-5243.

[28] Scollard, J.; McConville, D. *J. Am. Chem. Soc.* **1996**, *118*, 10008-10009.

[29] Small, B.; Brookhart, M.; Bennett, A. *J. Am. Chem. Soc.* **1998**, *120*, 4049-4050.

[30] Britovsek, V.; Gibson, B.; Kimberley, B.; Maddox, J.; McTavish, S.; Solan, G.; White, A.; Williams, D. *Chem. Commun.* **1998**, 849-850.

[31] Younkin, T.; Connor, E.; Henderson, J.; Friedrich, S.; Grubbs, R.; Bansleben, D. *Science* **2000**, *287*, 460-462.

[32] Wang, C.; Friedrich, S.; Younkin, T.; Li, R.; Grubbs, R.; Bansleben, D.; Day, M. *Organometallics* **1998**, *17*, 3149-3151.

[33] Fujita, T.; Tohi, Y.; Mitani, M.; Matsui, S.; Saito, M.; Nitabaru, M.; Sugi, K.; Makio, H.; Tsutsui, T. (Mitsui Chemicals, Inc.), *EP 0874005*, **1998**.

[34] Mitani, M.; Yoshida, Y.; Mohri, J.; Tsuru, K.; Ishii, S.; Kojoh, S.; Matsugi, T.; Saito, J.; Matsukawa, N.; Matsui, S.; Nakano, T.; Tanaka, H.; Kashiwa, N.; Fujita, T. (Mitsui Chemicals, Inc.), *WO 01/55231* A1, **2001**.

[35] Sugimura, K.; Ban, K.; Suzuki, Y.; Hayashi, T. Jpn. Laid-Open Appl. 09/302021, **1997**.

[36] Tjaden, E.; Casty, G.; Stryker, J. *J. Am. Chem. Soc.* **1993**, *115*, 9814-9915.

[37] Kolthammer, B.; Tracy, J.; Cardwell, R.; Rosen, R. US Patent 5,763,547, **1998**.

[38] Pell, K.; Wilson, D.; PCT Int. Appl. 98/45337, **1998**.

[39] Weinbert, W.H.; McFarland, E.; Goldwasser, I.; Boussie, T.; Turner, H.; Van Beek, J.; Murphy, V.; Powers, T. PCT Int. Appl. 98/03521, **1998**.

[40] Jungling, S.; Koltzenburg, S.; Mulhaupt, R. *J. Polym. Sci.* **1997**, *35*, 1-8.

[41] DeChelis, M.; Griffin, J.; Muhle, M. US Patent 5,405,922, **1995**.

[42] Griffin, J.; DeChellis, M.; Muhle, M. US Patent 5,462,999, **1995**.

[43] Goode, M.; Schreck, D.; Wenzel, T.; Williams, C. Eur. Pat. Appl. 780404 A2, **1997**.

[44] Agapiou, A.; Muhle, M.; Renola, G. US Patent 5,442,019, **1995**.

[45] Muhle, M.; Agapiou, A.; Renola, G. US Patent 5,652,666, **1997**.

[46] Devore, D.; Timmers, F.; Hasha, D.; Rosen, T.; Marks, T.; Deck, P.; Stern, C. *Organometallics* **1995**, *14*, 3132-3134.

[47] Hlatky, G.; Turner, H.; Eckman, R. *J. Am. Chem. Soc.* **1989**, *111*, 2728-2729.

[48] *Homogeneous Catalysis: The Applications and Chemistry of Catalysis by Soluble Transtition Metal Complexes;* Parshall, G.; Ittel, S.; John Wiley and Sons, Inc.: New York, **1992**, pp 57-59.

[49] Corradini, P.; Barone, V.; Fusco, R.; Guerra, G. *Eur. Polym. J.* **1979**, *15*, 1133-1141.

[50] Corradini, P.; Guerra, G.; Fusco, R.; Barone, V. *Eur. Polym. J.* **1980**, *16*, 835-842.

[51] Corradini, P.; Barone, V.; Fusco, R.; Guerra, G. *Gazz. Chim. Ital.* **1983**, *113*, 601-603.

[52] Arlman, E.; Cossee, P. *J. Catal.* **1964**, *3*, 99.

[53] Venditto, V.; Guerra, G.; Corradini, P. *Eur. Polym. J.* **1991**, *27*, 45-54.

[54] Allegra, G. *Makrolek. Chem.* **1971**, *145*, 235-246.

[55] Brookhart, M.; Ittel, S.; Johnson, L. *Chem. Rev.* **2000**, *100*, 1169-1203.

[56] Chung, T. *Macromolecules* **1988**, *21*, 865-869.

[57] Chung, T.; Rhubright, D. *Macromolecules* **1993**, *26*, 3019-3025.

[58] Schneider, M.; Schafer, R.; Mulhaupt, R. *Polymer* **1997** *38*, 2455-2459.

[59] Wilen, C.-E.; Auer, M.; Steinmann, A.; King, R.; Zweifel, H.; Drewes, R. *Macromolecules* **2000**, *33*, 5011-5026.

[60] Waymouth, R.; Kesti, M.; Coates, G. Appl. WO Patent Application 9412547 June 9, 1994 to Leland Stanford Junior University.

[61] Aaltonen, P.; Lofgren, B. *Macromolecules* **1995**, *28*, 5353-5357.

[62] Aaltonen, P.; Fink, G.; Lofgren, B.; Seppala, J. *Macromolecules* **1996**, *29*, 5255-5260.

[63] Galimberti, M.; Giannini, U.; Albizatti, E.; Caldari, S.; Abis, L. *J. Mol. Catal. A.* **1995**, *101*, 1-10.

[64] Tanaka, M.; Machida, S.; Uoi, M. U.S. Patent 4833224, June 27, 1989 to Idemitsu Kosan Co., Ltd., Japan.

[65] Novak, B.; Boffa, L. *Chem. Rev.* **2000** *100*, 1479-1493.

[66] Marques, M. M.; Correia, S. G.; Ascenso, J. R.; Ribeiro, A. F. G.; Gomes, P. T.; Dias, A. R.; Foster, P.; Rausch, M. D.; Chien, J. C. W. *J. Polym. Sci, Part A: Polym. Chem.* **1999**, *37*, 2457-2469.

[67] *Laboratory Studies of Heterogeneous Catalytic Processes;* Christofell, E. Elsevier: Amsterdam, **1989**.

[68] Soga, K.; Kaminaka, M. *Makromol. Chem. Phys.* **1993**, *194*, 1745-1755.

[69] Kaminaka, M.; Soga, K. *Polymer* **1992**, *33*, 1105-1107.

[70] Soga, K.; Uozumi, T.; Saito, M.; Shiono, T. *Macromol. Chem. Phys.* **1994**, *195*, 1503-1508.

[71] Hearn, A. *unpublished results.*

[72] Duchateau, R.; Abbenhuis, H.; van Santen, R.; Thiele, S.; van Tol, M. *Organometallics* **1998**, *17*, 5222-5224.

[73] Lee, D.; Yoon, K.; Lee, E.; Noh, S.; Byun, G.; Lee, C. *Macromol. Rapid Commun.* **1995**, 265-268.

[74] Noh, S.; Kim, S.; Kim, J.; Lee, D.; Yoon, K.; Lee, H.; Lee, S.; Huh, W. *J. Polym. Sci., A: Polym. Chem.* **1997**, *35*, 3717-3728.

[75] Yan, X.; Chernega, A.; Green, M.; Sanders, J.; Souter, J.; Ushioda, T. *J. Mol. Catal. A – Chem.* **1998**, *128*, 119-141.

[76] Noh, S.; Kim, J.; Jung, J.; Ra, C.; Lee, D.; Lee, H.; Lee, S.; Huh, W. *J. Organomet. Chem.* **1999**, *580*, 90-97.

[77] Daniele, S.; Hitchcock, P.; Lappert, M.; *Chem. Commun.* **1999**, 1909-1910.

[78] Novak, A.; Blake, A.; Wilson, C.; Love, J. *Chem. Commun.* **2002**, 2796-2797.

[79] Komon, Z.; Bu, X.; Bazan, G. *J. Am. Chem. Soc.* **2000**, *122*, 1830-1831.

[80] Li, L.; Metz, M.; Li, H.; Chen, M.; Marks, T.; Liable-Sands, L.; Rheingold, A. *J. Am. Chem. Soc.* **2002**, *124*, 12725-12741.

[81] Jiminez, G.; Royo, P.; Cuenca, T.; Herdtweck, E. *Organometallics* **2002**, *21*, 2189-2195.

[82] Fulton, J.; Hanna, T.; Bergman, R. *Organometallics* **2000**, *19*, 602-614.

[83] Fabre, S.; Findeis, G.; Trosch, J.; Gade, L.; Scowen, I.; McPartlin, M.; *Chem. Commun.* **1999**, 577-578.

[84] Schubart, M.; Mitchell, G.; Gade, L.; Kottke, T.; Scowen, I.; McPartlin, M. *Chem. Commun.* **1999**, 233-234.

[85] Schneider, A.; Gade, L.; Breuning, M.; Bringmann, G.; Scowen, I.; McPartlin, M. *Organometallics* **1998**, *17*, 1643-1645.

[86] Misumi, Y.; Ishii, Y.; Hidai, M.. *J. Chem. Soc., Dalton Trans.* **1995,** *21*, 3489-3496.

[87] Adams, R.; Barnard, T.; Lu, Z.; Wu, W.; Yamamoto, J. *J. Am. Chem. Soc.* **1994**, *116*, 9103-9113.

[88] Keaton, R.; Jayaratne, K.; Fettinger, J.; Sita, L. *J. Am. Chem. Soc.* **2000**, *122*, 12909-12910.

[89] Piers, W. Zhang, S. *Organometallics* **2001,** *20,* 2088-2092.

[90] Beck, S.; Geyer; A.; Brintzinger, H. H. *J. Chem. Soc., Chem. Commun.***1999**, 2477-2478.

[91] Fischer D.; Mulhaupt, R. *J. Organomet. Chem.* **1991**, *417*, C7-C11.

[92] Verkerk, U.; Fujita, M.; Dzwiniel, T.; McDonald, R.; Stryker, J. *J. Am. Chem. Soc.* **2002**, *124*, 9988-9989.

[93] Qi, G.; Erickson, N.; Stryker, J. *unpublished results.*

[94] Fujita, M.; Qi, G.; Verkerk, U.; Dzwiniel, T.; MacDonald, R.; Stryker, J. *Org. Lett.* **2004**, *6*, 2653-2656.

[95] Matsui, S.; Fujita, T. *Catalysis Today* **2001**, *66,* 63-73.

[96] Keim, W.; Kowalt, F.; Goddard, R.; Kruger, C. *Angew. Chem. Int. Ed. Engl.* **1978**, *17*, 466-467.

[97] Yoshida, Y.; Matsui, S.; Takagi, Y.; Mitani, M.; Nitabaru, M.; Nakano, T.; Tanaka, H.; Fujita, T. *Chem. Lett.* **2000**, *10,* 1270.

[98] Yoshida, Y.; Matsui, S.; Takagi, Y.; Mitani, T.; Nakano, T.; Tanaka, H.; Kashiwa, N.; Fujita, T. *Organometallics* **2001**, *20*, 4793-4799.

[99] Gibson, V.; Maddox, P.; Newton, C.; Redshaw, C.; Solan, G.; White, D.; Williams, D. *Chem. Commun.* **1998**, 1651-1652.

[100] Matsuo, Y.; Mashima, K.; Tani, K. *Organometallics* **2001**, *20*, 3510-3518.

[101] Matsuo, Y.; Mashima, K.; Tani, K. *Chem. Lett.* **2000**, *10*, 1114-1115.

[102] Yoshida, Y.; Saito, J.; Mitani, M.; Takagi, Y.; Matsui, S.; Ishii, S.; Nakano, T.; Kashiwa, N.; Fujita, T. *Chem. Commun.* **2002**, 1298-1299.

[103] Matsugi, T.; Matsui, S.; Kojoh, S.; Takagi, Y.; Inoue, Y.; Fujita, T.; Kashiwa, N. *Chem. Lett.* **2001**, *2*, 566-567.

[104] Matsugi, T.; Matsui, S.; Kojoh, S.; Takagi, Y.; Inoue, Y.; Fujita, T.; Kashiwa, N. *Macromolecules* **2002**, *35*, 4880-4887.

[105] Suzuki, Y.; Kashiwa, N.; Fujita, T. *Chem. Lett.* **2002**, *1*, 358-360.

[106] Matsui, S.; Tohi, Y.; Mitani, M.; Saito, J.; Makio, H.; Tanaka, H.; Nitabaru, M.; Nakano, T.; Fujita, T. *Chem. Lett.* **1999**, *28*, 1065-1066.

[107] Tsurugi, H.; Yamagata, T.; Tani, K.; Mashima, K. *Chem. Lett.* **2003**, *32*, 756-757.

Chapter 2 - Pre-organized ligand systems for bimetallic cooperativity

Interest in exploring the extent to which bimetallic cooperativity in an olefin polymerization catalyst can be *deliberately* constructed has directed our efforts to prepare novel polydentate ligands. In order to understand the nature of solid oxide supported catalysts and modified zeolite surfaces, new ligands must be constructed with two main design principles. First, there is a least some evidence to suggest bimetallic cooperativity at the active site of classical supported Z/N systems. Instead of using chelating ligands, we sought to evaluate sterically demanding ligand structures that encourage bimetallic bridging. The second principle follows from the first - the ease with which we are able to access the ligand and precatalyst remains paramount. To this end, the creation of a structurally simple, rigid ligand that enforces bimetallic cooperativity constitutes the major goal of this work.

Our group has previously reported[1,2] on the utitility of a novel preorganized tetradentate ligand system for coordination and catalysis (Figure 2.1). With a nearly square arrangement of oxygen atoms for metal binding, this in principle system allows for the incorporation of sterically isolating alkyl substituents adjacent to the binding site(s). In practice, however, only relatively small alkyl substituents have been successfully introduced.

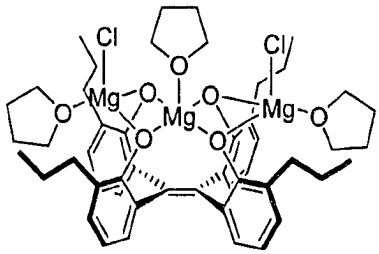

Figure 2.1 – Tetrakis(2-hydroxy-phenyl)ethene magnesium precatalyst[3]

Application of any commercial catalyst often depends on cost effective starting materials and syntheses. Recent progress in developing McMurray coupling methodology has reduced the synthesis of the parent ligand system to a three-step procedure[4] amenable to large-scale preparation. The introduction of the *n*-propyl substituents, however, consumes three additional steps.

With an eye to elucidating putative bimetallic active sites in classical Z/N catalysts and, in contrast to Fujita's[5] ligand chelation assertions, the effects of a relatively rigid, sterically hindered ligand and the imposition of bimetallic *complexation* remains the thrust of this work.[1,2,3,6,7] As Power[8] showed that increased nuclearity and pre-organization of metal centres led to novel polymetallic coordination structures, we postulated that by constructing the organic template so as to encourage at least indirect metal-metal interaction, the construct might form the basis for heterogeneous catalyst models. The phenoxide binding site in Figure 2.1 represents a host of other heteroatom–based ligand possibilities for heterogeneous models – including the amido– and imine–based systems reported by others in chelating ligand monometallic systems.

2.1 - Dibenzofuran

In this work, we intended to further simplify the ligand system and at the same time incorporate some additional themes. The sucess of *-amido* and *-oxo* type ligands has been well-documented[9,10,11,12] including, but not limited to, those which impose very high steric burden upon metal/ligand and metal/metal interactions. With this in mind, we targeted bidentate ligands based on the ***dibenzofuran*** core structure (Figure 2.2), with binding groups in the 4– and 6–positions and, where necessary, sterically isolating substituents at the 3– and 7–positions.

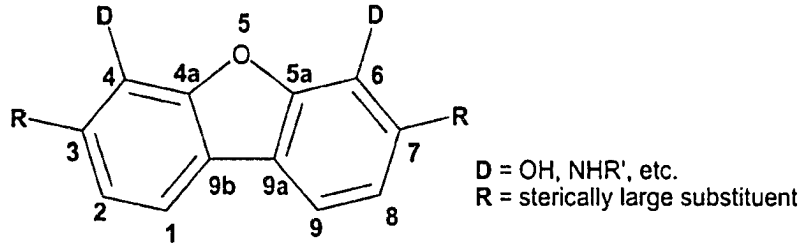

Figure 2.2 - Dibenzofuran and the accepted numbering structure[13]

The very weakly basic furan oxygen position (**5**, Figure 2.2) provides accessibility to possible hemi-labile ligand-metal interactions. The *amido–* or *oxo–* functionalization in the 4– and 6–positions encourages metal-ligand binding directly relevant to our interests: bridging *metal-metal* interactions. That is, the rigidly planar dibenzofuran ring system provides the essential function of this

ligand-oriented system: the binding sites are distant enough to avoid chelation about a single metal centre, forcing complexation of more than one metal (Figure 2.3).

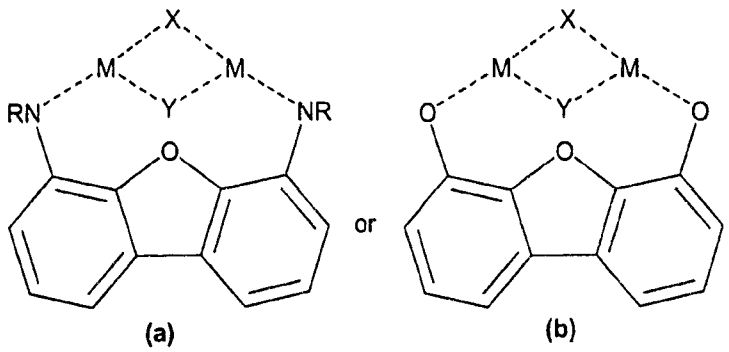

Figure 2.3 - Possible metal-metal interactions in (a) 4,6-*bis*(amido) dibenzofuran or (b) 4,6-*bis*(oxo)dibenzofuran

However, steric obligations at the active site have been neglected: the *bis*-4,6(oxygen) and primary amine functionalized parent structures (R = H) provide little steric isolation and little predilection for a simple bimetallic framework. Introduction of substantial steric bulk adjacent to the 4- and 6-oxygen substituents or attached to the amine nitrogen atoms (R = bulky alkyl) remains a considerable synthetic challenge. In fact, analysis of the existing literature provides an appreciation of the difficulty of adapting known synthetic routes to prepare the targeted dibenzofuran ligand systems.

2.2 - Electrophilic aromatic substitution using dibenzofuran

A review of the literature[13,14,15,16,17,18,19] reveals that dibenzofuran exhibits unique reactivity patterns when compared to similar aromatic substrates, such as phenols. Friedel-Crafts acylation,[20,21] Friedel-Crafts alkylation,[22] sulfonation,[23] and halogenation[24,25,26] of dibenzofuran universally give 2-substituted compounds as the major product. As well, Keumi and coworkers[14,27] report on the Friedel-Crafts benzoylation and benzylation of dibenzofuran, finding that the 2–position represents an average of 87% of the total reactivity of the 4 positions for benzoylation.

2.3 - Nitration of dibenzofuran

Literature studies on mixed-acid nitrations of dibenzofuran, however, indicate exclusive formation of 3-nitration products.[28,29] Keumi[14,27] offers no rationale for the anomalous reactivity patterns of dibenzofuran when standard concepts are used to explain electrophilic aromatic substitutions. Other researchers[30] have found that the nitration of dibenzofuran by HNO_3 in acetic anhydride results in 40% nitration at the 2– and 3–positions and 20% of 1-nitration product. Others[13,14] find that the nitration of the dibenzofuran parent using HNO_3 and H_2SO_4 occurs exclusively at the 3 and/or 7 positions. In fact, nitrations of dibenzofuran show a significant difference in behaviour when contrasted with Friedel-Crafts alkylations and acylations.[14] The ratio of 2- to 3-

isomer for nitration is dependant upon the nitrating agent, varying from 1.5 to 0.03. Most nitrations using Friedel-Crafts–type agents with alkyl nitrate/Lewis acid systems typically provide the 2–isomer whereas the 3–isomer is usually produced with nitric acid systems.[14] For example, the use of HNO_3 with TFA in CH_2Cl_2 provides almost exclusively 3-nitro-dibenzofuran (Equation 2.1).

Equation 2.1 - Nitration of dibenzofuran using a nitric acid system

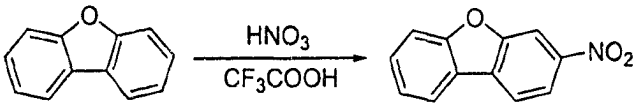

Eaborn[31] suggests that the 3–isomer is favoured by initial protonation of the furan oxygen by acids, leading to a change in the directing effects of dibenzofuran for electrophilic attack. (Scheme 2.1)

Scheme 2.1 - Eaborn's suggested mechanism of dibenzofuran nitration with nitric acid system

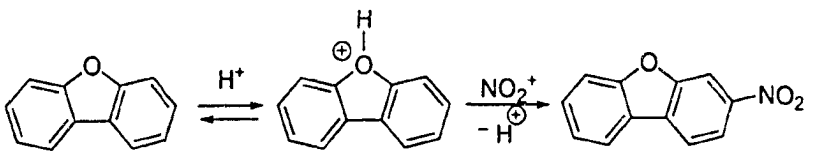

However, Keumi and co-workers[14] found no direct relationship between the amount of 3–isomer formed and the acidity of the medium used. They

suggest another possible mechanism (Scheme 2.2), where the nitronium atom is trapped initially by the furan oxygen, followed by intramolecular rearrangement.

Scheme 2.2 - Keumi's suggested mechanism of dibenzofuran nitration with a nitric acid system

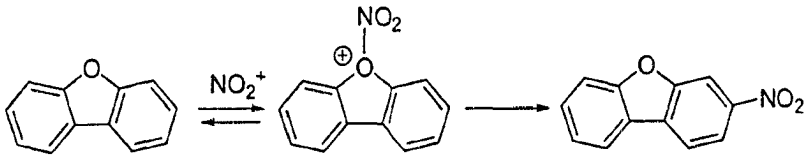

The authors do not speculate, however, how this rearrangement would preferentially afford the 3-isomer. Nevertheless, their exhaustive catalogue of trials[14] suggest that the positional preference is related to the concentration of nitronium ion associated with nitrate ion and molecular nitric acid (Equation 2.2–(a)).[32] They found consistency with other reports[33] of H_2SO_4/HNO_3 systems, wherein the active species is the nitronium ion (Equation 2.2–(b)). In fact, Keumi's empirical evidence is consistent with earlier reports from Olah,[34] which suggest an increase in the concentration of nitronium ion follows from an increase in the dialectric constant of the solvent or an increase in the concentration of nitric and sulfuric acid.[14]

Equation 2.2 - Proposed reacting species of nitronium ion

(a)

$$2HNO_3 \rightleftharpoons NO_2^+ + NO_3^- + H_2O$$

(b)

$$HNO_3 + 2H_2SO_4 \rightleftharpoons NO_2^+ + H_3O^+ + HSO_4^-$$

2.4 - Formation of 1,1,4,4,8,8,11,11-octamethyl-1,2,3,4,8,9,10,11-octahydro-dinaphtho[2,3-b;2',3'-d]furan and nitration

We postulated that if indeed no conditions were found for the regioselective 4,6-nitration of dibenzofuran, we might be able to induce nitration in the 4– and 6–positions by first adapting Bruson's protocol[35] for the Friedel-Crafts double alkylation of dibenzofuran. Although the Bruson found limited consistency with expected results, Abbott, in fact, reports exclusive 2–alkyl products from Friedel-Crafts alkylation of dibenzofuran.[22] By using this and our previous work[7] on the *tert*-butylation of the 4,6-*bis*(hydroxy)dibenzofuran as a model, we proposed that it might be possible to annulate selectively to give I (Scheme 2.3), followed by nitrating and subsequently reducing at the 4– and 6–positions.

Scheme 2.3 - Retrosynthetic strategy towards a sterically hindered 4,6-*bis*(amino)dibenzofuran structure.

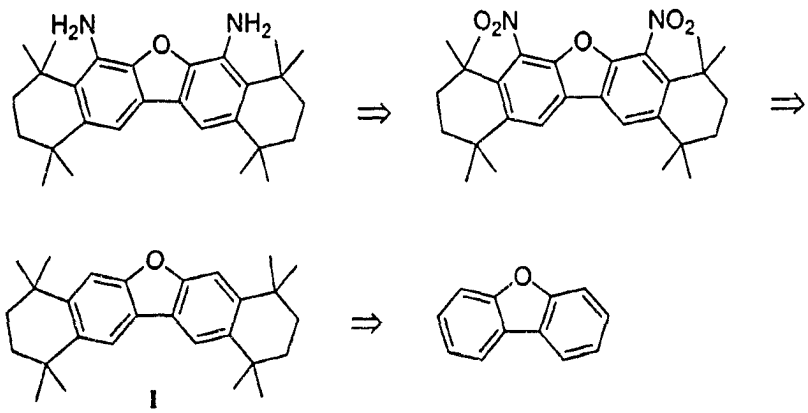

2.5 - Other Friedel-Crafts alkylations of dibenzofuran

Consideration was also given to constructing a hindered 4,6-*bis*(amino)dibenzofuran by way of methodology developed earlier by other members of our group,[7] initially by the Friedel-Crafts *tert*-butylation of dibenzofuran at the 2– and 7–positions or by exhaustive *tert*-butylation (Equation 2.3).

Equation 2.3 - Synthesis of 2,4,6,8-*bis*(*tert*-butyl)dibenzofuran

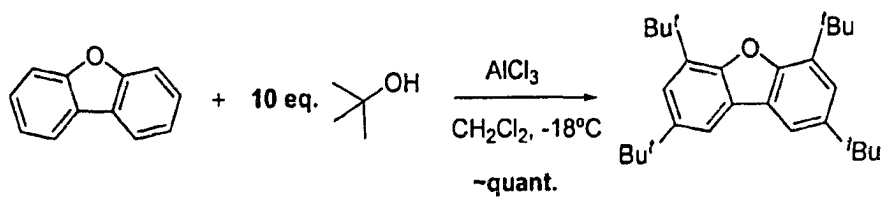

Aware of the work of Tashiro[36,37,38] and others[39,40,41] on the selective dealkylation of aromatic substrates by treatment with $AlCl_3$ in CH_3CN/benzene, we considered the possibility of adapting these procedures to selectively dealkylating and, subsequently nitrating the 4– and 6–positions.

2.6 - Dibenzofuranyl synthons

The reactivity patterns of dibenzofuran raise significant obstacles for both alkylation (for the introduction of steric bulk) and nitrogen introduction to give the required 4,6-dibenzofuran derivatives. However, the literature suggests that the introduction of appropriate functionality on monocyclic dibenzofuranyl *synthons* will be more promising. For example, the regioselective mono-nitration of biphenyl analogues is well known. With steric bulk already in place, the coupling of substituted benzene derivatives, either by *Ullman*-type[42,43,44] ether synthesis or through the oxidative coupling of phenols[45,46,47] might be accomplished efficiently (Scheme 2.4).

Scheme 2.4 - Retrosynthetic strategies towards alkylated dibenzofuran by way of (a) *Ullman*-type ether synthesis and (b) Oxidative coupling.

(a)

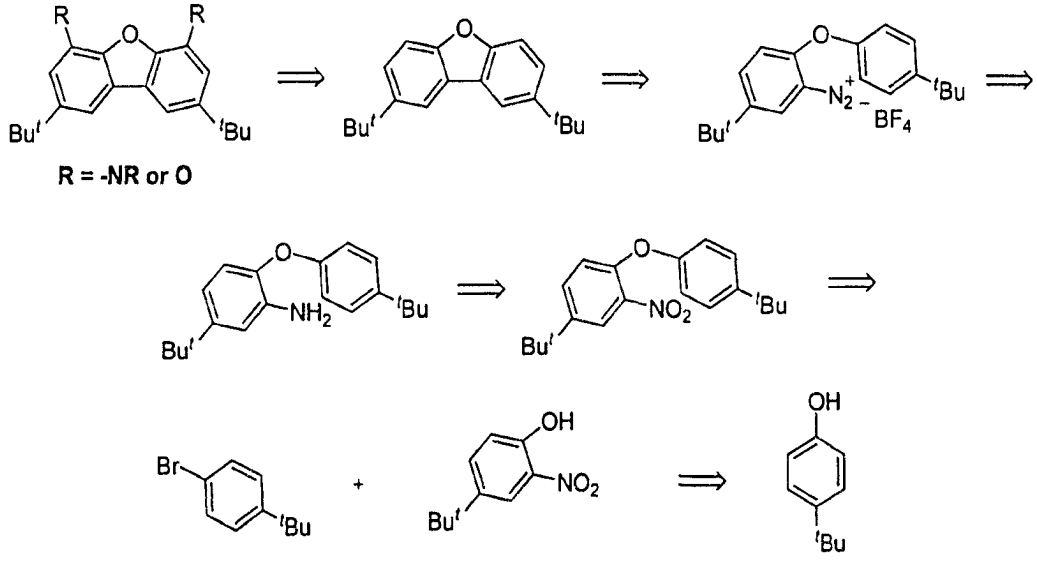

(b)

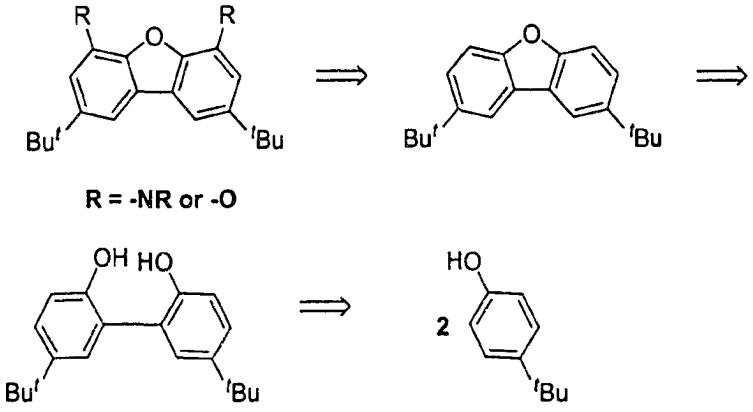

Eaborn[31,48] and others[30] have studied partial rate factors for dibenzofuran relative to diphenyl ether for protodetritiation,[31] protodetrimethylsilylation,[48] and nitration.[30] Their evidence suggests that the introduction of the biphenyl bond to diphenyl ether, the reactivity is lowered at both the positions *ortho* (4-) and *para*

(2-) to the oxygen atom of dibenzofuran. Taylor[49] also notes the same marked difference in reactivity patterns between dibenzofuran and diphenyl ether. Eaborn[48] proposes that the substituted phenyl group (9b) activation of the 1– and 3–positions results in competition from all positions, leading to uniform mixtures of isomers (Figure 2.4).

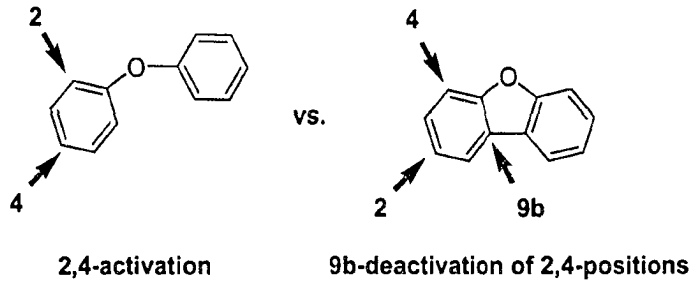

Figure 2.4 - Reactivity patterns of diphenyl ether and dibenzofuran

However, Eaborn[48] suggests that the principal source of the lowered reactivity in dibenzofuran could be ascribed to the oxygen lone pair contributing to resonance forms that impart some aromatic character to the furan ring.

Nevertheless, reactivity differences between the α– and β–positions of indane have been noted and would result from what is now known as the Mills-Nixon effect.[50] This anomaly has been postulated to be applicable to the case of dibenzofuran.[48,50] The transition state leading to 4-substitution will possess a 4a-9b bond (Figure 2.5 - **I**) that has higher double-bond character than in the ground state, leading to increased strain in the five–membered ring, destabilizing the transition state. In opposition, the transition state for the 2–substitution will possess a 4a-9b (Figure 2.5 - **II**) bond with less double-bond character than in the ground state, stabilizing this transition state and increasing the reactivity at

the 2–position. Hence, the reactivity of the 4–position will thus be lower, and the 2–position greater in dibenzofuran than what would be expected for diphenyl ether. In addition, it has been suggested[48,50] that the low reactivity of the 4–position may also be attributed to steric hindrance imposed by the lone-pair of the oxygen atom. However, the authors did not comment on the possibility of electronic effects playing a significant role in the relative stability of the transition states.

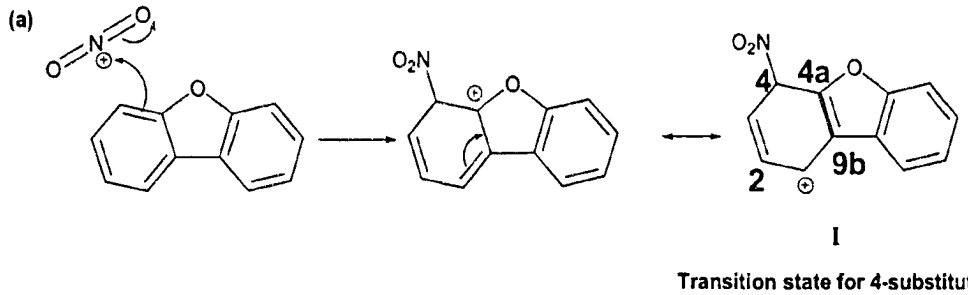

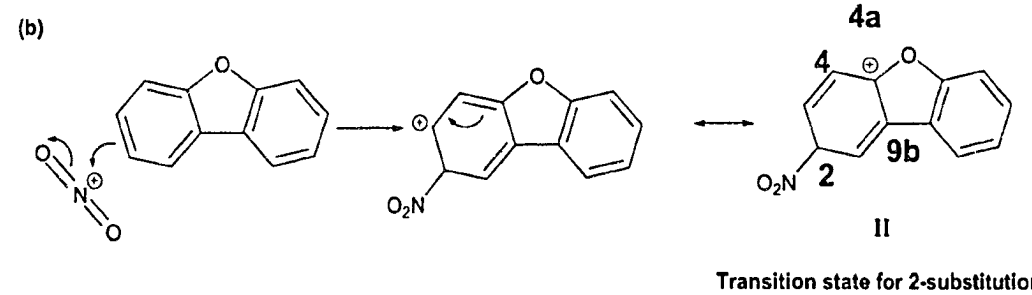

Figure 2.5 - Transition states for electrophilic substitution of dibenzofuran.

However, Billups and Boese[51] prepared structurally characterized tricyclobutabenzene (Figure 2.6), and confirmed calculations done by Stanger[52] and Siegel.[53] Siegel suggests[54] that that although the structure shows features of small strained rings (electron density deformations consistent with bent

bonds), no significant bond alternation is observed, where bond lengths of the central benzene are 1.40 and 1.38 angstroms for single and double bonds respectively. Their evidence thus appears to contradict arguments made for the Mills-Nixon effect for dibenzofuran. It remains unclear as to the rationale for some of the unique reactivity patterns in dibenzofuran.

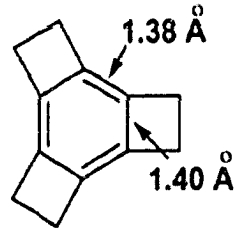

Figure 2.6 – Benzene bond lengths (angstroms) of tricyclobutabenzene.

2.7 - Directed *ortho*-metallation of dibenzofuran

Although Gilman's initial studies involved the directed *ortho*-metallation of anisole,[55] he reports extensively on dibenzofuran, including 4,6–double metallations[56] and electrophilic substitution reactions.[57] In fact, substantive reviews of directed *ortho*-metallations,[58,59] and other studies[56,60,61] on dibenzofuran reactivity, have shown the utility and scope of the methodology.

The directed *ortho*-metallation reaction is comprised of the deprotonation of a nominally non-acidic position *ortho* to a heteroatom containing a directed metallation group (DMG), **I** – Scheme 2.5. This deprotonation is usually effected by strong base, typically alkyllithium sources, resulting in an ortho lithiated species, **II**. The subsequent quench with an electrophilic agent yields a 1,2-disubstituted compound, **III**.

Scheme 2.5 - Directed *ortho*-metallation reaction[58]

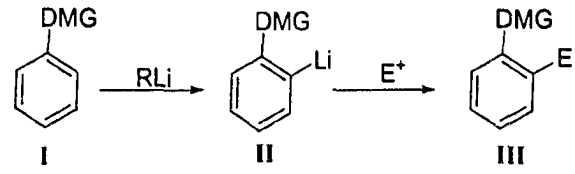

The directed *ortho*-metallation process generally involves the use of a powerful alkyllithium base in an organic solvent where solubilities are enhanced due to association into aggregates of well-known structure, ordinarily hexamers (in hydrocarbon solvents) or tetramers/dimers (in weakly basic solvents) (Table 2.1).

Table 2.1 - Aggregation of lithium reagents[58]

RLi	Solvent	Concentration (M)	Aggregate Species	Reference
MeLi	THF or Et_2O	0.2-1.2	tetramer	62
n-BuLi	C_6H_{12} or benzene	0.4-3.4	hexamer	63,64,65
	THF or Et_2O	0.1-0.7	tetramer-dimer	62,64 ,66,67,68
n-BuLi.TMEDA	*NA*	0.1	monomer	69
n-BuLi.TMEDA	*NA*	high	dimer	69
sec-BuLi	C_5H_{10}		tetramer-hexamer	70

Results of NMR spectroscopy,[70] X-ray structure determination,[71] and calculations[72] suggest that alkyllithium aggregates occur mostly as bridged structures, often consisting of electron-deficient bonding patterns of polar, multicovalent C–Li bonds. When in solution, these aggregates undergo rapid exchange of carbon-lithium and lithium-ligand bonds, often resulting in conformational interconversions.[58] Basic solvents, such as Et_2O and THF, cause

dissociation through a Lewis acid-base reaction, solvating the aggregate (eg., the addition of THF induces $(n\text{-BuLi})_6$ to reaggregate into $(n\text{-BuLi}\bullet THF)_4$). Bidentate TMEDA and tridentate PMDETA effectively break down such alkyllithium aggregates to monomers and dimers, effectively increasing their basicity. In the case of TMEDA, spectroscopic studies[69,71] indicate that the dominant species is in the form $(RLi\bullet TMEDA)_2$ with the lithium tetracoordinate (Figure 2.7).

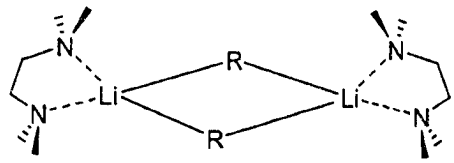

Figure 2.7 - Coordination sphere of $(RLi\bullet TMEDA)_2$[73,74]

2.8 - Alkylation of 4,6-*bis*(hydroxy)dibenzofuran

As others in our group have previously shown,[7] facile introduction of hydroxy groups in the 4– and 6–positions of dibenzofuran can be accomplished via double *ortho*-metallation followed by $B(OMe)_3$ quench and subsequent peroxide oxidation, furnishing the 4,6–diol in fair to good yield (Equation 2.4).

Equation 2.4 - Formation of 4,6-*bis*(hydroxy)dibenzofuran

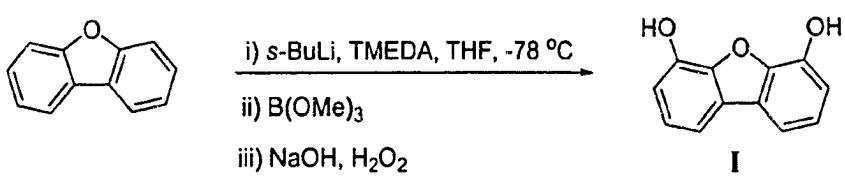

I

56%

We also considered the possibility of adapting known methodology[7,35] to further modify the 4,6-*bis*(hydroxy)dibenzofuran **I** (Equation 2.4), providing an entry point to sterically encumbered *oxo*- ligand systems (Figure 2.8).

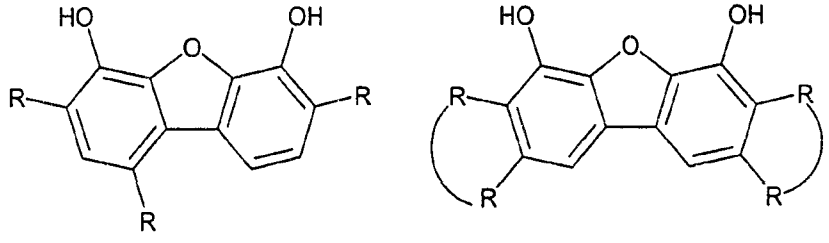

R = ^{t}Bu **R = annulated alkyl**

Figure 2.8 - Possible sterically encumbered 4,6-*bis*(hydroxy)dibenzofuran compounds

2.9 - Metal catalyzed coupling of dibenzofuran and amines

The use of an aryl boronic acid or halide in the metal–catalyzed coupling with various amines is well–known.[75,76,77,78,79,80,81,82,83,84,85] As we had previously shown[7] good success with introducing the boronic acid in the 4– and 6–positions of dibenzofuran, and being aware of literature protocol for the preparation of 4,6-*bis*(iodo)dibenzofuran,[86] we considered these compounds to be promising entry points for the preparation of hindered amines (Equation 2.5).

Equation 2.5 - Preparation of 4,6-dibenzofuranylbisboronic acid **2** and 4,6-*bis*(iodo)dibenzofuran.

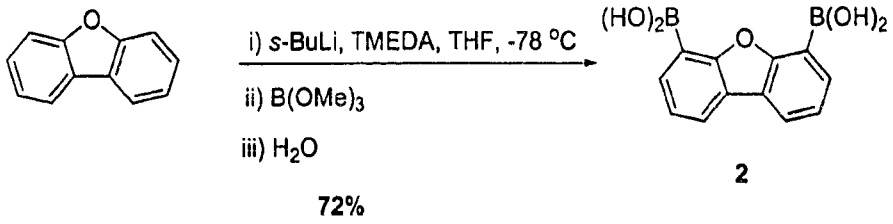

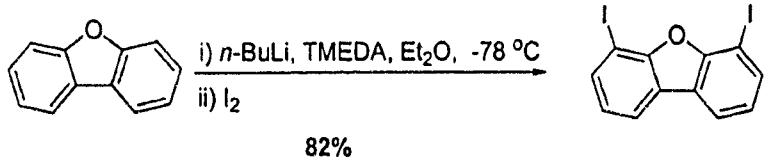

Several coupling methodologies were available, including the use of either copper or palladium, and are discussed in Chapter 3.

2.10 - Nitrodesilylation

Ipso-nitro substitution of aromatic silyl analogues had been achieved by Eaborn[87] using HNO_3 (Equation 2.6).

Equation 2.6 - Eaborn's nitrodesilylation reaction

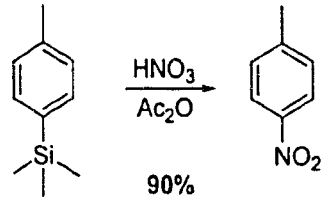

Although the authors did not use dibenzofuran as a substrate, we considered that silylation of a double metallated dibenzofuran intermediate, followed by nitrodesilylation constitutes yet another potential entry point to the 4,6-*bis*(amino)dibenzofuran construct (Scheme 2.6).

Scheme 2.6 - Retrosynthetic strategy using nitrodesilylation towards 4,6-*bis*(amino)dibenzofuran.

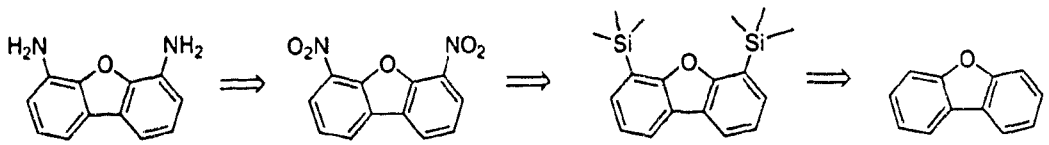

Based on the precedent of many of the aforementioned strategies, we have recognized several efficient proposals for the synthesis of targeted ligand systems, this synthetic work is detailed in Chapter 3.

Notes and References

[1] Verkerk, U.; Fujita, M.; Dzwiniel, T.; McDonald, R.; Stryker, J. *J. Am. Chem. Soc.* **2002**, *124*, 9988-9989.

[2] Fujita, M.; Qi, G.; Verkerk, U.; Dzwiniel, T.; MacDonald, R.; Stryker, J. *Org. Lett.* **2004**, *6*, 2653-2656.

[3] Fujita, M. PhD thesis. *University of Alberta* **2001**.

[4] Chung, M-K. *unpublished results.*

[5] Matsui, S.; Fujita, T. *Catalysis Today* **2001**, *66*, 63-73.

[6] Qi, G.; Stryker, J. *unpublished results.*

[7] Dzwiniel, T. *unpublished results.*

[8] Olmstead, M.; Sigel, G.; Hope, H.; Xu, X.; Power, P. *J. Am. Chem. Soc.* **1985**, *107*, 8087-8091.

[9] Li, L.; Metz, M.; Li, H.; Chen, M.; Marks, T.; Liable-Sands, L.; Rheingold, A. *J. Am. Chem. Soc.* **2002**, *124*, 12725-12741.

[10] Mitani, M.; Mohri, J.; Yoshida, Y.; Saito, J.; Ishii, S.; Tsuru, K.; Matsui, S.; Furuyama, R.; Nakano, T.; Tanaka, H.; Kojoh, S.; Matsugi, T.; Kashiwa, N.; Fujita, T. *J. Am. Chem. Soc.* **2002**, *124*, 3327-3336.

[11] Jiminez, G.; Royo, P.; Cuenca, T.; Herdtweck, E. *Organometallics* **2002**, *21*, 2189-2195.

[12] Keim, W.; Kowalt, F.; Goddard, R.; Kruger, C. *Angew. Chem. Int. Ed. Engl.* **1978**, *17*, 466-467.

[13] Sargent, M.; Stransky, P. *Adv. Het. Chem.* **1984**, *35*, 1-80.

[14] Keumi, T.; Tomioka, N.; Hamanaka, K.; Kakihara, H.; Fukushima, M.; Morita, T.; Kitajima, H. *J. Org. Chem.* **1991**, *56*, 4671-4677.

[15] Hand, E.; Johnson, S.; Baker, D. *J. Org. Chem.* **1997**, *62*, 1348-1355.

[16] Zeller, K.P.; Berger, S. *J. Chem. Soc., Perkin Trans. II* **1976**, *6*, 54-58.

[17] Radner, F.; Eberson, L. *J. Chem. Res.* **1996**, *8*, 2016-2030.

[18] Gilman, H.; Ingham, R. *J. Am. Chem. Soc.* **1953**, *75*, 4843-4845.

[19] Gilman, H.; Cheney, L. *J. Am. Chem. Soc.* **1939**, *61*, 3149-3156.

[20] Whaley, W.; White, C. *J. Org. Chem.* **1953**, *18*, 309-312.

[21] Johnson, R.; Willis, H.; Gilman, H. *J. Am. Chem. Soc.* **1954**, *76*, 6407-6408.

[22] Abbott, R. US Patent 2,500,732. Mar. 14, 1950.

[23] Wendland, R.; Smith, C. Muraca, R. *J. Am. Chem. Soc.* **1949**, *71*, 1593-1594.

[24] Oita, K.; Johnson, R.; Gilman, H. *J. Org. Chem.* **1955**, *20*, 657-659.

[25] Whitmore, F.; Langlois, D. *J. Am. Chem. Soc.* **1933**, *55*, 1518-1520.

[26] Gilman, H.; Brown, G.; Bywater, W.; Kirkpatrick, W. *J. Am. Chem. Soc.* **1934**, *56*, 2473-2475.

[27] Keumi, T.; Nakamura, M.; Kitamura, M.; Tomioka, N.; Kiitajima, H. *J. Chem. Soc., Perkin Trans. II* . **1985**, 909-913.

[28] Keumi, T.; Yamada, H.; Takashashi,; Kitajima, H. *Bull. Chem. Soc. Jpn.* **1962**, *55*, 629-633.

[29] Yamashiro, S. *Bull. Chem. Soc. Jpn.* **1941**, *16*, 61-62.

[30] Dewar, M.; Urch, D. *J. Chem. Soc.* **1957**, 345-347.

[31] Baker, R.; Eaborn, C. *J. Chem. Soc.* **1961**, 5077-5080.

[32] Hughes, E.; Ingold, C.; Reed, R. *J. Chem. Soc.* **1950**, 2400-2409.

[33] Ingold, C.; Millen, D.; Poole, H. *J. Chem. Soc.* **1950**, 2576-2582.

[34] Olah, G.; Kuhn, S.;. *J. Am. Chem. Soc.* **1962**, *84*, 3684-3687.

[35] Bruson, H.; Kroege, J. *J. Am. Chem. Soc.* **1940**, *1*, 36-44.

[36] Tashiro, M.; Watanabe, H.; Tsuge, O. *Org. Prep. Proced. Int.* **1974**, *6*, 117-124.

[37] Tashiro, M.; Yamato, T. *J. Org. Chem.* **1985**, *50*, 2939-2942.

[38] Tashiro, M.; Yamato, T.; Kobayashi, K.; Arimura, T. *J. Org. Chem.* **1987**, *52*, 3196-3199.

[39] Yamato, T.; *Hasegawsis* **1979**, 921-926.

[40] Yamato, T.; Arimuraa, K.; Saruwatari, Y.; Doamekpor, L. *Chem. Ber.* **1993**, *126*, 1435-1441.

[41] Yamato, T.; Arimura, T.; Tashiro, M. *J. Chem. Soc., Perkin Trans II* **1987**, 1-7.

[42] Ullmann, F. *Ber. Dtsh. Chem. Ges.* **1903**, *36*, 2382-2384.

[43] Lindley, J. *Tetrahedron* **1984**, *40*, 1433-1456.

[44] Goodbrand, H.; Hu, N. *J. Org. Chem.* **1999**, *64*, 670-674.

[45] Yamato, T.; Hasegawa, K.; Saruwatari, Y.; Doamekpor, L. *Chem. Ber.* **1993**, *126*, 1435-39.

[46] Aarts, V.; Grootenhuis, P.; Reinhoudt, D.; Czech, A.; Czech, B.; Bartsch, R. *Recl. Trav. Chim. Pays Bas* **1988**, *107*, 94-103.

[47] Sartori, G.; Maggi, R.; Bigi, F.; Grandi, M. *J. Org. Chem.* **1993**, *58*, 271-7273.

[48] Eaborn, C.; Sperry, J. *J. Chem. Soc.* **1961**, 4921-4928.

[49] Taylor, R. *J. Chem. Soc. B*, **1968**, 1559-1564.

[50] Vaughan, G.; Welch, G.; Wright, G. *Tetrahedron*, **1965**, *21*, 1665-1669.

[51] Boese, R.; Blaser, D.; Billups, W.; Haley, M.; Maulitz, A.; Mohler, D.; Vollhardt, K. *Angew. Chem.* **1994**, *106*, 321-325.

[52] Stanger, A. *J. Am. Chem. Soc.* **1991**, *113*, 8277-8280.

[53] Baldridge, K.; Siegel, J. *J. Am. Chem. Soc.* **1991**, *114*, 9583-9587.

[54] Siegel, J. *Angew. Chem. Int. Ed. Engl.* **1994**, *33*, 1721-1723.

[55] Gilman, H.; Bebb, R. *J. Am. Chem. Soc.* **1939**, *61*, 109-112.

[56] Gilman, H.; Gorisch, R. *J. Org. Chem.* **1957**, *22*, 6, 687-689.

[57] Johnson, R.; Willis, H.; Gilman, H. *J. Am. Chem. Soc.* **1949**, *71*, 1593-1595.

[58] Snieckus, V. *Chem. Rev.* **1990**, *90*, 879-933.

[59] Gschwend, H.; Rodriguez, H. *Org. React. (N.Y.)* **1979**, *26*, 1.

[60] Jean, F.; Tartar, A.; Melnyk, O. *Tetrahedron Lett.* **1995**, *36*, 7657-7660.

[61] Radner, F.; Eberson, J. *J. Chem. Res.* **1996**, *8*, 2016-2030.

[62] West, P.; Waack, R. *J. Am. Chem. Soc.* **1967**, *89*, 4395-4399.

[63] Margerison, D.; Newport, J. *Trans. Far. Soc.* **1963**, *59*, 2058-2063.

[64] Lewis, H.; Brown, T. *J. Am. Chem. Soc.* **1970**, *92*, 4664-4670.

[65] Eastham, J. *J. Am. Chem. Soc.* **1964**, *86*, 1071-1076.

[66] Quirck, R.; Kester, D. *J. Organomet. Chem.* **1974**, *72*, C23-C25.

[67] McGarrity, J.; Ogle, C. *J. Am. Chem. Soc.* **1985**, *107*, 1805.

[68] McGarrity, J.; Ogle, C.; Brich, Z.; Looslie, H. *J. Am. Chem. Soc.* **1985**, *107*, 1810-1811.

[69] Langer, A.; *Adv. Chem. Ser. No. 130* **1974**, 22-28.

[70] Fraenkel, G.; Henrichs, M.; Hewitt, M.; Su, B. *J. Am. Chem. Soc.* **1984**, *106*, 255-256.

[71] Setzer, W.; Schleyer, P. *Adv. Organomet. Chem.* **1985**, *24*, 353-358.

[72] Schleyer, P. *Pure Appl. Chem.* **1984**, *56*, 151-157.

[73] Nichols, M.; Williard, P.; *J. Am. Chem. Soc.*, **1993**, *115*, 1568-1572.

[74] Barnett, N.; Mulvey, R.; Clegg, W.; O'Neil, R. *J. Am. Chem. Soc.* **1993**, *115*, 1573-1574.

[75] Lam, P.; Clark, C.; Saubern, S.; Adams, J.; Winters, M.; Chan, D.; Combs, A. *Tetrahedron Lett.* **1998**, *39*, 2941-2944.

[76] Evans, D.; Katz, J.; West, T. *Tetrahedron Lett.* **1998**, *39*, 2937-2940.

[77] Hartwig, J. *Angew. Chem. Int. Ed. Engl.* **1998**, *37*, 2046-2067.

[78] Enguehard, C.; Allouchi, H.; Gueiffier, A.; Buchwald, S. *J. Org. Chem.* **2003**, *68*, 4367-4370.

[79] Kwong F.; Buchwald, S. *Org. Lett.* **2003**, *5*, 793-796.

[80] Klapars A.; Huang X.; Buchwald, S. *J. Am. Chem. Soc.* **2002**,*124*, 7421-7428.

[81] Kwong F.; Klapars, A.; Buchwald, S. *Org. Lett.* **2002**, *4*, 581-584.

[82] Klapars, A.; Antilla, J.; Huang, X.; Buchwald, S. *J. Am. Chem. Soc.* **2001**, *123*, 7727-7729.

[83] Antilla, J.; Buchwald, S. *Org. Lett.* **2001**,*3*, 2077-2079.

[84] Kiyomori, A.; Marcoux, J.; Buchwald, S. *Tetrahedron Lett.* **1999**, *40*, 2657-2660.

[85] Chan, D.; Monaco, K.; Wang, R.P.; Winters, M. *Tetrahedron Lett.* **1998**, *39*, 2933-2936.

[86] Tsang, K.; Diaz, H.; Graciani, N.; Kelly, J. *J. Am. Chem. Soc.* **1994**, *116*, 3988-4005.

[87] Eaborn, C.; Salih, Z.; Walton, D. *J. Chem. Soc. Perkin Trans. II* **1972**, 172-179.

Chapter 3 - Results and Discussion

The foregoing chapter details our investigation of routes to sterically encumbered *oxo*–, *imino*–, and *amido*–containing ligands. From classical methodology to novel applications of known chemistry, our goal remained the same - a short and efficient synthesis of desired compounds.

3.1 - Strategies towards alkylating dibenzofuranyl substrates

Early work was focused on introducing bulky alkyl groups on previously known compounds.[1] Concurrently, we explored the use of classical methodology towards introducing nitrogen synthons in the 4– and 6– positions of dibenzofuran.

3.1.1 - Alkylation of 4,6-*bis*(hydroxy)dibenzofuran

Increasing the steric burden through the introduction of cyclohexyl rings led our initial attempts to functionalize 4,6-*bis*(hydroxy)dibenzofuran **1** (Equation 3.1), first synthesized previously in our group.[1]

Equation 3.1 - Formation of 1,1,4,4,8,8,11,11-octamethyl-1,2,3,4,8,9,10,11-octahydro-5,7-dihydroxy-dinaphtho[2,3-b;2',3'-d]furan (1)

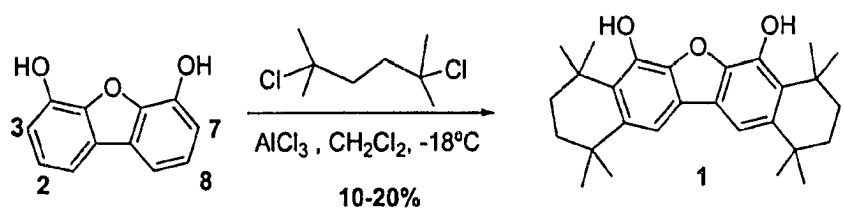

We knew the alkylation of 4,6-*bis*(hydroxy)dibenzofuran could be effected, as the introduction of *tert*-butyl groups was accomplished in acceptable yield.[1] (Equation 3.2)

Equation 3.2 - Alkylation of 4,6-*bis*(hydroxy)dibenzofuran

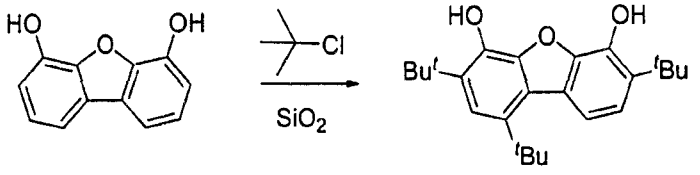

57%

We considered the possibility that if the 3– and 7– positions of 4,6-*bis*(hydroxy)dibenzofuran were activated towards Friedel-Crafts alkylation (Figure 3.1) over the 2– and 8– positions, statistical arguments might suggest wanted isomer formation could be effected using double alkylation.

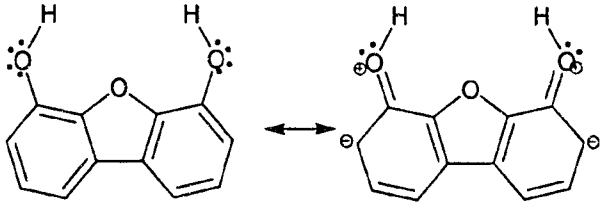

Figure 3.1 - 3,7 - Activation of dibenzofuran towards Friedel-Crafts alkylation

For our purposes, the reaction could involve initial alkylation at either the *ortho*– or *meta*–positions to yield the desired product. In the event, we found that

not only were extra equivalents of Lewis acid required to drive the reaction to completion (as judged by the disappearance of starting material by TLC), product isolation proved to be difficult, with crude ^{1}H NMR spectroscopic analysis suggesting the formation of several isomers (Figure 3.2).

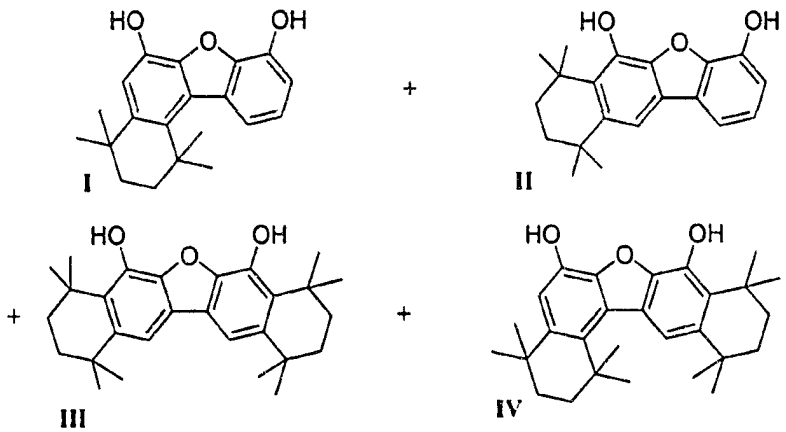

Figure 3.2 - Possible regioisomeric preferences for Friedel-Crafts alkylation of dibenzofuran

Our observations indicated little preference for product **III** formation, with the possibility of other unwanted isomer formation (**I, II, IV**). As well, other *inter*-molecular alkylations between dibenzofuranyl parents may also be possible. Nevertheless, no NMR spectroscopic comparison of products was possible due to the difficulties in isolation and separation, consistent with Bruson's findings.[2] Stepwise cyclohexyl ring annulation each with one equivalent of substrate may have served to improve the ease of purification and identification. However, no attempts were made to explore this option. Several attempts were made to improve the selectivity of the desired product by varying Lewis acids ($FeCl_3$,

$AlCl_3$), stoichiometry (0.5 – 10 equiv.), solvent (1,2-dichloroethane, THF, ether) and temperature conditions (-18 °C to reflux). In all trials, no conditions were found which improved the regioselectivity (by crude ^1H NMR spectroscopic analysis).

Overall, our results are consistent with previous reports of Abbott,[3] suggesting that positions 2– and 8– may be most activated by the furan oxygen of dibenzofuran, leading to a preponderance of unwanted isomer mixtures.

3.2 - Metal catalyzed coupling of dibenzofuran and amines

The use of an aryl boronic acid template was regarded as a promising entry point for the preparation of hindered amines, considering the wealth of metal-catalyzed methodologies Chan,[4,5] Evans,[6] Hartwig[7] and Buchwald[8,9,10,11,12,13,14] have developed for the coupling of aryl boronic acids and amines. As mentioned earlier, the introduction of the boronic acid groups in the 4– and 6–positions of dibenzofuran was established by others in our group.[1]

However, both Cundy[15] (Scheme 3.1) and Buchwald[9] report significant reduction in yield and reaction rate when coupling *ortho*-substituted phenyl boronic acids with various amines.

Scheme 3.1 - Cundy's[15] attempts at Cu–catalyzed aryl boronic acid coupling

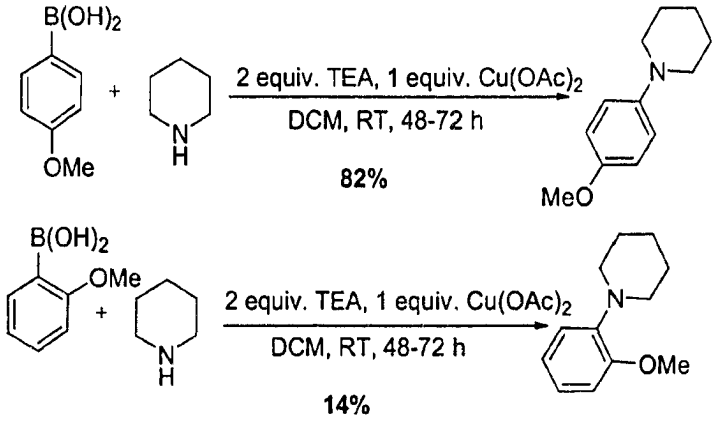

Unfortunately, all attempts at copper(II)–catalyzed coupling[4] of the 4,6-dibenzofuranylbisboronic acid and *tert*-butylamine, including the conditions shown in Equation 3.4, were not successful.

Equation 3.4 - Attempted copper–catalyzed boronic acid and amine coupling

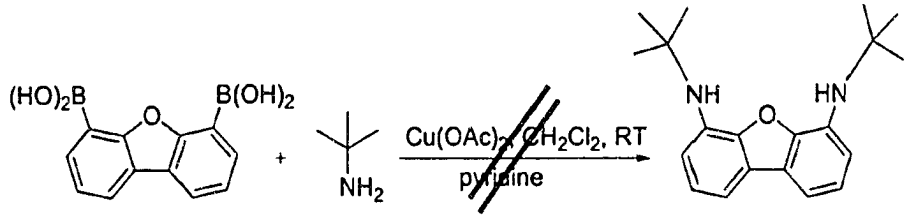

The literature offers no examples of using *tert*-butylamine as a substrate for cross-coupling, despite the exhaustive catalogue of primary amine sources reported.[8,9,10,11,12,13,14] Discussions with Buchwald[16] indicated no rationale for our inability to achieve the same success with *tert*-butyl amine under similar

conditions. In fact, ^{1}H NMR spectroscopy of the crude products suggested that only mono– and/or di–deboronation products were obtained. Following literature procedures to avoid deboronation using myristic acid or 2,6-lutidine and other hindered amines,[17] we were again unsuccessful, producing only deboronation products. Cundy[15] and Buchwald[13] suggest steric arguments could be a factor in the failure to couple *ortho*–substituted arylboronic acids. However, in our trials of 4,6-dibenzylfuranylbisboronic acid and *tert*-butylamine, we might expect to see at least some coupling to form the mono–alkylamino product. As we encountered only deboronation products in all trials, it is not clear that steric factors alone account for the lack of product formation.

We were able, however, to affect the *bis*–iodination of dibenzofuran in better yield than was reported in the literature[18] (Equation 3.5).

Equation 3.5 - Synthesis of 4,6-*bis*(iodo)dibenzofuran

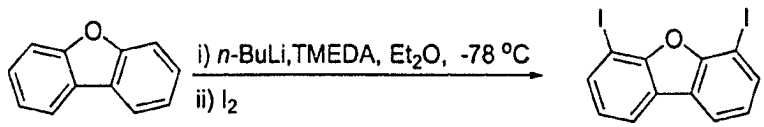

87%

However, adaptation of published protocols[8,11,13] in the copper–catalyzed coupling of 4,6-*bis*(iodo)dibenzofuran and *tert*-butylamine provided no desired product. In fact, we were able to affect only the *de*-iodination of the 4,6-*bis*(iodo)dibenzofuran substrate. Buchwald[10] suggests possible deactivation of the catalytic cycle through the formation of **I** – Scheme 3.2.

Scheme 3.2 - Possible mechanistic pathways for the Cu–catalyzed coupling of amines and aryl halides[10,19]

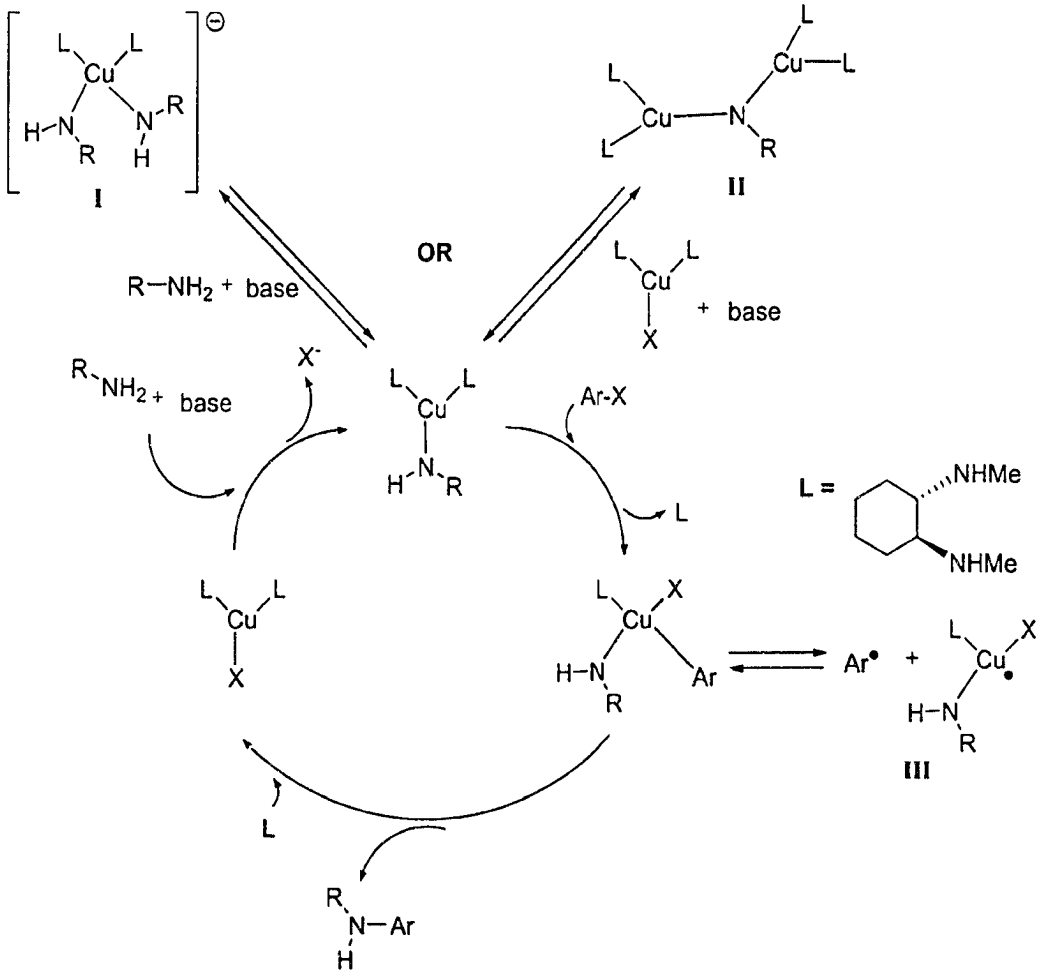

In our system, the use of 4,6-*bis*(iodo)dibenzofuran and *tert*-butylamine suggests deactivation through **II** – (*above*) or homolytic pathways **III** – (*above*) also possible. However, the rationale is not clear as to how the process may be occuring.

All attempts to prepare 4,6-*bis*(*tert*-butylamino)dibenzofuran through the $Pd(dba)_2$–catalyzed coupling of 4,6-*bis*(iodo)dibenzofuran and *tert*-butylamine[4,5] were also not successful, as ^1H NMR spectroscopic analysis of the crude

products indicated no 4,6-*bis*(amino)dibenzofuran product. Although Buchwald reports the variation of solvent or halide may play an important role in the oxidative addition step of the catalytic cycle, we did not investigate the role of either solvent or halide source.

Instead we looked to 4,6-*bis*(amino)substitution on dibenzofuran with the intent of introducing steric bulk on the amino groups.

3.3 - Strategies toward 4,6-*bis*(amino)dibenzofuran functionalization

Initial attempts to effect 4,6-nitration of the dibenzofuran parent followed a literature protocol[20,21] using HNO_3 and H_2SO_4. The analysis of crude products by ^1H NMR spectroscopy was consistent with the expected 3,6-dinitrodibenzofuran formation. Nevertheless, we attempted to alter the regioselectivity by using less harsh reagents,[22] such as $NaNO_2$ in AcOH.[20,21] An analysis of the ^1H NMR spectra of the crude reaction mixture, however, suggested no nitration products whatsoever were obtained.

3.3.1 - 1,1,4,4,8,8,11,11-octamethyl-1,2,3,4,8,9,10,11-octahydro-dinaphtho [2,3- b;2',3'-d]furan formation and nitration.

Consistent with earlier attempts to alkylate the 4,6-*bis*(hydroxy)dibenzofuran, adaptation of Bruson's[23] and other's[24,25] methodologies to the regioselective Friedel-Crafts alkylation of dibenzofuran itself also faired poorly (Equation 3.6). In fact, we were left with the desired product in

only an approximately 5% yield (as judged by ^{1}H NMR spectroscopy of crude product mixtures).

Equation 3.6 - Attempts toward Friedel-Crafts alkylation of dibenzofuran

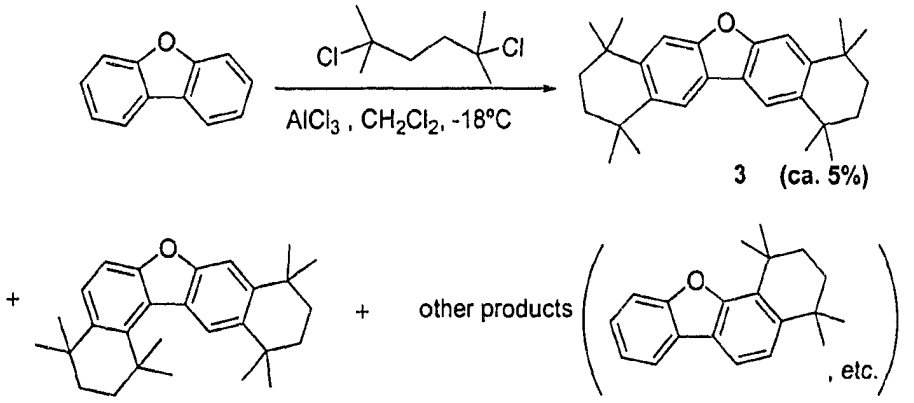

Although steric factors might have suggested otherwise, there again appears to be little preference for the symmetric annulation of the two 6–membered rings (Figure 3.3), despite our expectation of selective initial alkylation at the 2– and 8–positions.

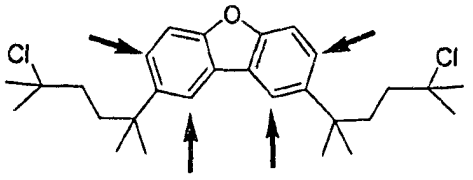

Figure 3.3 - Possible isomers leading to the *bis*-dibenzofuran alkylated products

Although nitration of **3** using $NaNO_2$ and AcOH was unsuccessful,[22] we were able to obtain 1,1,4,4,8,8,11,11-octamethyl-1,2,3,4,8,9,10,11-octahydro-

dinaphtho[2,3-b;2',3'-d]furan **5** by nitration of **3** with HNO_3 and H_2SO_4, followed by reduction with hydrogen catalyzed by 10% Pd/C (Scheme 3.3).

Scheme 3.3 - Nitration and reduction of 1,1,4,4,8,8,11,11-octamethyl-1,2,3,4,8,9,10,11-octahydro-dinaphtho[2,3-b;2',3'-d]furan

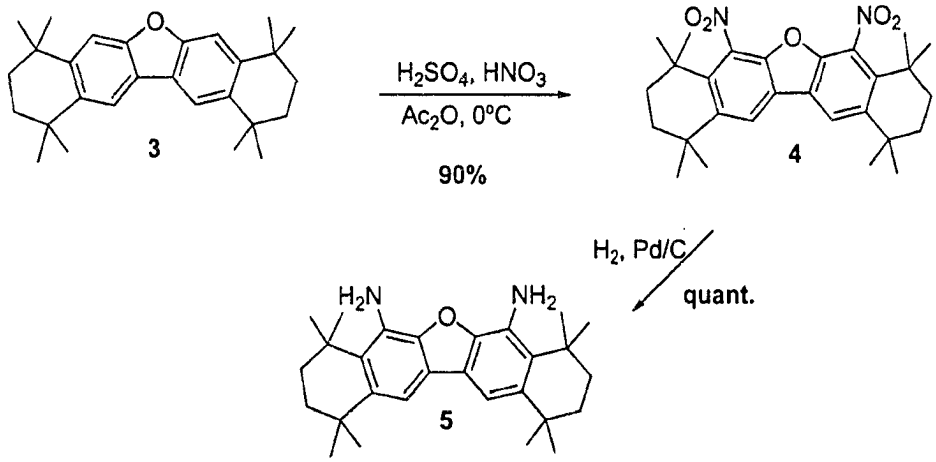

Nevertheless, initial low yields of annulated compound **3** effectively retired this strategy.

3.3.2 - Other Friedel-Crafts alkylations of dibenzofuran

Having a significant quantity of the *tert*-butylated dibenzofuran **6** prepared earlier by others in our group,[1] we next adapted Tashiro's procedures[26,27,28,29] for dealkylation of related biphenyl analogues. Repeated trials designed to selectively remove the 4– and 6–*tert*-butyl groups of **6** (Equation 3.7), including

variation of Lewis acid concentration and solvent ratio ($AlCl_3$ in CH_3NO_2/benzene) were met with poor results, with the desired product found in less than 10% of the crude reaction products (by ^1H NMR spectroscopic analysis).

Equation 3.7 - Selective dealkylation of *bis*(2,4,6,8-*tert*-butyl)dibenzofuran

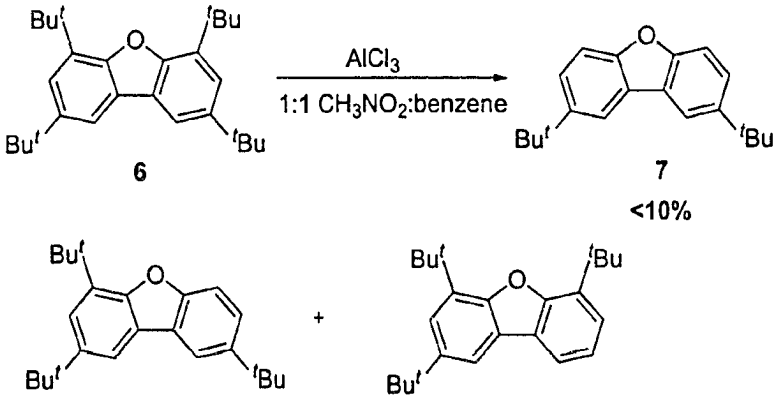

We did, however, successfully *mono*–nitrate 2,8-*bis*(*tert*-butyl)dibenzofuran **7**, using HNO_3 and H_2SO_4 (Equation 3.8), but were not able to introduce a second nitro group. Subsequent attempts using a larger excess of HNO_3 resulted in unwanted side products, including dealkylated, and apparently, rearranged isomers (crude ^1H NMR) (Equation 3.9).

Equation 3.8 - Nitration of 2,8-*bis*(*tert*-butyl)dibenzofuran

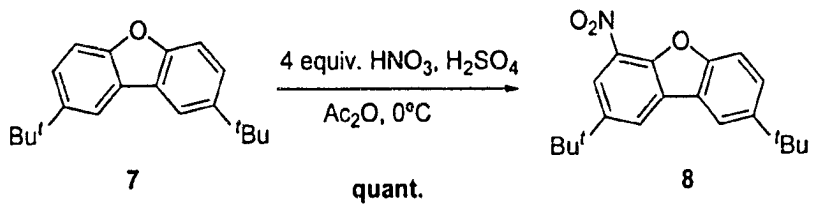

Equation 3.9 - Regioselective dealkylation and nitration of 2,8-*bis*(*tert*-butyl)dibenzofuran.

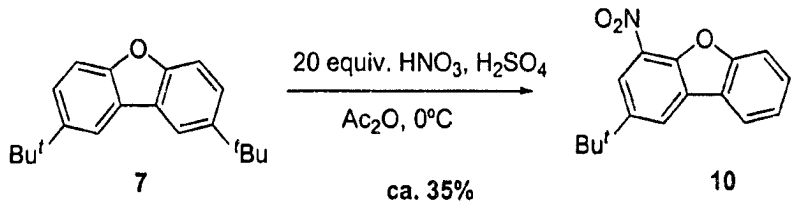

As a result of the dealkylation observed, we considered the possibility of using the same HNO_3/H_2SO_4 conditions to selectively remove the 4– and 6–*tert*-butyl groups from 2,4,6,8-*bis*(*tert*-butyl)dibenzofuran **6** and nitrate in situ (Equation 3.10). However, repeated trials with varying conditions and stoichiometry were not successful.

Equation 3.10 - Attempts towards regioselective dealkylation and nitration dibenzofuran.

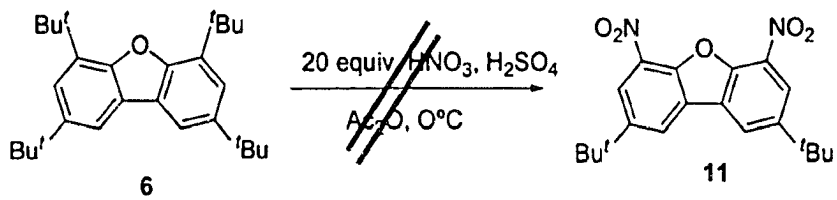

3.3.3 - Nitrodesilylation of dibenzofuran derivatives

Because we had previously shown that the double metallation of dibenzofuran was quantitative by quenching the intermediate with D_2O

(disappearance of the 4– and 6–protons by ^{1}H NMR spectroscopy), we trapped the dianion intermediate with trimethylsilyl chloride. In the event, the reaction afforded 4,6-*bis*(trimethylsilyl)dibenzofuran **12** in good yield (Equation 3.11).

Equation 3.11- Synthesis of 4,6-*bis*(trimethylsilyl)dibenzofuran.

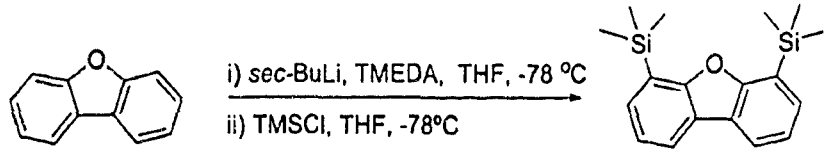

85% **12**

Attempted nitrodesilylation of **12** followed an adaptation of a literature protocol, using HNO_3.[30] In the event, analysis of the crude ^{1}H NMR spectrum of the crude product suggested that no 4,6-*bis*(nitro)dibenzofuran product was formed; instead, 2,8-*bis*(nitro)-4,6-*bis*(trimethylsilyl)dibenzofuran **13**, as well as mono– and di–*proteo*desilylated products were obtained, as judged by spectroscopic analysis (Equation 3.12).

Equation 3.12- Attempts to nitrodesilylate compound **12.**

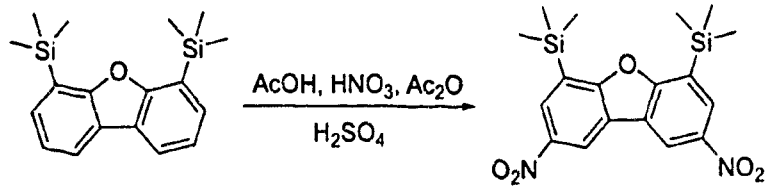

12 **~20 %** **13**

Repeated trials of the reaction with $AgNO_3$ under various conditions[30] also provided no 4,6-*bis*(nitro)dibenzofuran (Equation 3.13), but did give several

products (by crude ^{1}H NMR spectroscopy), with the greatest percentage of product consistent with the mono–substitution product **14**.

Equation 3.13 - Attempts to nitrodesilylate dibenzofuran

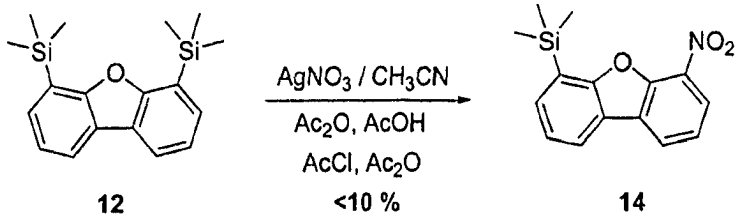

12 **<10 %** **14**

Eaborn and co-workers[30] have rationalized that at higher temperatures, nitrodesilylation is favoured over separate C–Si bond cleavage and subsequent nitration. However, Eaborn did not evaluate *ortho*-oxygen substituted substrates similar to dibenzofuran. We subsequently sought to control the suspected *over*-nitration of *bis*(4,6-trimethylsilyl)dibenzofuran **12** by first protecting the 2– and 8–positions with alkyl groups (Scheme 3.4).

Scheme 3.4 - Attempts to nitrodesilylate of dibenzofuran substrates.

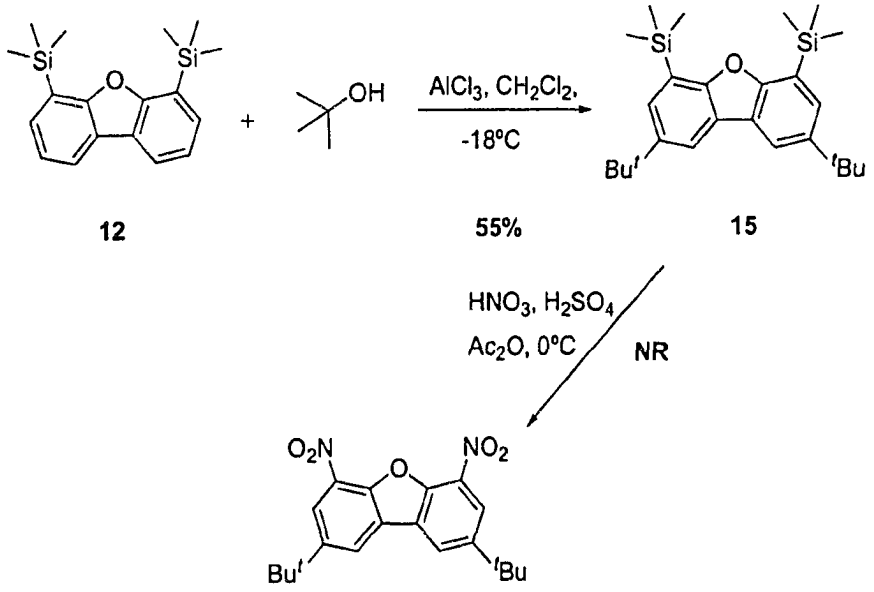

We were indeed able to effect the Friedel-Crafts alkylation of 4,6-*bis*(trimethylsilyl)dibenzofuran **12** in good yield; however repeated attempts at nitrodesilylation resulted only in complex mixtures of products, as judged by the analysis of the ^{1}H NMR spectrum of the crude product.

3.4 - Dibenzofuranyl synthons

Concurrently, synthesizing 4,6-*bis*(nitro)dibenzofuran was explored using monocyclic dibenzofuranyl synthons, with the hope of exploiting the known chemistry of simple phenols and biphenyl ethers.

3.4.1 - Oxidative coupling

Should we effect oxidative coupling of an appropriately substituted phenol, the nucleophilic dehydration of the product may yield the desired dibenzofuran in a short, efficient synthesis (Scheme 3.5).

Scheme 3.5 - Proposed efficient route to hindered dibenzofuran construct with steric bulk.

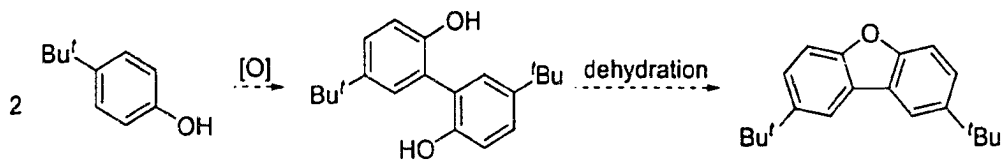

Attempted oxidative coupling of simple phenols, however, showed little promise, although others have reported the facile conversion of substituted phenols to biphenyl compounds.[31,32,33] Several reagents and conditions were attempted (Table 3.1).

Table 3.1 - Oxidative coupling trials.

Substrate	Reagent	Solvent	Conditions
4-*tert*-butylphenol	*tert*-butylperoxide	neat	120 -150 °C
	VCl_4	CCl_4	RT
	chloranil[a]	neat	210 °C
	DDQ[b]	neat	210 °C
	$AlCl_3$, chloranil	$MeNO_2$	RT
	$AlCl_3$, DDQ	$MeNO_2$	RT
4-*tert*-butyl-2-nitrophenol	$AlCl_3$, chloranil	$MeNO_2$	RT

a: chloranil*:* 2,3,5,6-tetrachlorobenzoquinone *b:* 2,3-dichloro-5,6-dicyano-1,4-benzoquinone

3.4.2 - Ullman-type ether synthesis

Although oxidative coupling methodology proved unsatisfactory, an Ullman-type ether synthesis was more promising. Before attempting the coupling reaction,[34,35,36,37,38] 4-*tert*-butylbromobenzene **17** was prepared by adapting an existing literature protocol.[39,40,41,42,43] This was accomplished by low temperature dropwise addition of Br_2 to a mixture of the Fe° and *tert*-butylbenzene **16** (Equation 3.14).

Equation 3.14 - Bromination of *tert*-butylbenzene.

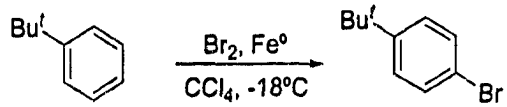

16 quant. 17

Ullman-type ether synthesis of the aryl halide **17** and 4-*tert*-butylphenol was then cleanly effected under standard Cu–catalyzed conditions[37,38] (Equation 3.15).

Equation 3.15 - Ullman-type ether synthesis.

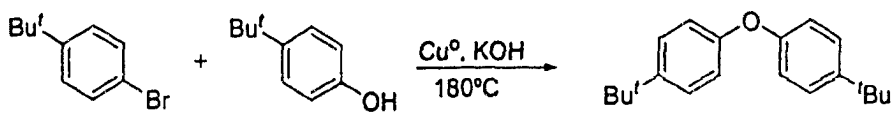

17 ~70%

Whitesides[44] suggests that when the Cu(I) salt is used instead of Cu°, the process occurs through the copper(I) complexation with the phenoxide anion, followed by nucleophilic phenoxide attack (Scheme 3.6).

Scheme 3.6 - Suggested mechanism for the Ullman ether synthesis.[44]

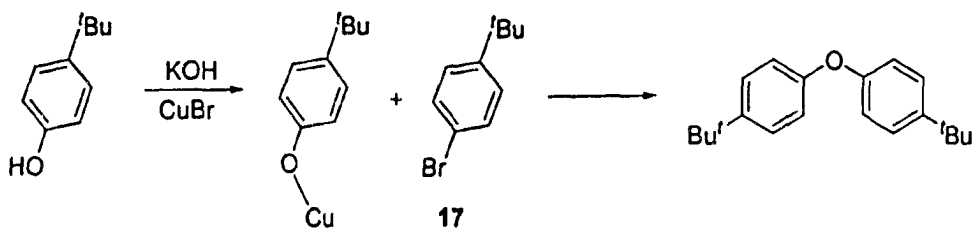

Accordingly, we expected that the introduction of the electron-withdrawing nitro group *ortho* to the bromo position on **17** would activate the direct nucleophilic substitution. The nitration of 4-*tert*-butylbromobenzene **17** under mild conditions ($NaNO_2$) followed the literature procedure[22] and met with little success. More effective were harsher conditions, using HNO_3 and H_2SO_4,[43] providing 2-nitro-4-*tert*-butyl-bromobenzene **18** exclusively in good yield (Equation 3.16).

Equation 3.16 - Nitration of 4-*tert*-butylbromobenzene.

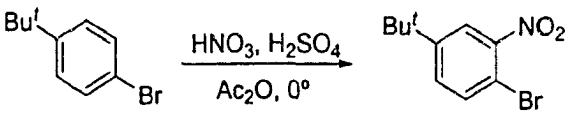

17 **80 %** **18**

Subsequent *Ullman*-type[35,36,45] ether synthesis of the 2-nitro-4-*tert*-butylbromobenzene **18** with 4-*tert*-butylphenol **19** is outline in Scheme 3.7. The results were consistent with expectation and results of Lindley,[37] wherein the *ortho*–nitro group functionalization serving to increase the yield of the coupling reaction. Subsequent reduction of the diarylether **20** to 2-amino-4-*tert*-butylbromobenzene **21** (H_2, 10% Pd/C) was quantitative and diazotization with $NaNO_2$ and $NaBF_4$ produced 2-diazo-4,4'-di-*tert*-butyldiphenylether tetrafluoroborate **22** in fair yield.

Scheme 3.7 - Synthesis of 2-diazo-4,4'-*tert*-butyldiphenylether tetrafluoroborate.

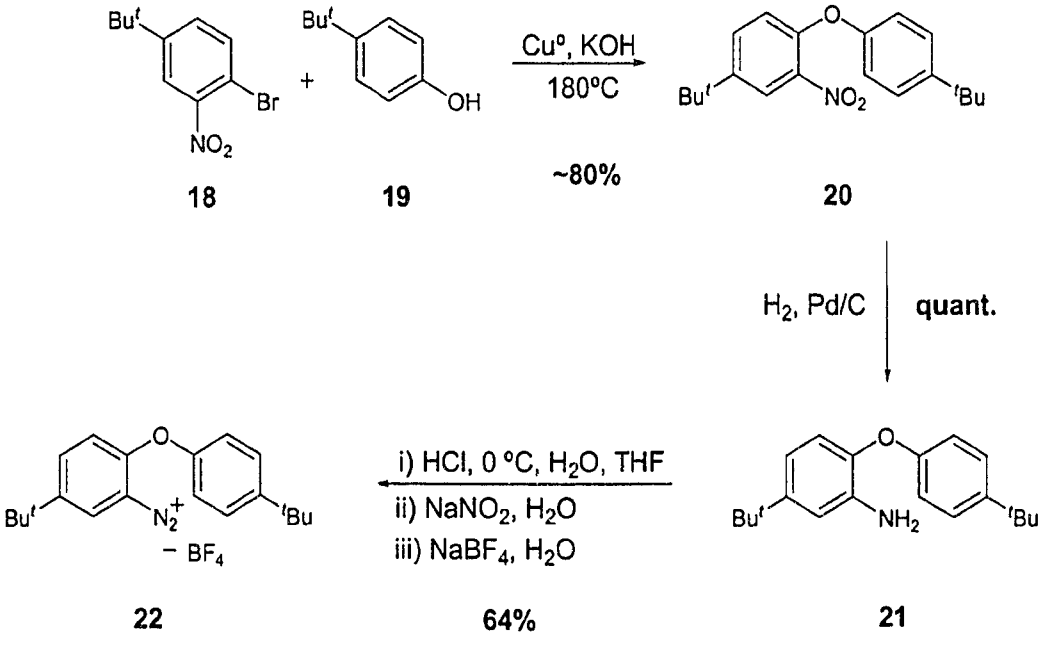

Although the annelation of the diphenylether diazonium salt **22** to give the 2,8-substituted dibenzofuran has been shown to occur in good yield,[46] concommitant development of more convergent strategies took precedence over our completion of this final step.

3.5 - Directed *ortho*-metallation

At this stage in our investigation, Maruoka and co-workers reported[47] that 4,6-*bis*(amino)dibenzofuran could be prepared in three steps: (1) directed double metallation of dibenzofuran; (2) azidotization of the double-metallated intermediate; and (3) reduction of the 4,6-*bis*(azido) product using $LiAlH_4$.

However, Maruoka's brief communication completely lacked experimental detail and compound characterization. Attempts at directed double metallation and subsequent azidotization using Maruoka's protocol showed only moderate success in our hands – with less than ideal selectivity for the 4,6–*bis*(azido) vs. the 4-*mono*(azido) product (Equation 3.17). Subsequent trials involved varying the temperature of the double metallation step (from 0 to -78 °C) and changing reagent concentrations, but no increase in selectivity was found.

Equation 3.17 - Synthesis of 4,6-*bis*-(azido)dibenzofuran from tosyl azide.

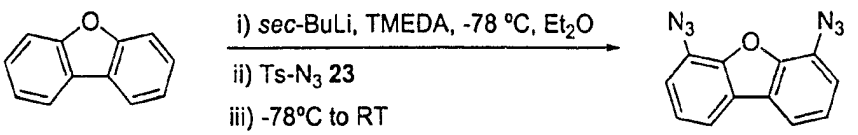

60% **24**

Using a directed *ortho*–metallation and subsequent azide quench, Greco and co-workers[48,49] studied azido transfers on 3,4-disubstituted indoles. Commenting on Greco's work, Scriven suggested[50] that the mechanism of azido transfer may be driven by the reduction at sulfur (Scheme 3.8).

Scheme 3.8 - Scriven's suggested mechanism of azide transfer.[50]

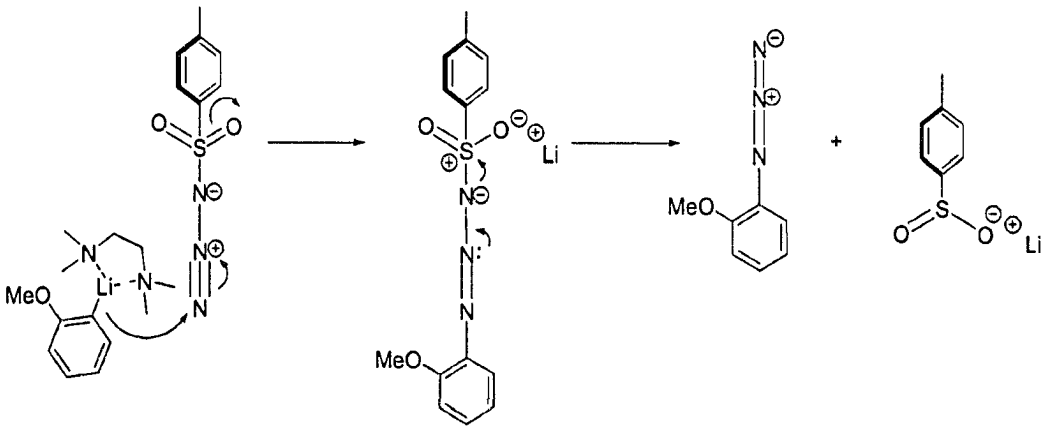

I

Zanirato,[51] however, suggests the azido transfer mechanism follows the decomposition of the triazene lithium salt **I** (Scheme 3.8). If we to considered another resonance form for the intermediate **II** (Scheme 3.9), other degradation pathways become possible, especially if an aqueous work-up may favour the thermodynamic elimination of N_2 (**III** through **V** Scheme 3.9).

Scheme 3.9 - Degradation pathways of a triazene lithium salt

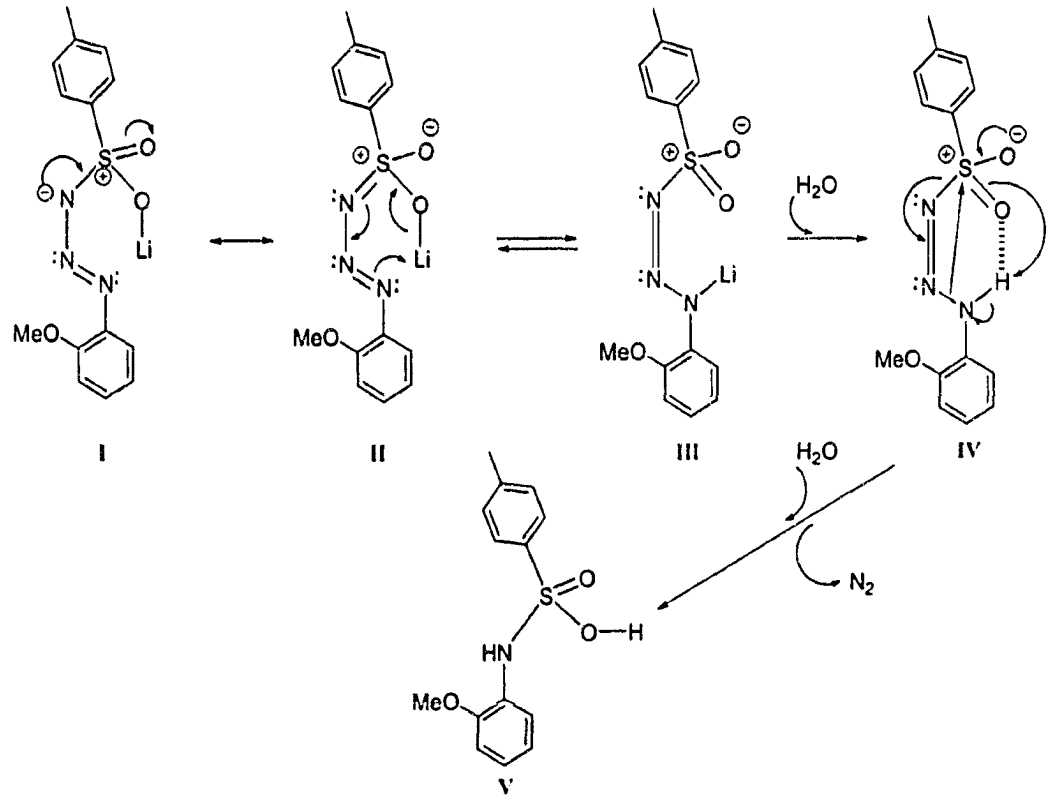

An analogous four membered intermediate **VI** (Scheme 3.10) is thought to occur in the reaction of an azide with triphenylphosphine,[52,53] with the elimination of N_2 occuring via a four–membered transition state.

Scheme 3.10 - Reaction of an azide with triphenylphosphine.

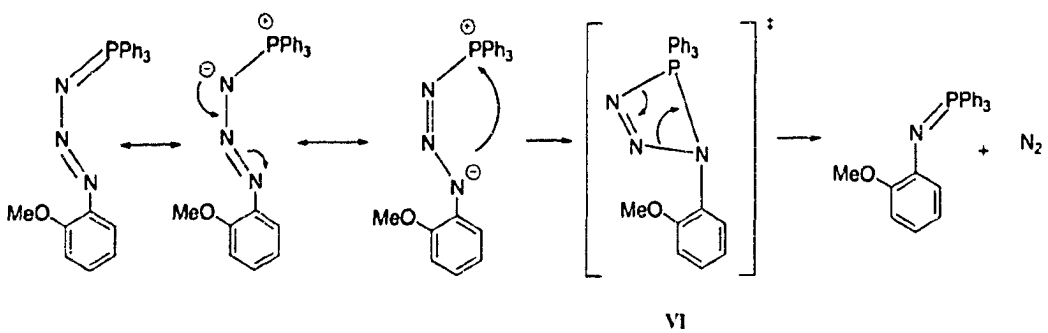

In all our trials, no examination of the crude reaction mixtures was undertaken. No release of gas was observed during the aqueous work–up, which might be expected should degradation be occuring in the manner seen in Scheme 3.9.

3.5.1 - Other Azide Sources

In an effort to increase the selectivity for the formation of 4,6-*bis*(azido)dibenzofuran, we explored the use of other azide sources, as shown in Equations 3.18 – (a) and (b).

Equation 3.18 - Other sulfonyl azide sources

(a)

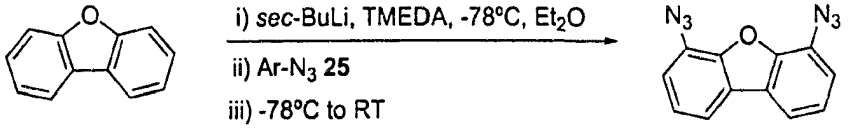

60%

24

(b)

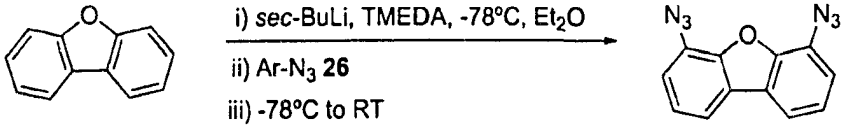

48%

24

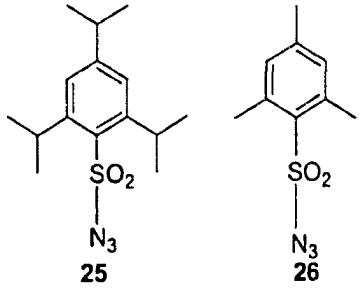

25 **26**

Although the overall yields in these reactions are comparable, more notable is the *bis* vs. *mono* selectivity, as summarized in Table 3.2.

Table 3.2 - Comparison of azide sources and *bis* vs. *mono* selectivities

Azide Source	Overall Yield	*Bis* Selectivity
Ts-N_3 - **23**	60%	1.5 : 1
Mes-N_3 - **25**	60%	4 : 1
Tris-N_3 - **26**	48%	2.13 : 1

Although the desired selectivity for 4,6-*bis*(azido)dibenzofuran could be affected in the order of **25** > **26** ≥ **23**, a qualitative examination into the relative conversion rates was not completed and it is not clear how these preferences are realized.

The selectivity differences observed for azido transfer may also be consistent with competing intermolecular *lateral*-lithiation reactions (Equation 3.19), where the acidity differences and/or steric access to the lateral position of the sulfonyl group are expected to be in the order of Ts>Mes≥Tris. Should this competition indeed be relevant, our results would be consistent with such expectations.

Equation 3.19 - Possible competing intermolecular *lateral*-lithiations

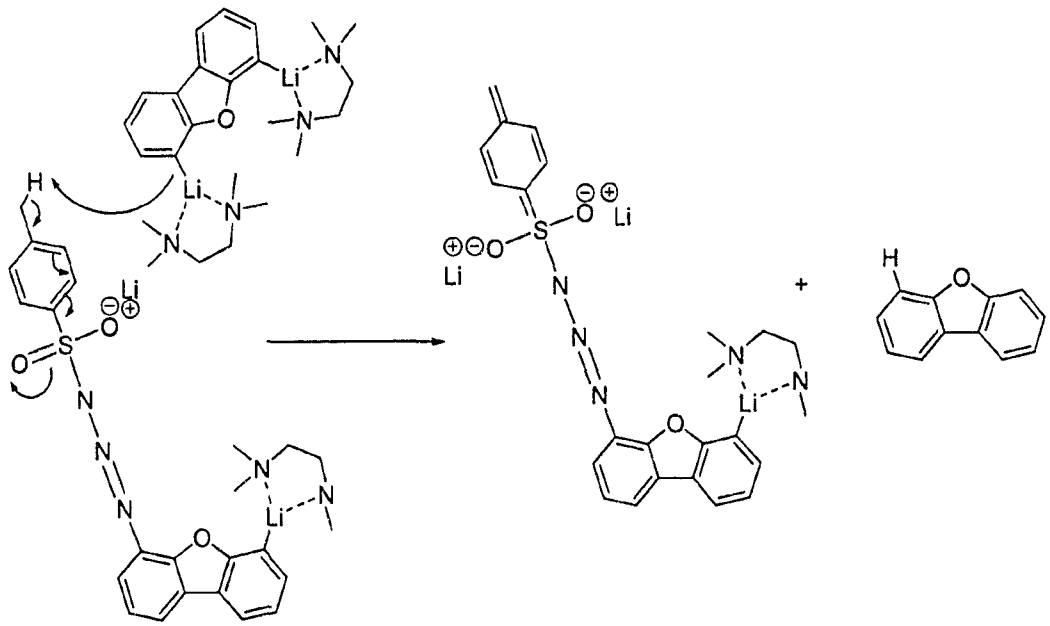

In addition to varying the azide source in the 4,6-*bis*(azido)dibenzofuran formation, we sought also to reduce the cost of reagents by exploring other alkyllithium sources.

3.5.2 - Coordinated amine and alkyllithium sources

As well as the use of other alkyllithium sources, we sought to increase the overall yield and selectivity for the *bis*(azide) over the *mono*(azide) by substituting TMEDA with another lithium sequestering reagent. It has been suggested by Bauer[54] that at low temperature, anisole and *n*-BuLi exist as a tetrameric aggregate (**a** – Scheme 3.11), and that upon addition of one equivalent of

TMEDA, a 1:1 *n*-BuLi•TMEDA dimer and free anisole are formed **(b)**. Bauer suggests that coordination sites at Li are then slowly taken up by the anisole oxygen, accompanied by an agostic Li–H interaction **(c)**. Irreversible deprotonation follows to give the *ortho*-lithiated species **(d)** and the *n*-BuLi•TMEDA **(e)**, both of which then undergo aggregation.

Scheme 3.11 - Suggested mechanism of aggregation and directed ortho metallation for an anisole, *n*-BuLi and TMEDA system

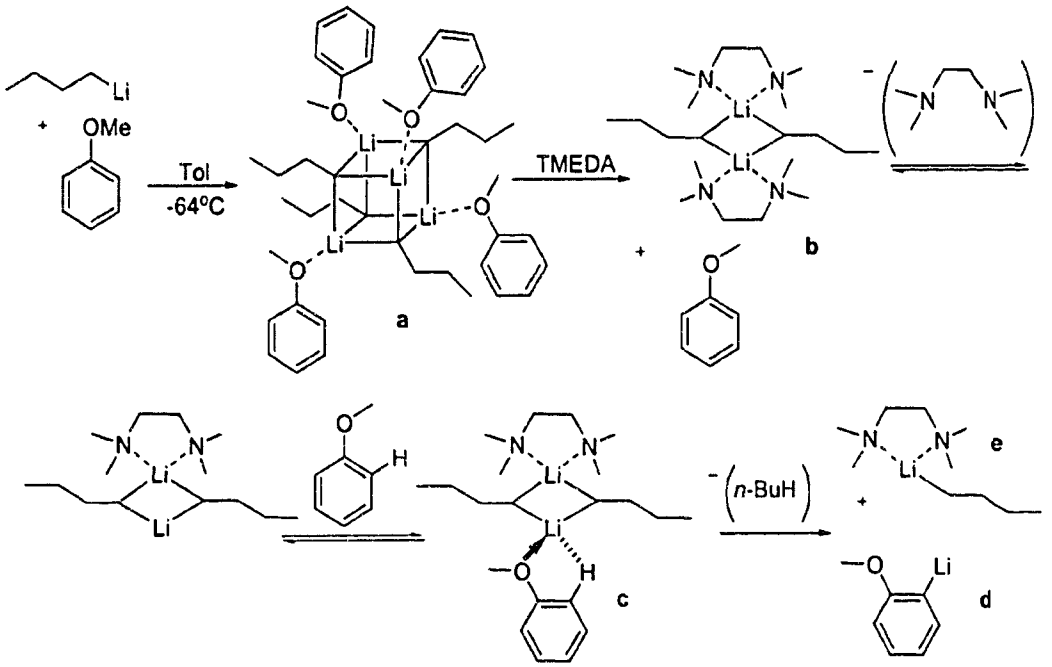

MNDO calculations[54] support the formation of structure **c**, suggesting that both kinetic and thermodynamic factors play significant roles in the directed ortho metallation process.

Based on this analysis, any agostic lithium–oxygen interactions in the deprotonation of dibenzofuran could be interrupted by the use of a tridentate

coordinating reagent such as PMDETA. However, the distance of the furan oxygen from lithium in either the 4– or 6–positions suggests that no agostic interaction is possible.

In trials with PMDETA, we found that we could effect the formation of 4,6-*bis*(azido)dibenzofuran, using *n*-BuLi as base, with a slight increase in yield (Equation 3.20). This procedure is favoured, considering the lower cost and greater reliability of *n*-BuLi over *sec*-BuLi.

Equation 3.20 - Formation of 4,6-*bis*(azido)dibenzofuran from PMDETA and *n*-BuLi.

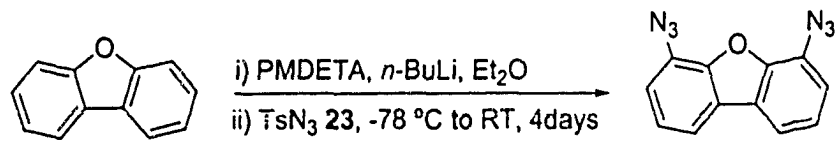

68% **24**

No azide formation (by TLC analysis) was apparent when mesitylenesulfonyl azide was used to quench the PMDETA–coordinated dilithiodibenzofuran intermediate.

Interestingly, in all trials using PMDETA or TMEDA and *sec*-BuLi or *n*-BuLi, Et_2O was the solvent that afforded the most complete conversion to desired 4,6-*bis*(azido)dibenzofuran. This observation is consistent with that of Brown,[55] who suggested that THF inhibits the rate of aggregate exchange.

It is clear that electronic effects play a more dominant role than steric effects in our ability to increase the overall *bis*-selectivity. Accordingly, we might have expected at least some *bis*–product formation from the use of mesitylene

sulfonyl azide and *n*-BuLi/PMDETA. However, the significant increase in steric bulk on the dibenzofuranyl structure imposed by the combination of PMDETA and the mesitylenesulfonyl group may dominate, inhibiting any azide transfer at all.

In other studies by Charette[56] on azide transfer to chiral enolates, the rate of azide transfer could be increased in several ways: as the enolate counterion became more electropositive ($Li^+ << Na^+ < K^+$); as the azide transfer agent became both more electron–rich and sterically demanding (*p*-nitrobenzenesulfonyl azide < tosyl azide < trisyl azide); and if the reaction quench ocurred in AcOH instead of H_2O. However, we did not explore the transmetallation of the Li ion nor did we attempt to quench with acid.

3.6 - Synthesis of sterically hindered *N*-containing ligands from 4,6-*bis*-(azido)dibenzofuran

In addition to concurrent efforts to increase the yield and *bis*(azido) selectivity, we explored the facile reduction of 4,6-*bis*(azido)dibenzofuran through classical methodology.

3.6.1 - Reduction of 4,6-*bis*(azido)dibenzofuran

The reduction of the 4,6-*bis*(azido)dibenzofuran **24** with $LiAlH_4$[47] provided our first entry into useful quantities of 4,6-*bis*(amino)dibenzofuran **27** (Equation

3.21). The conversion of **27** into sterically encumbered amines and imines then became the focus of our investigations.

Equation 3.21 - Reduction of 4,6-*bis*(azido)dibenzofuran.

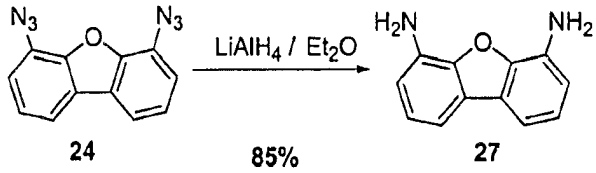

24 85% 27

3.6.2 - Hindered secondary amines by nucleophilic addition

Early attempts to add bulky alkyl substituents to the 4,6-*bis*(amino)dibenzofuran involved both Lewis acid catalyzed and classical base assisted alkylation methodologies (Equation 3.22).

Equation 3.22 - Nucleophilic addition of 4,6-*bis*(amino)dibenzofuran on *tert*-butylamine.

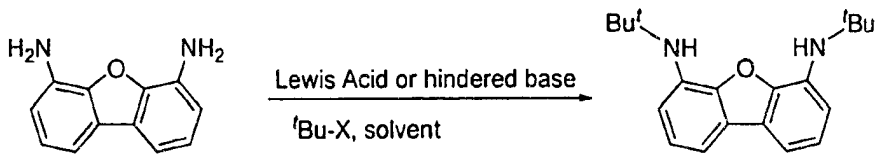

Several procedures were evaluated, with an eye to determining the most useful combination of Lewis acid, solvent, *tert*-butyl source, and hindered base. Although analysis of crude ^{1}H NMR spectra suggested little or no product formation, a summary of conditions and reagents are presented in Table 3.3.

Table 3.3 - Trial summaries of nucleophilic addition of 4,6-*bis*(amino)dibenzofuran.

Trial	Alkyl substrate	Lewis acid	Base	Solvent	Conditions
1	*tert*-butyl-Cl	$TiCl_4$	None	THF	-78 °C
2	*tert*-butyl-Cl	$TiCl_4$	None	CH_2Cl_2	-78 °C
3	*tert*-butyl-Cl	$TiCl_4$	None	1,2-dichloroethane	-78 °C
4	*tert*-butyl-Cl	None	2,4,6-tri-*tert*-butylpyridine	1,2-dichloroethane	-25 °C
5	*tert*-butyl-Cl	None	2,6-lutidine	1,2-dichloroethane	-18 °C
6	*tert*-butyl-OH	None	2,4,6-tri-*tert*-butylpyridine	1,2-dichloroethane	-25 °C
7	*tert*-butyl-Br	$SnCl_4$	None	Toluene	RT
8	TMS-Cl	None	NaH	Et_2O	0 °C
9	TMS-Cl	None	*n*-BuLi	Et_2O	-78 °C
10	TMS-Cl	None	*n*-BuLi	pyridine	RT to 80 °C, bomb
11	Ac_2O	None	None	Et_2O	RT
12	Ac_2O	None	pyridine	Et_2O	RT

Limited success was achieved following the vague precedent set by Maruoka and co-workers.[47] The alkylation with trityl cation led to some formation of the desired *bis*(tritylation) product (Equation 3.23). Unfortunately, repeated attempts to purify the crude reaction product by MPLC (SiO_2, 20 : 1 toluene / CH_2Cl_2) resulted in partial decomposition, presumably by trityl ionization.

Equation 3.23 - Addition of trityl tetrafluoroborate to 4,6-*bis*(amino)dibenzofuran

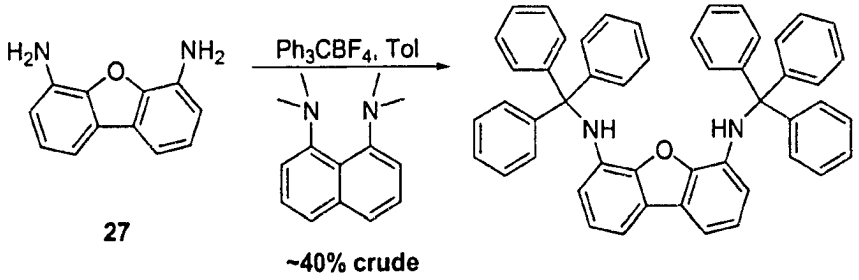

27

~40% crude

3.6.3 - Attempted reductive amination of 4,6-*bis*(amino)dibenzofuran

We next investigated classical reductive amination methodology[57,58,59,60,61] for the introduction of bulky amine substituents, treating the *bis*(amine) **27** with acetone and activated molecular sieves, followed by addition of either TMS-CN or MeLi (Equation 3.24).

Equation 3.24 - Attempted reductive amination of 4,6-*bis*(amino)dibenzofuran.

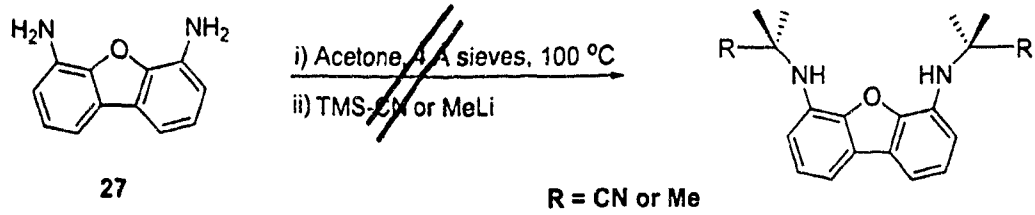

27

R = CN or Me

Monitoring the addition of MeLi (*ii* - Equation 3.24) indicated no product formation (by TLC and analysis of the crude product by ^{1}H NMR spectroscopy), consistent with the observations of Krespan,[62] who found that treatment of an acetone–derived imine with an alkyllithium suffered from competing deprotonation (Scheme 3.12).

Scheme 3.12 - Competing deprotonation of an acetone–derived imine.

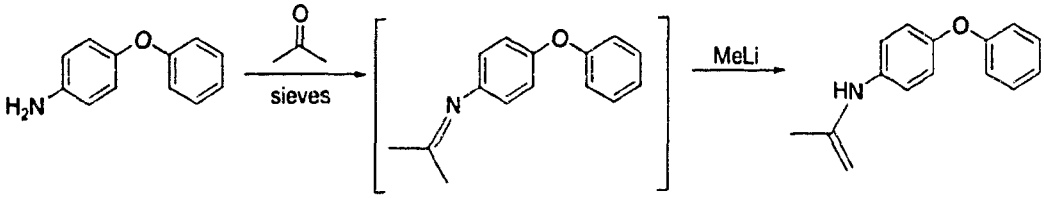

All ketone–derived imine substrates with acidic α-hydrogen atoms proved problematic in the reductive amination. We were nonetheless interested in sterically encumbered *bis*(imine) analogues as ligands themselves. Sugimura[63] and Fujita[64] reported that related arylimine–based early and late metal catalysts showed high activity for ethylene polymerization. Following a known procedure,[65] condensation of 4,6-*bis*(amino)dibenzofuran **27** with the known aldehyde **29**[66] providing 4,6-*bis*-(2-hydroxy-3-*tert*-butyl-4-methylbenzylimino)dibenzofuran **30** for ongoing investigations of coordination chemistry and catalysis. (Equation 3.25).

Equation 3.25 - Synthesis of 4,6-*bis*-(2-hydroxy-3-*tert*-butyl-4-methylbenzylimino)dibenzofuran.

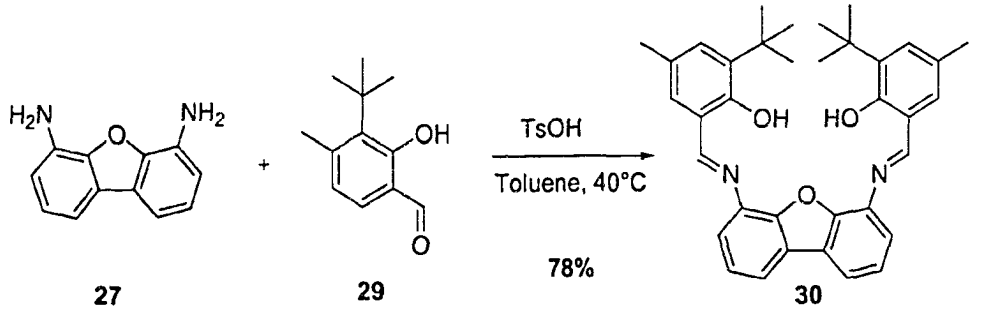

27 **29** **30**

3.7 - 4,6-*Bis*(azido)dibenzofuran and the Staudinger reaction

Thus aware of the difficulty in preparing sterically encumbered *bis*(alkylamino)dibenzofuran compounds by classical methodologies, we revisited the reactivity of 4,6–*bis*(azido)dibenzofuran formation, with specific emphasis on the *Staudinger*[67] reaction.

3.7.1 - Mechanism of the Staudinger reaction

The Staudinger reaction is the transformation of an alkyl azide with a phosphine to give an intermediate iminophosphorane, which when treated with water, decomposes to the phosphorus oxide and secondary amine (Equation 3.26). The reaction is thought to proceed without participation of free radicals or nitrene intermediates[52,53] and with retention of configuration at the phosphorous atom.[68]

Equation 3.26 - The Staudinger reaction

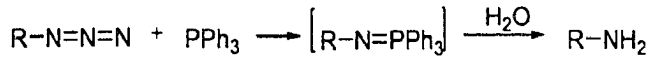

Using ^{15}N labelling, Bock and Schnoller[69,70] found that the N–R bond in a phosphazide was found to transfer to a phosphazo product without cleavage of the N–R bond (Equation 3.27).

Equation 3.27 - ^{15}N labelling and the Staudinger reaction

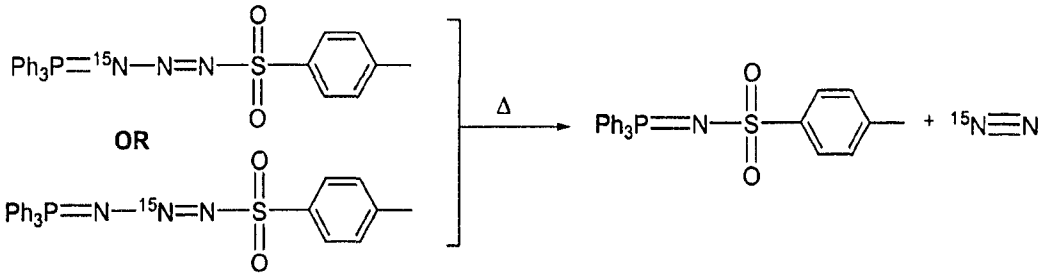

The reaction of phosphorus (III) and an azide is thought[52,71,72] to be accelerated by donor groups on the azide. The phosphazide is then believed to decompose to the iminophosphorane through an intramolecular mechanism via a 4-membered transition state[52,69] (Equation 3.28).

Equation 3.28 - Staudinger intermediate and products

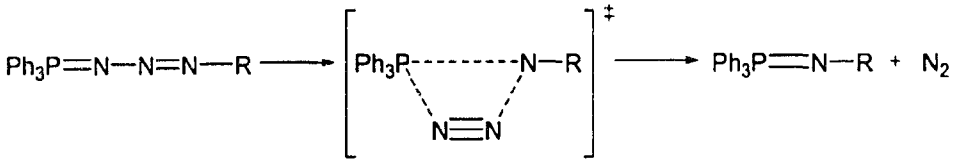

3.7.2 - Utility of the Iminophosphorane

Letsinger and coworkers[73] originally showed that a slight modification of this "one-pot" process may be used to prepare amines by hydrolysis of the iminophosphorane intermediate using ammonium hydroxide.

Iminophosphoranes are, in fact, much more valuable intermediates, undergoing *Wittig*-type reactions with aldehydes,[74] ketenes,[75] and in some cases, ketones[50,76,77] (Scheme 3.13).

Scheme 3.13 - Mechanism of iminophosphorane attack on an aldehyde[78]

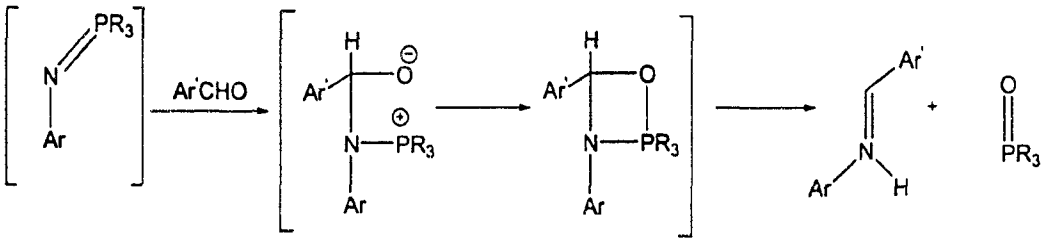

The use of the iminophosphorane to access *bis*(amine) derivatives required the 4,6-*bis*(triphenylphosphiniminyl)dibenzofuran intermediate **31**. Initial trials realized this target in excellent yield (Equation 3.29).

Equation 3.29 - Synthesis of 4,6-*bis*(triphenylphosphiniminyl))dibenzofuran

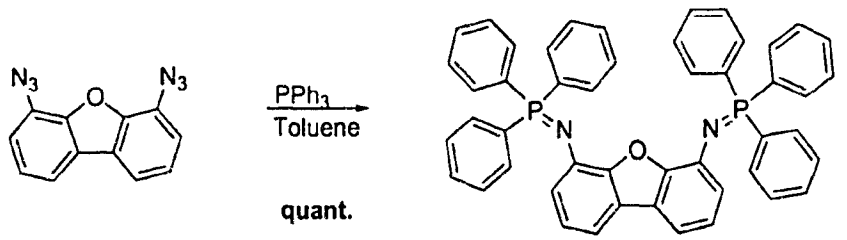

24 **31**

Although literature protocol[79] calls for Et_2O solvent, we found the substitution of toluene was more successful. Schrock[80] and others[62]

demonstrated that condensation of amines and hexafluoroacetone was effective for the synthesis of sterically demanding fluorinated *tert*-butylamines. We were thus interested in the direct reaction of the iminophosphorane **31** with hexafluoroacetone. This we were able to do, isolating the 4,6-*bis*-(1,1,1,3,3,3-hexafluoro-2-propylimino)dibenzofuran **32** in good yield (Equation 3.29), by using an excess of the gaseous ketone.

Equation 3.30 - Synthesis of 4,6-*bis*(1,1,1,3,3,3-hexafluoro-2-propylimino) dibenzofuran.

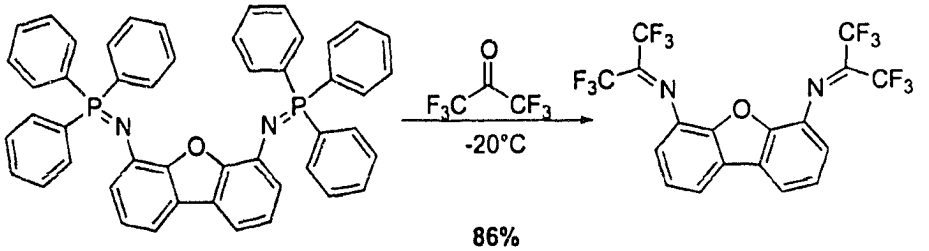

86%

31 **32**

With no possibility of competing deprotonations, the *bis*(imine) **32** was treated with MeLi or PhLi, leading to the isolation of two hindered *bis*(amine) ligand systems **33** and **34** (Equation 3.31).

Equation 3.31 - Synthesis of (a) 4,6-*bis*-(1,1,1,3,3,3-hexafluoro-2-methyl-2-propylamino)dibenzofuran **33** (b) 4,6-*bis*-(1,1,1,3,3,3-hexafluoro-2-phenyl-2-propylamino)dibenzofuran **34**.

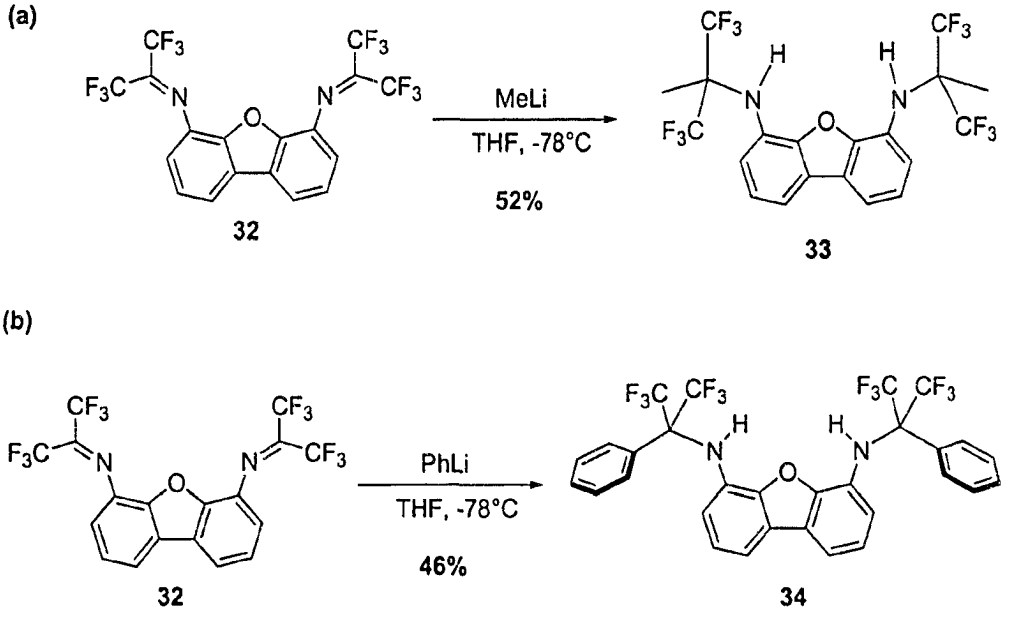

Most appealing is the versatility of this procedure. The entire sequence can be done *in situ*, directly converting 4,6-*bis*(azido)dibenzofuran **24** to the final *bis*(amine) product in reasonable yield (Scheme 3.14).

Scheme 3.14 - One pot synthesis of 4,6-*bis*-(1,1,1,3,3,3-hexafluoro-2-methyl-2-propylamino)dibenzofuran.

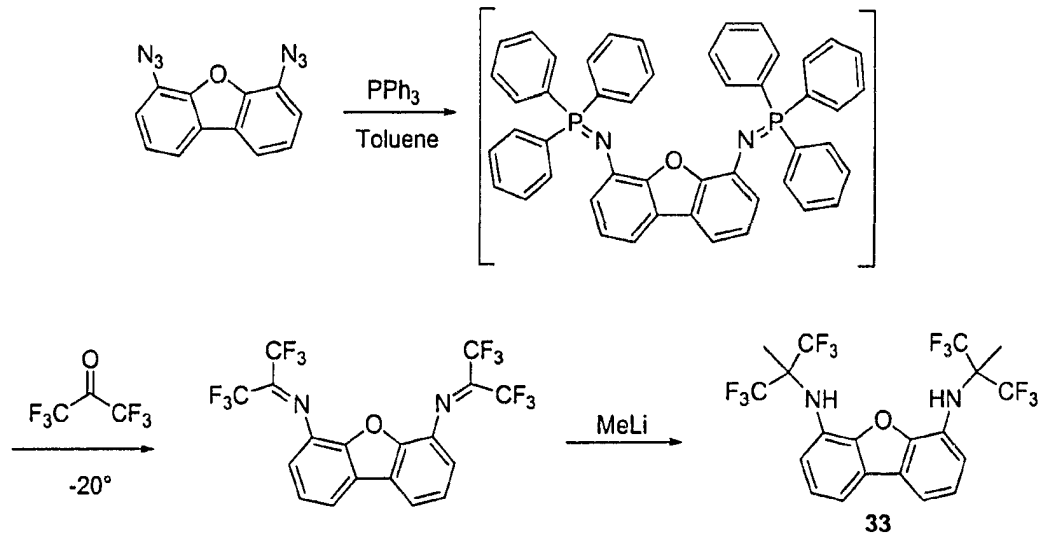

45% overall

Bis(alkylamines) structures **33** and **34** were confirmed in the solid state by X-ray crystallography (see Appendix A for complete reports). Structure **33** (Figure 3.4) is consistent with expectation, with the hexafluoro–*tert*-butyl groups found on opposite sides of the dibenzofuranyl plane, minimizing their interaction. Interestingly, the phenyl analogue **34** was not found in this arrangement (Figure 3.5). Rather, the phenyl groups are seen on the same side of the dibenzofuranyl plane. Each demonstrates the potential of this pre-organized ligand design, with the sterically encumbered alkyl amino environments presenting a unique, hindered environment for coordinating early or late metals.

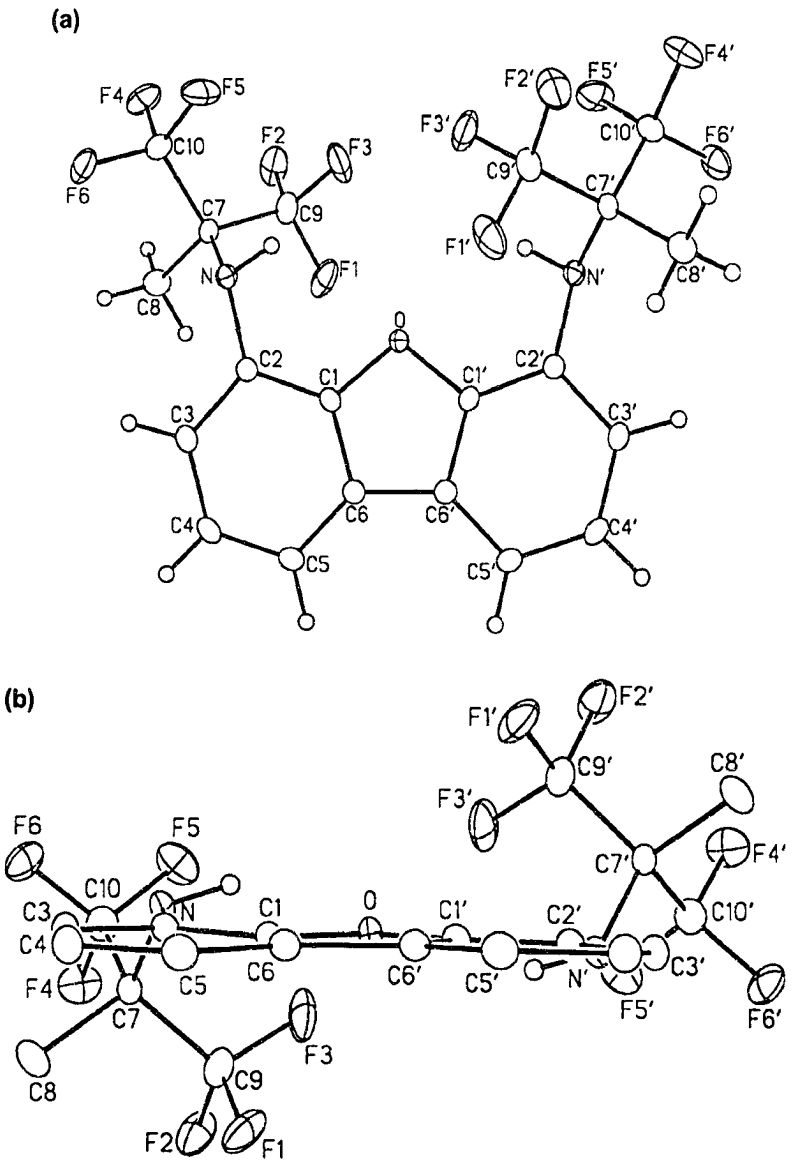

Figure 3.4 - (a) Front and (b) edge–on Ortep diagrams of hindered amine **33**. Non-hydrogen atoms are represented by Gaussian ellipsoids at the 20% probability level. Hydrogen atoms are shown with arbitrarily small thermal parameters.

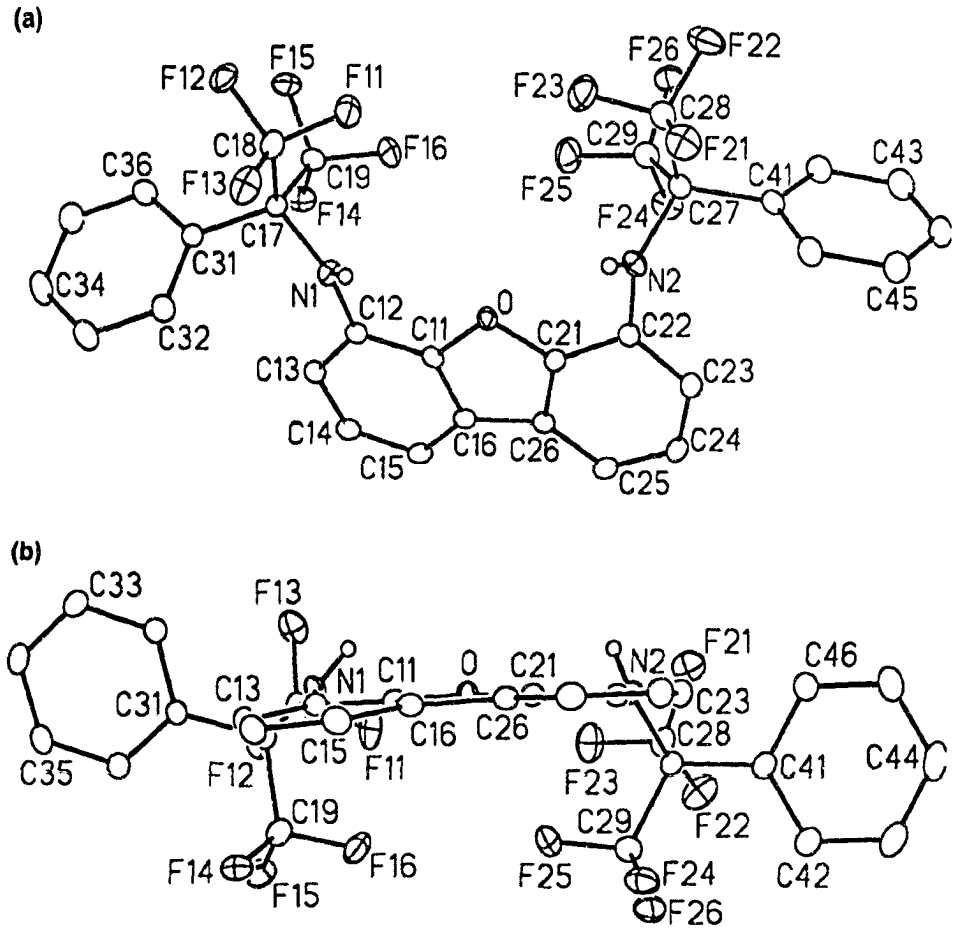

Figure 3.5 - Front (a) and side view (b) Ortep diagrams of hindered amine **34** Non-hydrogen atoms are represented by Gaussian ellipsoids at the 20% probability level. The hydrogen atoms of the amino groups are shown with arbitrarily small thermal parameters; all other hydrogens are not shown.

We also sought to save a step in the synthesis of the *bis*(imine) **31** (Equation 3.25), by adopting Staudinger methodology. Thus quenching the *bis*(iminophosphorane) **24** with aldehyde **29** afforded the desired *bis*(imine) **27** in moderate yield (Equation 3.32).

Equation 3.32 - Staudinger mediated synthesis of 4,6-*bis*-(2-hydroxy-3-*tert*-butyl-4-methylbenzylimino)dibenzofuran.

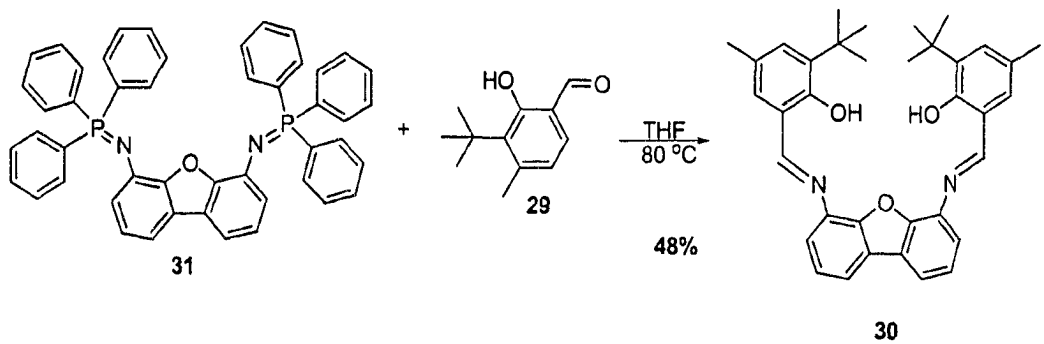

31 29 30

We investigated the applicability of this procedure to other carbonyl substrates. Unfortunately the reaction with pentafluoroacetophenone gave no imine formation in repeated trial reactions. However, using a more electron–rich phosphine in the Staudinger reaction, increased reactivity of the intermediate iminophosphorane was observed. The reaction of tricyclohexylphosphine (PCy_3) with 4,6-*bis*(azido)dibenzofuran provided the intermediate *bis*(iminophosphorane) (Scheme 3.15), which, when condensed with pentafluoroacetophenone and followed directly by treatment with MeLi, gave some product formation, which by ^1H NMR spectroscopic analysis of the crude material suggested the formation of *bis*(amine) (Scheme 3.15).

Scheme 3.15 - Attempted synthesis of 4,6-*bis*(1-pentafluorophenyl-3-aceto-propylamino)dibenzofuran.

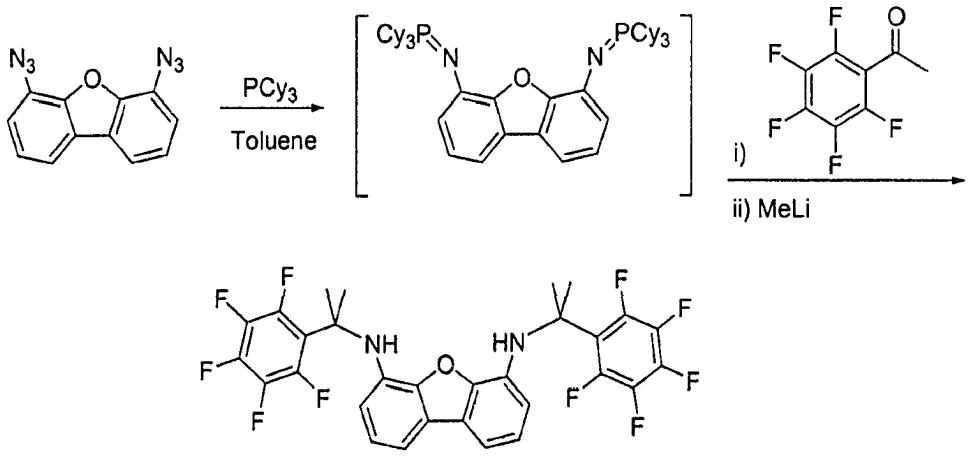

~40% crude

However, all attempts to use other activated ketones, such as trifluorobenzophenone (eg. Scheme 3.16) were not successful. In other trials, the prior addition of a Lewis acid ($SnCl_4$, $TiCl_4$) to activate the ketone substrate (pentafluorophenylacetone) showed no improvement, giving no product formation upon treatment with alkyllithium.

Scheme 3.16 - Attempted synthesis of 4,6-*bis*(1,3-phenyl-2-methyl-propylamino) dibenzofuran.

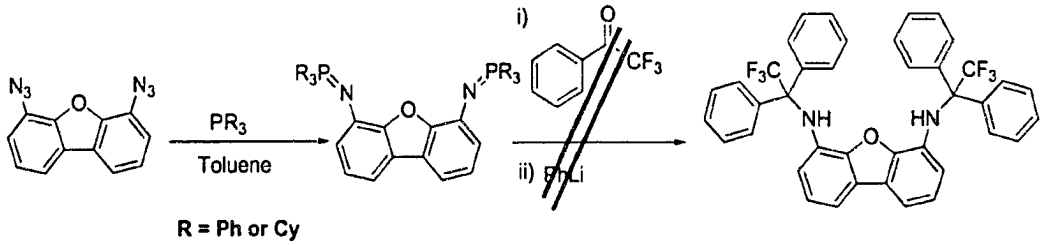

R = Ph or Cy

The literature has little to reveal about the relative nucleophilicity of iminophosphorane substrates. However, recent reports from Charette[81] on the reaction of trimethylsilyl azide with PMe_3 underline the utility of using electon–rich phosphines in Staudinger methodology.

3.8 - Conclusion and Future Work

With an efficient route now available to sterically encumbered *bis*(imino) and *bis*(amino) compounds, a detailed investigation of respective early and late transition metal coordination chemistry and catalysis is possible.

Directed double metallation of dibenzofuran can be effected using less costly and more reliable alkyllithium sources in combination with coordinating amines. An examination of other azide transfer reagents and work-up methodology will direct efforts to improve the yield and *bis*–selectivity in the synthesis of 4,6-*bis*(azido)dibenzofuran.

The use of the Staudinger process has shown excellent utility in the preparation of secondary amines. Future investigations will undoubtedly be concerned with exploring other electron–rich phosphines in the preparation of iminophoshoranes capable of condensing with novel carbonyl sources.

Notes and References

---

[1] Dzwiniel, T. *unpublished results.*

[2] Bruson, H.; Kroege, J. *J. Am. Chem. Soc.* **1940**, *1*, 36-44.

[3] Abbott, R. US Patent 2,500,732. Mar. 14, 1950.

[4] Chan, D.; Monaco, K.; Wang, R-P.; Winters, M. *Tetrahedron Lett.* **1998**, *39*, 2933-2936.

[5] Lam, P.; Clark, C.; Saubern, S.; Adams, J.; Winters, M.; Chan, D.; Combs, A. *Tetrahedron Lett.* **1998**, *39*, 2941-2944.

[6] Evans, D.; Katz, J.; West, T. *Tetrahedron Lett.* **1998**, *39*, 2937-2940.

[7] Hartwig, J. *Angew. Chem. Int. Ed. Engl.* **1998**, *37*, 2046-2067.

[8] Enguehard, C.; Allouchi, H.; Gueiffier, A.; Buchwald, S. *J. Org. Chem.* **2003**, *68*, 4367-4370.

[9] Kwong F.; Buchwald, S. *Org. Lett.* **2003**, *5*, 793-796.

[10] Klapars A.; Huang X.; Buchwald, S. *J. Am. Chem. Soc.* **2002**,*124*, 7421-7428.

[11] Kwong F.; Klapars, A.; Buchwald, S. *Org. Lett.* **2002**, *4*, 581-584.

[12] Klapars, A.; Antilla, J.; Huang, X.; Buchwald, S. *J. Am. Chem. Soc.* **2001**, *123*, 7727-7729.

[13] Antilla, J.; Buchwald, S. *Org. Lett.* **2001**,*3*, 2077-2079.

[14] Kiyomori, A.; Marcoux, J.; Buchwald, S. *Tetrahedron Lett.* **1999**, *40*, 2657-2660.

[15] Cundy, D.; Forsyth, S. *Tetrahedron Lett.* **1998**, *39*, 7979-7982.

[16] *"S. Buchwald, personal communication, June, 2001."*

[17] Kiyomori, A.; Marcoux, J.; Buchwald, S. *Tetrahedron. Lett.* **1999**, *40*, 2657-2660.

[18] Tsang, K.; Diaz, H.; Graciani, N.; Kelly, J. *J. Am. Chem. Soc.* **1994**, 116, 3988-4005.

[19] Bacon, R. G. R.; Karim, A. *J. Chem. Soc., Perkin Trans. I* **1973**, 272-278.

[20] Yamashiro, S. *Bull. Chem. Soc. Jpn.* **1941**, *16*, 61-67.

[21] Keumi, T.; Yamada, H.; Takashashi,; Kitajima, H. *Bull. Chem. Soc. Jpn.* **1962**, *55*, 629-634.

[22] de la Breteche, M.; Billion, M.; Ducrocq, C. *Bull. Soc. Chim. Fr.* **1996**, *133*, 973-977.

[23] Bruson, H.; Kroege, J. *J. Am. Chem. Soc.* **1940**, *62*, 36-43.

[24] Abbott, R. US Patent 2,500,732, **1950.**

[25] Monsanto Chemicals Ltd., French Patent 1,351,472, **1964.**

[26] Tashiro, M.; Watanabe, H.; Tsuge, O. *Org. Prep. Proced. Int.* **1974**, *6*, 117.

[27] Tashiro, M.; Yamato, T.; Kobayashi, K.; Arimura, T. *J. Org. Chem.* **1987**, *52*, 3196-3199.

[28] Tashiro, M. *Synthesis* **1979**, 921-926.

[29] Yamato, T.; Arimura, T.; Tashiro, M. *J. Chem. Soc., Perkin. Trans. 1*, **1987**, 1-7.

[30] Eaborn, C.; Salih, Z.; Walton, D. *J. Chem. Soc. Perkin Trans. 2* **1972,** 172-179.

[31] Yamato, T.; Hasegawa, K.; Saruwatari, Y.; Doamekpor, L. *Chem. Ber.* **1993**, *126*, 1435-39.

[32] Aarts, V.; Grootenhuis, P.; Reinhoudt, D.; Czech, A.; Czech, B.; Bartsch, R. *Recl. Trav. Chim. Pays Bas* **1988**, *107*, 94-103.

[33] Sartori, G.; Maggi, R.; Bigi, F.; Grandi, M. *J. Org. Chem.* **1993**, *58*, 7271-7273.

[34] Ullmann, F. *Ber. Dtsh. Chem. Ges.* **1903**, *36*, 2382-2384.

[35] Higginbottom, R.; Suschitzky, H. *J. Chem. Soc.* **1962**, *2*, 2367.

[36] Zeller, K.; Berger, S. *J. Chem. Soc. Perkin Trans. 2* **1977**, 54.

[37] Lindley, J. *Tetrahedron* **1984**, *40*, 1433-1456.

[38] Goodbrand, H.; Hu, N. *J. Org. Chem.* **1999**, *64*, 670-674.

[39] Jones, L.; Foster, J. *J. Org. Chem.* **1970**, *35*, 1777-1781.

[40] Colle, T.; Lewis, E. *J. Am. Chem. Soc.* **1979**, *101*, 1810-1813.

[41] Yamato, T.; Komine, M.; Nagano, Y. *OPPI Briefs.* **1997**, *29*, 301-314.

[42] Vogel's Textbook of Practical Organic Chemistry, 5th edition. London: Longman Scientific and Technical, 1989, pg 1254.

[43] Prasad, V.; Panapoulous, A.; Rubin, J. *Tetrahedron Lett.* **2000**, *41*, 4065-4068.

[44] Whitesides, G.; Sadowski, J.; Lilburn, J. *J. Am. Chem. Soc.*, **1974**, *96*, 2829-2835.

[45] Brewster, R.; Groering, T. *Org. Synthesis*, Col. Vol. II, 445.

[46] Wassmundt, F.; Pedemonte, R. *J. Org. Chem.* **1995**, *60*, 4991-4994.

[47] Hanawa, H.; Kii, S.; Maruoka, K. *Adv. Syn. Cat.* **2001**, *343*, 1, 57-60.

[48] Kozikowski, A.; Greco, M. *Tetrahedron Lett.* **1982**, *23*, 2005.

[49] Kozikowski, A.; Greco, M. *J. Org. Chem.* **1984**, *49*, 2310.

[50] Scriven, E.; Turnbull, K. *Chem. Rev.* **1988**, *88*, 297-362.

[51] Spagnolo, P.; Zanirato, P.; Gronowitz, S. *J. Org. Chem.* **1982**, *47*, 3177.

[52] Leffler, J.; Temple, *J. Am. Chem. Soc.* **1967**, *89*, 5235-5245.

[53] Goldwhite, H.; Gysegem, P.; Schow, S.; Swyke, C. *J. Chem. Soc. Dalton Trans.* **1975**, *1*, 16-18.

[54] Bauer, W.; Schleye, P. *J. Am. Chem. Soc.* **1989**, *111*, 7191-7198.

[55] Brown, T. *Pure Appl. Chem.* **1970**, *23*, 447-454.

[56] Evans, D.; Britton, T. *J. Am. Chem. Soc.* **1987**, *109*, 6881-6883.

[57] Mai, K.; Patil, G. *Syn .Commun.* **1985**, *15*, 157-164.

[58] Gmeiner, P.; Kartner, A.; Junge, D. *Tetrahedron Lett.* **1993**, *34*, 4325-4326.

[59] Hunter, D.; Racok, J.; Rey, A.; Ponce, Y. *J. Org. Chem.* **1988**, *53*, 6, 1278-1281.

[60] Baumann, R.; Davis, W.; Schrock, R. *J. Am. Chem. Soc.* **1997**, *119*, 3830-3831.

[61] Buchmeiser, M.; Schrock, R. *Inorg. Chem.* **1995**, *34*, 3553-3554.

[62] Middleton, W.; Krespan, C. *J. Org. Chem.* **1965**, *30*, 1398-1402.

[63] Sugimura, K.; Ban, K.; Suzuki, Y.; Hayashi, T. Jpn. Laid-Open Appl. 09/302021, **1997**.

[64] Fujita, T.; Tohi, Y.; Mitani, M.; Matsui, S.; Saito, M.; Nitabaru, M.; Sugi, K.; Makio, H.; Tsutsui, T. (Mitsui Chemicals, Inc.), *EP 0874005*, **1998.**

[65] Mitani, M.; Mohri, J.; Yoshida, Y.; Saito, J.; Ishii, S.; Tsuru, K.; Matsui, S.; Furuyama, R.; Nakano, T.; Tanaka, H.; Kojoh, S.; Matsugi, T.; Kashiwa, N.; Fujita, T. *J. Am. Chem. Soc.* **2002**, *124*, 3327-3326.

[66] Higginbottom, R.; Suschitzky, R. *Chem. Eur. Jour.* **1996**, *2*, 974-980.

[67] Staudinger, H.; Meyer, J. *Helv. Chim. Acta.* **1919**, *2*, 635.

[68] Horner, L.; Winkler, H. *Tetrahedron Lett.* **1964**, *5*, 175-179.

[69] Bock, H.; Schnoller, M. *Angew. Chem.* **1968**, *80*, 667-672.

[70] Bock, H.; Schnoller, M. *Chem. Ber.* **1969**, *102*, 38-42.

[71] Horner, L.; Gross, A. *Liebigs Ann.* **1955**, *117*, 591-596.

[72] Leffler, J.; Tsuno, Y. *J. Org. Chem.* **1963**, *28*, 902-906.

[73] Mungall, W.; Greene, G.; Heavner, G.; Letsinger, R. *J Org. Chem.* **1975**, *40*, 1659-1662.

[74] Schmidbaur, H.; Jonas, G. *Chem Ber.* **1967**, *100*, 1120-1124.

[75] Shaw, R.; Fitzsimmons, B.; Smith, B. *Chem. Rev.* **1962**, *62*, 247-280.

[76] Wiberg, N.; Schwenk, G.; Schmid, K. *Chem Ber.* **1972**, *105*, 1209-1214.

[77] Boezio, A.; Solberghe, G.; Lauzon, C.; Charette, A. *J. Org. Chem.* **2003**, *68*, 3242-3245.

[78] Gololobov, Y.; Zhnurova, I.; Kasukin, F. *Tetrahedron* **1981**, *32*, 437-472.

[79] Richard, J. *J. Org. Chem.* **1992**, *57*, 625-629.

[80] Buchmeiser, M.; Schrock, R. *Inorg. Chem.* **1995**, *34*, 3553-3554.

[81] Boezio, A.; Solberghe, G.; Lauzon, C.; Charette, A. *J. Org. Chem.* **2003**, *68*, 3242-3245.

Chapter 4 - Experimental

Instruments and Analysis: Nuclear Magnetic Resonance (NMR) spectra for ^{1}H and ^{13}C nuclei were recorded on a Varian Unity-Inova 300 (^{1}H, 300 MHz), Varian Unity-Inova 500 (^{1}H, 500 MHz) or Varian Unity-Inova 400 (^{1}H, 400 MHz) spectrometer. ^{19}F NMR spectra were recorded on a Varian Unity-Inova 400 (^{19}F, 400 MHz) spectrometer. NMR spectra were obtained at 27°C (300 K) unless otherwise noted. Chemical shifts (ppm, δ) are reported relative to tetramethylsilane (TMS) standard, and coupling constants (J) are reported in Hz. 'Apparent' coupling constants such as a doublet of doublets appearing as triplets are reported as J_{obs} or J. Assignment of quaternary (4°) or tertiary (3°) for aromatic carbons in ^{13}C NMR spectroscopy is tentative and based on relative intensity of signals in broadband ^{1}H-decoupled spectra. High resolution mass spectra were obtained on a Kratos MS-50 spectrometer (electron impact ionization (EI)) and elemental analyses were performed by the University of Alberta Microanalysis Laboratories. FTIR spectra were obtained on Nicolet Magna IR 750 or Nicolet 20SX spectrophotometer. Single crystal X-ray diffraction studies were performed in the X-ray Crystallography Laboratory at the University of Alberta Department of Chemistry by Dr. Robert McDonald and Dr. Mike Ferguson. Details of structure determinations are included in the Appendix.

Reaction Conditions: All manipulations on air sensitive compounds were performed under an argon or nitrogen atmosphere using standard Schlenk techniques, or in a Vacuum Atmospheres He-553-2 Dri-lab equipped with a Mo-41-1 inert gas purifier and a CD-882 Dri-Cold Freezer maintained at –35°C.

Thin Layer Chromatography (Silica Gel 60 F-254) was visualized by quenching of UV induced fluorescence or phosphomolybdic acid reagent. Flash chromatography and MPLC (Medium Pressure Liquid Chromatography) were performed on silica gel 60 (230-400 mesh, Silicycle). MPLC was performed using a FMI Lab Pump Model RP-SYX using standard Michel-Millar Teflon adaptors. Celite filtrations were performed using Celite 545 on a fritted glass funnel under vacuum. Flasks for moisture or air sensitive reactions were either flame-dried immediately before use or placed in a 120 °C oven overnight before use. Cylindrical Pyrex vessels equipped with Kontes k-826510 Teflon stopcocks are referred to as "reaction bombs."

Materials: Unless indicated otherwise, all solvents and reagents were purchased from commercial vendors and used as received. Sensitive materials were kept and used under appropriate conditions to maintain quality. The following solid materials were purified before use: commercial dibenzofuran (technical, 90%) was dissolved in a minimum volume of dry CH_2Cl_2, passed through a silica plug, evaporated, and recrystallized in the cold from dry tetrahydrofuran (THF); dihydrodicyanobenzoquinone (DDQ) and chloranil were recrystallized from dry THF. The following solvents/liquid reagents were dried and stored as indicated before use: benzene, THF, diethyl ether (Et_2O), hexane, and pentane were distilled from sodium benzophenone ketyl; toluene was distilled over sodium and degassed; trimethylsilyl chloride (TMS–Cl) was held at reflux for 4h over CaH_2 before collecting: acetone was stirred over boric anhydride (B_2O_3) for 2h, then distilled and used immediately; acetonitrile (MeCN)

was distilled from CaH_2 freshly before use; 1,2-dichloroethane was passed through neutral alumina and stored over activated 4 Å molecular sieves under N_2; *para*-toluenesulphonyl (Ts) azide was prepared from TsCl and NaN_3 according to published procedure[1] and purified by dissolving the TsN_3 in dry, degassed Et_2O and then passing it through a plug of alumina; *tert*-butylamine ($^tBuNH_2$) was distilled from solid NaOH and pyridine was distilled from solid KOH before use. 2,6-Lutidine was distilled from $AlCl_3$ and then redistilled. Tetramethylethylenediamine (TMEDA) and pentamethyldiethylenetriamine (PMDETA) were freshly distilled from metallic sodium before use; 2,5-dimethyl-2,5-dichlorohexane was prepared by dissolving 2,5-dihydroxy-2,5-dimethylhexane in concentrated HCl followed by bubbling HCl gas through the solution. 2,4,6,8-tetrakis(*tert*-butyl)dibenzofuran was prepared by Trevor Dzwiniel in the Stryker group.[2] The following compounds were prepared according to or by adaptation of literature protocols: trimethylsilyliodide[3]; copper(II) acetate[4]; $Pd(dba)_2$[5]; 4,6-*bis*(iodo)dibenzofuran[6]; 4-*tert*-butyl-bromobenzene[7,8,9]; 4-*tert*-butyl-2-nitro-bromobenzene[10,11,12]; 4,4'-di-*tert*-butyl-2-nitro-diphenylether[13]; 2-hydroxy-3-*tert*-butyl-5-methyl-benzaldehyde[14].

1,1,4,4,8,8,11,11-octamethyl-1,2,3,4,8,9,10,11-octahydro-5,7-dihydroxy-dinaphtho[2,3-b;2',3'-d]furan (1)

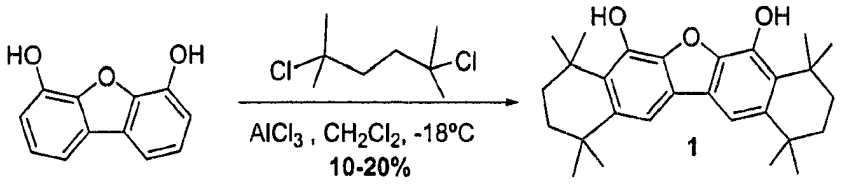

To a solution of 4,6-*bis*(hydroxy)dibenzofuran (0.500 g, 2.5 mmol) and 2,5-dichlorodimethylhexane (1.008 g, 5.5 mmol, 2.2 eq.) in CH_2Cl_2 (5 mL) at -18 °C under N_2 was added slowly by canula a suspension of $AlCl_3$ (1.363 g, 10.5 mmol) in CH_2Cl_2. The mixture was allowed to warm to RT and monitored by TLC. After stirring 48 h, additional aliquots of CH_2Cl_2 (15 mL), $AlCl_3$ (0.200 g) and dichlorodimethylhexane (0.250 g) were added. The reaction was quenched by slow addition of H_2O (20 mL) after 48 h. The organics fraction was separated and the aqueous phase extracted with CH_2Cl_2 (3 x 15 mL). The organic fractions were combined, washed with H_2O (15 mL), dried over Na_2SO_4 and evaporated in vacuo to yield a crude mixture **1**,1,4,4,8,8,11,11-octamethyl-1,2,3,4,8,9,10,11-octahydro-5,7-dihydroxy-dinaphtho[2,3-b;2',3'-d]furan **1** (~108 mg, 10-20%) and other uncharacterised products. ^1H NMR (300 MHz, $CDCl_3$): 7.77 (s, 2H, H1/H9), 1.82-1.65 (2 m, 8H, CH_2), 1.76 (s, 6H, CH_3), 1.30 (s, 6H, CH_3).

1,1,4,4,8,8,11,11-octamethyl-1,2,3,4,8,9,10,11-octahydro-dinaphtho[2,3-b;2',3'-d]furan (3)

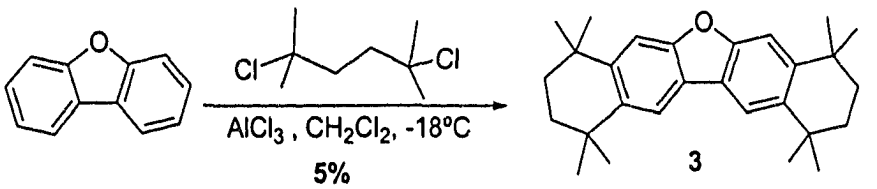

The following is an adaptation of a published preparation.[15]

To a solution of dibenzofuran (1.00 g, 5.95 mmol) and 2,5-dichloro-2,5-dimethylhexane (2.4 g, 13.1 mmol, 2.2 eq) in CH_2Cl_2 (10 mL) at –18 °C under N_2 was added slowly by canula a suspension of anhydrous $AlCl_3$ (3.600 g, 27.0 mmol, 4.5 eq) in CH_2Cl_2 (10 mL) under N_2. Resultant suspension was allowed to warm to RT overnight. Reaction was monitored by TLC for the disappearance of starting material and quenched after 22.5 h with the dropwise addition of H_2O (15 mL). The products were extracted with CH_2Cl_2 (3 x 15 mL), dried over Na_2SO_4 and evaporated in vacuo to yield a crude mixture of products. These were separated by MPLC (silica, 2 x 30 cm, cyclohexane). Fractions containing the desired product were combined and the solvent evaporated in vacuo. Recrystallization from cyclohexane/pentanes yielded 1,1,4,4,8,8,11,11-octamethyl-1,2,3,4,8,9,10,11-octahydro-dinaphtho[2,3-b;2',3'-d]furan **3** (113.4 mg, 5%) as an yellow oil. R_f = 0.25 (1 : 1 - cyclohexane : TBME). IR (CH_2Cl_2, cast) 2959 (s), 2922 (s), 2858 (s), 1617 (m), 1485 (s), 1470 (m), 1419 (s), 1360 (s), 1280 (m), 1200 (s), 1156 (s) cm^{-1}. ^1H NMR (300 MHz, acetone-d_6): δ 8.06 (s, 2H, H1/H9), 7.48 (s, 2H, H4/H6), 1.78 (s, 8H, CH_2), 1.37 (s, 12H, CH_3), 1.36 (s,

12H, CH_3) HRMS (EI) *m/z* : Calcd for $C_{28}H_{36}O$: 388.27661. Found 388.27659 (100.00 %) [M^+].

1,1,4,4,8,8,11,11-octamethyl-4,6-*bis*(nitro)dibenzofuran (4)

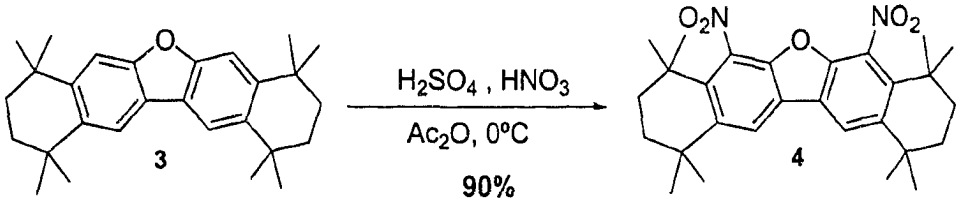

To a solution of 1,1,4,4,8,8,11,11-octamethyl-1,2,3,4,8,9,10,11-octahydro-dinaphtho[2,3-b;2',3'-d]furan **3** (50 mg, 0.15 mmol) in CH_2Cl_2 (5 mL) under N_2 at 0 °C was added glacial AcOH (10 mL), H_2SO_4 (18.3 µL dropwise) and concentrated HNO_3 (22 µL). The reaction was allowed to warm to RT and progress was monitored by TLC. After 2.5 h, the solution was recooled to 0 °C and additional aliquots of H_2SO_4 (18.3 µL) and HNO_3 (22 µL) were added dropwise and the reaction was allowed to stir overnight. The crude mixture was quenched by the addition of saturated $NaHCO_3$ (20 mL) and extracted with CH_2Cl_2 (3 x 10 mL). The combined organic extracts were washed with H_2O (2 x 15 mL), dried over Na_2SO_4 and evaporated in vacuo. MPLC (silica, 2 x 30 cm, 9:1 cyclohexane : Et_2O) was performed on the crude mixture, yielding 1,1,4,4,8,8,11,11-octamethyl-1,2,3,4,8,9,10,11-octahydro-5,7-dinitro-dinaphtho[2,3-b;2',3'-d]furan **4** (0.064 g, 0.14 mmol, 90%) as an off-white solid. R_f = 0.08 (1:1 cyclohex : EtOAc). IR (CH_2Cl_2, cast) 2963, 2931, 1552, 1369, 877 cm^{-1}. ^1H NMR (300 MHz, acetone-d_6): δ 7.99 (s, 2H, H1/H9), 1.83 (m, 4H, CH_2)

1.74 (m, 4H, CH_2), 1.44 (s, 6H, CH_3), 1.41 (s, 6H, CH_3). HRMS (EI) *m/z* : Calcd for $C_{28}H_{34}N_2O_5$: 478.24677. Found 478.24522 (100.00 %) [M^+].

1,1,4,4,8,8,11,11-octamethyl-1,2,3,4,8,9,10,11-octahydro-5,7-diamino-dinaphtho[2,3-b;2',3'-d]furan (5)

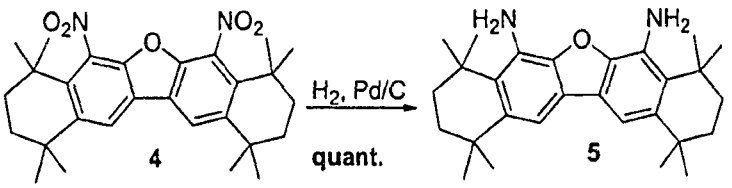

To a solution of 1,1,4,4,8,8,11,11-octamethyl-1,2,3,4,8,9,10,11-octahydro-5,7-dinitro-dinaphtho[2,3-b;2',3'-d]furan **4** (0.050 g, 0.1 mmol) in EtOAc (5 mL) at RT was added Pd/C (10%, ~40 mg, ~0.1 mol %). Air in the Schlenk flask was evacuated under vacuum and filled with N_2. To this suspension was attached a balloon charged with H_2. Reaction was allowed to stir for ~72h, at which point TLC analysis indicated the reaction was complete. The crude suspension was filtred through celite and the solvent evaporated in vacuo to yield 11,1,4,4,8,8,11,11-octamethyl-1,2,3,4,8,9,10,11-octahydro-5,7-diamino-dinaphtho[2,3-b;2',3'-d]furan **5** (0.041 g, 0.1 mmol, 100%) as an off-white solid. R_f = 0.55 (1:1 cyclohex : EtOAc). ^{1}H NMR (300 MHz,acetone-d_6): δ 7.60 (s, 2H, H1/H9), 5.32 (s, 4H, br, NH_2), 1.76-1.64 (m, 4H, CH_2) 1.66 (m, 4H, C-H_2), 1.48 (s, 12H, CH_3), 1.29 (s, 12H, CH_3). HRMS (EI) *m/z* : Calcd for $C_{28}H_{38}N_2O$: 418.29840. Found 418.29824 (100.00 %) [M^+].

2,8-*bis*(*tert*-butyl)dibenzofuran (7)

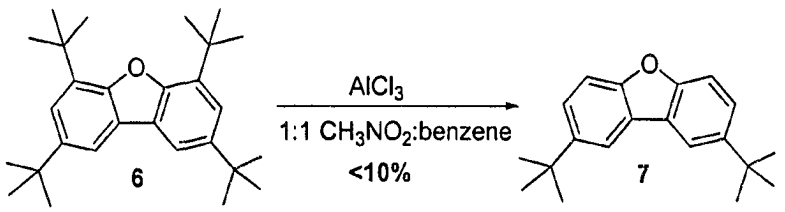

To a solution of 2,4,6,8-tetrakis(*tert*-butyl)dibenzofuran **6** (0.200 g, 0.5 mmol) in benzene (4 mL) under N_2 at 10 °C was added slowly by canula a suspension of $AlCl_3$ (0.120 g, 0.9 mmol, 1,8 equiv.) in CH_3NO_2/benzene (1.8 mL, 1:1) at 10 °C under N_2. The mixture was allowed to stir 2 h at 10 °C. Ice (2 g) was added and the crude product was extracted with CH_2Cl_2 (3 x 10 mL). The combined organics were washed with brine (10 mL), dried over Na_2SO_4, and evaporated in vacuo to yield 2,8-*bis*(*tert*-butyl)dibenzofuran **7** (7.3 mg, 0.026 mmol, 10 %) as a yellow oil. R_f = 0.6 (5:1 Hex : EtOAc). ^{1}H NMR (300 MHz, acetone-d_6): δ 7.94 (dd, J = 7.6, 1.3 Hz, 2H, H1/H9), 7.42 (dd, J = 7.6, 1.3 Hz, 2H, H4/H6), 7.30 (t, J_{obs} = 2.1 Hz, 2H, H3/H7), 1.60 (s, 18H, CH_3).

4,6-*bis*(trimethylsilyl)dibenzofuran 12

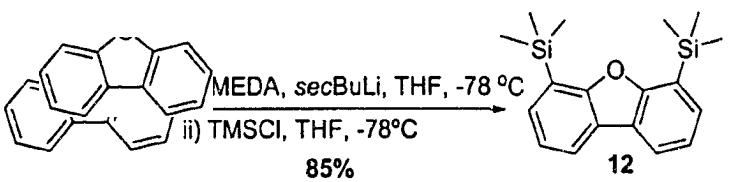

The following is an adaptation of a published preparation.[16]

To a deoxygenated solution of dibenzofuran (10.0 g, 59.5 mmol) in THF (100 mL) under N_2 was added TMEDA (27.6 g, 237.9 mmol, 4 equiv.) by syringe. The resultant solution was cooled to –78 °C in a dry ice/acetone bath. To this

solution was added slowly by canula *sec*-BuLi (105.3 mL, 136.9 mmol, 1.3 M in cyclohexane). The pale yellow suspension was allowed to warm to RT and stirred overnight. The resulting yellow suspension was then re-cooled to –78 °C and added slowly by canula to a solution of TMSCl (64.86 g, 595 mmol, 10 equiv.) in THF (50 mL) at –78 °C . The solution was allowed to stir for 2h and quenched by pouring into H_2O (200 mL) at 0 °C. The crude mixture was extracted with CH_2Cl_2 (3 x 75 mL). The combined organic phases were dried over powdered Na_2SO_4 and evaporated in vacuo. The solid crude product was recrystallized from cold pentanes to yield 4,6-*bis*(trimethylsilyl)dibenzofuran **12** (15.8 g, 50.6 mmol, 85%) as pale yellow crystals. R_f = 0.5 (cyclohex). ^{1}H NMR (300 MHz, acetone-d_6): δ 8.12 (H1/H9, 2H, dd J = 7.6, 1.4 Hz), 7.58 (H3/H7, 2H, dd, J = 7.6, 1.4 Hz), 7.38 (H2/H8, 2H, t, J_{obs} = 7.6 Hz), 0.48 (CH_3, 18 H, s).

Bis(2,8-dinitro-4,6-trimethylsilyl)dibenzofuran 13

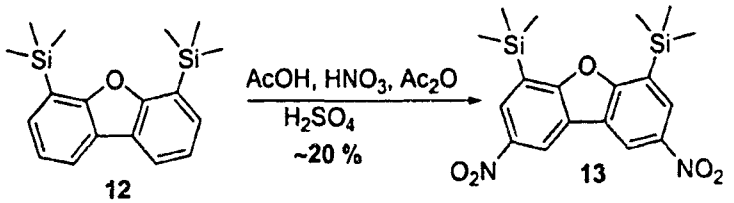

A solution of 4,6-*bis*(trimethylsilyl)dibenzofuran **12** (0.339 g, 1.08 mmol) in AcOH (13 mL) was prepared and held at 50 °C under N_2. One drop of conc. H_2SO_4 was added to the solution above immediately before a solution of HNO_3 (0.26 mL) in Ac_2O (1.1 mL) at 0°C was added dropwise to the 50 °C solution. The mixture was allowed to stir overnight until TLC indicated the disappearance of starting

material. The crude mixture was diluted with H_2O (20 mL). The organic phase was separated and the aqueous extracted with CH_2Cl_2 (3 x 15 mL). The organic fractions were combined, dried over powdered Na_2SO_4 and evaporated in vacuo to yield a mixture of products (~150 mg), presumably including *bis*(2,8-dinitro-4,6-trimethylsilyl)dibenzofuran **13** (~90 mg, 0.0001 mmol, ~20 %) as a yellow oil. R_f = 0.2 (cyclohex). ^1H NMR (300 MHz, acetone-d_6): δ 8.34 (d, J = 8.3 Hz, 2H, H1/H9), 7.96 (d, J = 8.3 Hz, 2H, H3/H7), 0.50 (s, 12H, $SiCH_3$)

Bis(2,8-_tert_-butyl-4,6-trimethylsilyl)dibenzofuran 15

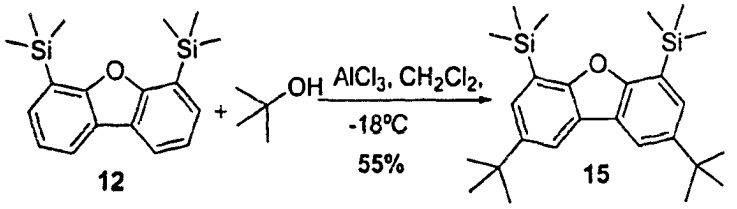

To a solution of 4,6-*bis*(trimethylsilyl)dibenzofuran **12** (148 mg, 0.5 mmol) and *tert*-butyl alcohol (93 mg, 1.26 mmol, 2.5 equiv.) in CH_2Cl_2 (4 mL) under N_2 at -18 °C was added a suspension of $AlCl_3$ (330 mg, 2.5 mmol, 5 equiv.) in CH_2Cl_2 (5 mL) slowly by canula. The mixture was allowed to warm to RT and monitored by TLC. Additional portions of *tert*-butyl alcohol (3 equiv.) and $AlCl_3$ (3 equiv.) were added after 12 h. After stirring an additional 12 h, TLC analysis indicated disappearance of starting material. The reaction was quenched by the addition of H_2O (10 mL) and the crude product extracted with CH_2Cl_2 (3 x 15 mL). The combined organic fractions were dried over Na_2SO_4 and evaporated in vacuo. The crude product was purified by MPLC (silica, 1.5 x 20 cm, 1:1

hexanes:cyclohexane) yielding *bis*(2,8-*tert*-butyl-4,6-trimethylsilyl)dibenzofuran **15** (0.1168 g, 0.28 mmol, 55 %) as a yellow oil. R_f = 0.4 (1:1 cyclohex : hex). ^{1}H NMR (300 MHz, acetone-d_6): δ 8.00 (d, *J* = 2.0 Hz, 2H, H1/H9), 7.47 (d, *J* = 2.0 Hz, ~2H, H3/H7), 1.43 (s, 18H, Si-CH_3) 1.61 (s, 18 H, CH_3).

para-*tert*-butylbromobenzene 17

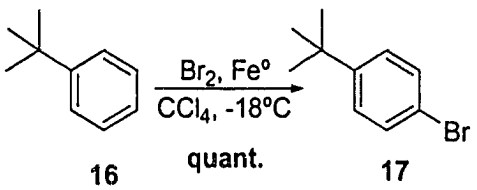

16 17

The following is an adaptation of a published preparation.[4,5,7]

To a solution of *tert*-butylbenzene **16** (5.0 g, 37.9 mmol) in CCl_4 at –18 °C under N_2 was added Fe° (250 mg, 4.5 mmol, 0.1 eq.). To this suspension was added dropwise by syringe Br_2 (5.9 g, 37.5 mmol, 1.0 eq.). The reaction was followed by TLC and allowed to warm to RT while stirring a total of 3.5 h. The reaction was then quenched with the addition of $NaHSO_3$ (10 mL). The aqueous fraction was separated and the organic washed with $NaHCO_3$ (10 mL), H_2O (10 mL), dried over Na_2SO_4 and evaporated in vacuo to yield *para-tert*-butylbromobenzene[4,5,7] **17** (8.0 g, 37.9 mmol, 100 %) as a yellow oil, spectroscopically identical to the known material. R_f = 0.8 (EtOAc). ^{1}H NMR (300 MHz, $CDCl_3$): δ 7.40-7.36 (complex m, AA' of AA'BB'), 7.25-7.22 (complex m, BB' of AA'BB'), 1.28 (s, 9H, CH_3).

2-nitro-4-*tert*-butylbromobenzene 18

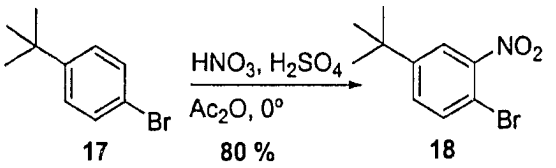

17 **80 %** **18**

The following is an adaptation of a published preparation.[10,11,12]

To a solution of *para-tert*-butylbenzene **17** (0.615 g, 2.8 mmol) in Ac_2O (4 mL) under N_2 at 0 °C was added dropwise by syringe conc. H_2SO_4 (1.0 mL, 6.4 eq.) and HNO_3 (1.0 mL, 5.4 eq.). The reaction mixture was allowed to stir 15 min. at 0 °C and allowed to warm to RT over 45 min. The solution was poured into ice (25 g) and the crude product was extracted with CH_2Cl_2 (3 x 20 mL). The combined organics were dried over Na_2SO_4 and evaporated in vacuo. MPLC (silica, 1.5 x 15 cm, hexanes) was performed on the crude mixture. The fractions containing the desired product were combined and evaporated in vacuo to yield 2-nitro-4-*tert*-butylbromobenzene[10,11,12] **18** (0.614 g, 2.2 mmol, 80 %) as a orange oil, spectroscopically identical to the known material. R_f = 0.1 (hexanes). ^1H NMR (300 MHz, $CDCl_3$): δ 7.90 (d, *J* = 2.3 Hz, 1H, H3), 7.61 (d, *J* = 8.5 Hz, 1H, H6), 7.42 (dd, *J* = 8.5, 2.3 Hz, 1H, H5), 1.32 (s, 9H, CH_3).

2-nitro-4,4'-*tert*-butyldiphenylether 20

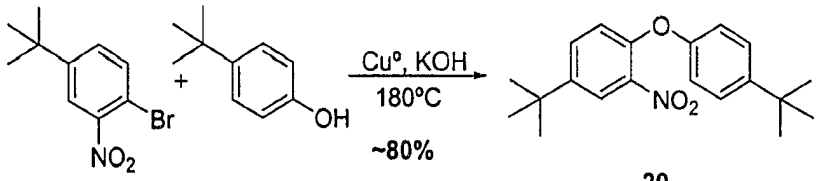

18 **19** **20**

The following is an adaptation of a published preparation.[13]

A mixture of *para-tert*-butylphenol **19** (4.57 g, 30.41 mmol) and KOH (2.55 g, 45.6 mmol, 1.5 eq.) under N_2 was heated while stirring to 130 °C for 1 h. The mixture was then stirred under vacuum for an additional hour at which time 2-nitro-4-(*tert*-butyl)bromobenzene **18** (7.82 g, 30.41 mmol, 1.0 eq.) and powdered Cu° (200 mg, 3.1 mmol, 0.1 eq.) were added at once. To the flask was added an air condensor and the mixture heated to 180 °C for an additional 2 h. The crude mixture was cooled to RT, CH_2Cl_2 (50 mL) was added, and the resulting solution filtered through celite, washed with H_2O (20 mL), dried over Na_2SO_4 and evaporated in vacuo to yield 2-nitro-4,4'-*tert*-butyldiphenylether[13] **20** (7.86 g, 24.3 mmol, 80 %) as a yellow oil. This compound was not further purified. Crude mixture R_f = 0.2, 0.25 (cyclohex). ^{1}H NMR (300 MHz, acetone-d_6): δ 7.96 (d, J = 2.4 Hz, 1H, H3), 7.72 (dd, J = 8.7, 2.4 Hz, 1H, H5), 7.45 (d, J=8.9 Hz, 2H, H2'/H6'), 7.03 (d, J = 8.7 Hz, 1H, H6), 6.98 (d, J = 8.9 Hz, 2H, H3'/H5'), 1.36 (s, 9H, CH_3), 1.32 (s, 9H, CH_3).

2-amino-4,4'-*bis*(*tert*-butyl)diphenylether 21

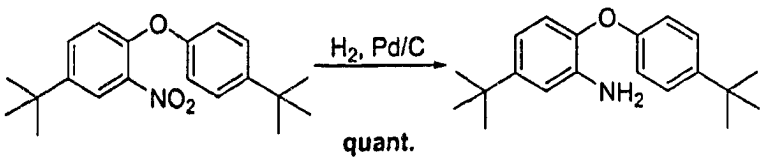

20 **21**

To the crude 2-nitro-4,4'-*bis*(*tert*-butyl)diphenylether **20** (7.86 g, 24.3 mmol) in EtOAc (50 mL) under N_2 was added Pd/C (10%, 1.0 g, 3 mol%). To this suspension was affixed a balloon filled with H_2. The suspension was stirred at RT overnight. The crude mixture was then filtered through celite and the solvent evaporated in vacuo. CH_2Cl_2 (100 mL) was added to the crude mixture and then washed with H_2O (20 mL), brine (20 mL), dried over Na_2SO_4, and evaporated in vacuo to yield 2-amino-4,4'-*bis*(*tert*-butyl)diphenylether **21** (7.22 g, 24 mmol, ~100%) as a pale yellow oil. This compound was not further purified. Crude mixture R_f = 0.1, 0.3 (2:1 Hex : EtOAc). ^1H NMR (300 MHz, CD_2Cl_2): δ 9.0 (m, 3H,), 8.2 (m, 4H), 3.76 (s, br, 2H, NH_2), 0.28 (s, 9H, C4H_3), 0.16 (s, 9H, C4'H_3).

2-diazo-4,4'-*bis*(*tert*-butyl)diphenylether tetrafluoroborate 22

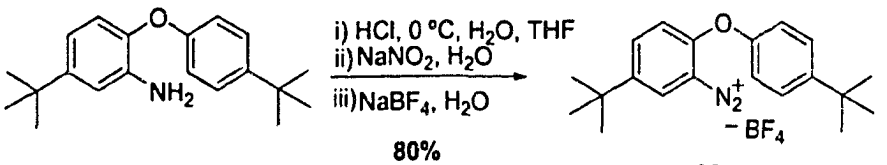

21 **22**

To a suspension of 2-amino-4,4'-*bis*(*tert*-butyl)diphenylether **21** (3.98 g, 13.58 mmol) in THF (5 mL) at 0 °C under N_2 was added dropwise conc. HCl (5.33 mL)

in H_2O (16 mL). To this solution was added dropwise a solution of $NaNO_2$ (1.27 g, 18.4 mmol, 1.35 eq.) in H_2O (10 mL) and the resultant suspension was allowed to warm to RT while stirring for 40 min. The reaction was quenched by the addition of excess sulfamic acid (500 mg) and the suspension was filtered through celite. To the filtrate was added a solution of $NaBF_4$ (3.2 g, 29.0 mmol, 2.1 eq.) in H_2O (10 mL), resulting in the formation of a precipitate. The solution was filtered and EtOAc (35 mL) added. The aqueous layer was separated and the organic solvent evaporated in vacuo to yield 2-diazo-4,4'-*bis*(*tert*-butyl)diphenylether tetrafluoroborate **22** (3.96 g, 0.010 mmol, 80%) as yellow solid. ^1H NMR (300 MHz, CD_2Cl_2): δ 7.31 (d, J = 8.9 Hz, 1H), 6.86 (m, 3H), 6.74 (m, 3H), 1.29 (s, 9H, CH_3), 1.28 (s, 9H, CH_3).

4,6-*bis*(azido)dibenzofuran 24

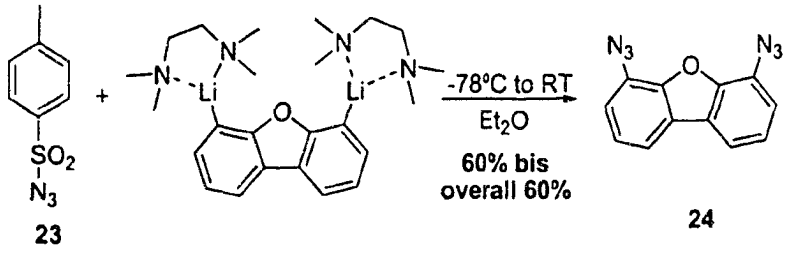

To a degassed, stirred solution of dibenzofuran (5.0 g, 29.8 mmol) and TMEDA (13.8 g, 17.8 mL, 119.0 mmol) in Et_2O (350 mL) at –78 °C was added by canula *sec*-BuLi (50.5 mL, 65.6 mmol, 1.3 M in cyclohexane). The pale yellow suspension was allowed to warm to room temperature overnight. This yellow suspension was then cooled to –78 °C and added by canula to a solution of *para*-

toluenesulfonyl azide **23** (56 g, 283 mmol, 10 equiv.) in Et_2O (50 mL) at room temperature.[17] The solution turned a deep maroon over 2 h, was stirred an addition 4 h, and then quenched by the addition of H_2O (100 mL). The organic layer was separated, washed again with H_2O (3 x 100 mL), brine (50 mL), dried over powdered Na_2SO_4, filtered and the solvent evaporated *in vacuo*. The resultant oily maroon residue was purified by MPLC (silica, 1% Et_2O / hexane). Combined fractions (Rf = 0.3, 10% Et_2O in hexanes) containing product were evaporated *in vacuo* and recrystallized in the cold from Et_2O to yield **24** (4.47 g, 17.88 mmol, 60%) as pale yellow crystals. R_f = 0.2 (20:1 Hex : EtOAc). IR (CH_2Cl_2, cast) 2298 (s), 1595 (m), 1489 (m), 1361 (s) cm^{-1}. ^1H NMR (500 MHz, $CDCl_3$): δ 7.65 (d, J = 7.8 Hz, 2H, H1/H9), 7.30 (t, J_{obs} = 7.8 Hz, 2H, H2/H8), 7.11 (d, J = 7.87, 2H, H3/H7). ^{13}C NMR (125 MHz, $CDCl_3$): δ 147.5 (C4A/C5A, 4°), 125.7 (C9A/C9B, 4°) 125.2 (C4/C6, 4°), 124.1 (C3/C7, 3°), 117.9 (C1/C9, 3°), 117.0 (C2/C8, 3°). HRMS (EI) *m/z* : Calcd for $C_{12}H_6N_6O$: 250.06031. Found 250.06063 [M^+].

4,6-*bis*(amino)dibenzofuran 27

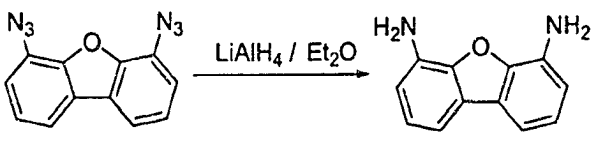

24 **85%** **27**

To a solution of 4,6-*bis*-azidodibenzofuran **24** (2.6 g, 10.4 mmol) in Et_2O (100 mL) at –78 °C was added a suspension of $LiAlH_4$ (1.18 g, 31.2 mmol) in

Et_2O/toluene (50/75 mL) dropwise by canula. The suspension was stirred and allowed to warm to RT overnight. The disappearance of starting material was followed by TLC (silica, 2:1 EtOAc : hexane) for an additional 8 h. The yellow solution was quenched by the addition of H_2O (1.2 mL), then 10% NaOH (1.2 mL), followed by H_2O (3.5 mL). The resulting precipitate of aluminum salts was filtered and the organic layer was separated. The aqueous phase was extracted again with Et_2O (3 x 50 mL). The combined organic phases were washed with brine (25 mL), dried over powdered Na_2SO_4, and evaporated *in vacuo*. The crude organic residue was purified by MPLC (silica, EtOAc : hexane, 2:1) and recrystallized from Hex : Et_2O : (1 : 10) to yield 4,6-*bis*(amino)dibenzofuran **27** (1.75 g, 8.84 mmol, 85%) as pale yellow crystals. R_f = 0.05 (2:1 Hex : EtOAc). IR (CH_2Cl_2, cast) 3336 (s), 3203 (m), 3045 (w), 1646 (s), 1617 (s), 1598 (s), 1497 (m), 1444 (m), 1433 (s), 1330 (m), 1289 (m), 1186 (m), 1042 (w) cm^{-1}. ^1H NMR (300 MHz, $CDCl_3$): δ 7.35 (dd, J = 7.7, 1.1 Hz, 2H, H1/H9), 7.14 (t, J_{obs} = 7.7 Hz, 2H, H2/H8), 6.82 (dd, J = 7.7, 1.1 Hz, 2H, H3/H7), 4.04 (s, br, 4H). ^{13}C NMR (125 MHz, $CDCl_3$): δ 144.8 (C4A/C5A, 4°), 131.9 (C9A/C9B, 4°), 125.3 (C4/C6, 4°), 123.4 (C3/C7, 3°), 112.8 (C1/C9, 3°), 110.8 (C2/C8, 3°). HRMS (EI) *m/z* : Calcd for $C_{12}H_{10}N_2O$: 198.07931 Found 198.07932 (100.00 %) [M^+]. Anal. Calcd for $C_{12}H_{10}N_2O$: C, 72.71; H, 5.08; N, 14.13. Found C, 72.32; H, 5.43; N, 14.08.

4,6-*bis*(2-hydroxy-3-*tert*-butyl-4-methylbenzylimino)dibenzofuran 30.

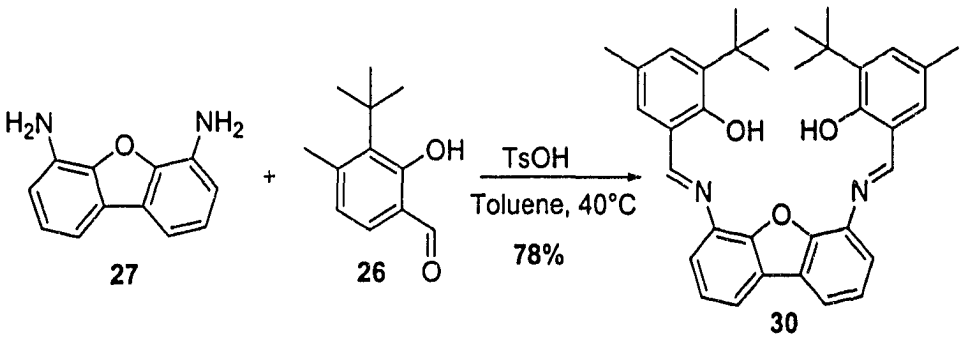

To a solution of 4,6-*bis*(amino)dibenzofuran **27** (1.05 g, 5.3 mmol) in toluene (10 mL) was added 2-hydroxy-3-*tert*-butyl-4-methylbenzaldehyde[14] **26** (3.05 g, 15.8 mmol) and *p*-TsOH (5 mg, 0.02 mmol, 0.005 equiv.). The suspension was heated to 40 °C for 24 h. The solvent was evaporated *in vacuo* and the crude product purified by MPLC (silica, 1 : 1 hexanes : EtOAc) to yield 4,6-*bis*-(2-hydroxy-3-*tert*-butyl-4-methylbenzylimino)dibenzofuran **30** (2.26 g, 4.14 mmol, 78%) as a fine yellow powder. R_f = 0.2 (20:1 EtOAc : Hex). IR (CH_2Cl_2, cast) 2955 (m), 2912 (m), 2869 (w), 1616 (s), 1577 (s), 1484 (s), 1463 (w), 1438 (w), 1390 (w), 1360 (w), 1322 (w), 1267 (w), 1232 (w), 1211 (w), 1182 (s), 1162 (w), 1137 (w), 1063 (w), 1023 (w) cm^{-1}. ^1H NMR (300 MHz, $CDCl_3$): δ 9.26 (s, 2H, H imine), 7.87 (dd, *J* = 7.2, 1.6 Hz, 2H, H1/H9), 7.50-7.41 (m, 4H, H3/H7, H2/H8), 7.23 (d, *J* = 2.0, 2H, Ph H6), 7.1 (d, *J* = 1.6 Hz, 2H, Ph H4), 2.30 (s, 6H, Ph CH_3), 1.50 (s, 18H, Ph $C(CH_3)_3$). HRMS (EI) *m/z* : Calcd for $C_{36}H_{38}N_2O_3$: 546.28827. Found 546.28830 (100.00 %) [M^+]. Anal. Calcd for $C_{36}H_{38}N_2O_3$: C, 79.09; H, 7.01; N, 5.12. Found C, 78.60; H, 6.83; N, 4.90.

4,6-*bis*(triphenylphosphiniminyl)dibenzofuran 31

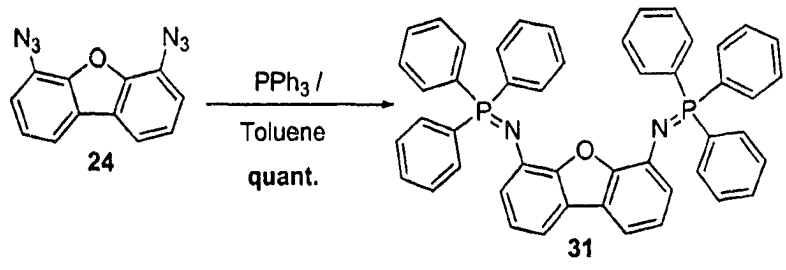

To a suspension of 4,6-*bis*(azido)dibenzofuran **24** (4.3 g, 17.2 mmol) in toluene (25 mL) at 0 °C was added by canula a solution of triphenylphosphine (9.46 g, 36.1 mmol) in toluene (25 mL). The resulting yellow solution was allowed to warm to RT and stirred overnight. The resultant yellow suspension was verified for the disappearance of starting material by TLC analysis. Solvents were evaporated *in vacuo* and the crude yellow precipitate was triturated with dry Et_2O (3 x 50 mL). The combined organic phases were evaporated *in vacuo* to yield 4,6-*bis*-(triphenylphosphiniminyl)dibenzofuran **31** (12.3, 17.2 mmol, 100%) as a yellow powder, which was not further purified. R_f = 0.45 (10:1 Hex : EtOAc). IR (CH_2Cl_2, cast) 3053 (m), 1611 (m), 1580 (s), 1487 (s), 1435 (s), 1423 (s), 1408 (s), 1366 (s), 1338 (s), 1292 (m), 1210 (m), 1184 (m), 1167 (m), 1146 (s), 1090 (m), 1032 (m), 1020 (w), 998 (w), 914 (w), 858 (w) cm^{-1}. ^1H NMR (300 MHz, $CDCl_3$): δ 7.94-7.87 (m, 12H), 7.52-7.41 (m, 6H), 7.41-7.39 (m, 12H), 7.21 (d, J = 7.6 Hz, 2H H1/H9), 6.84 (t, J_{obs} = 7.6 Hz, 2H, H2/H8), 6.55 (d, J = 7.6 Hz, 2H, H3/H7). ^{13}C NMR (125 MHz, $CDCl_3$): δ 151.4 (d, $^1J_{P\text{-}C}$ = 19.8 Hz, $^{31}P\text{-}C_{arom}$), 137.2, 133.1 (d, $^3J_{P\text{-}C}$ = 9.9 Hz, $^{31}P\text{-}C\text{-}C\text{-}C_{arom}$), 132.1, 131.7 (d, $^4J_{P\text{-}C}$ = 2.7 Hz, $^{31}P\text{-}C\text{-}C\text{-}C\text{-}C_{arom}$), 131.3, 128.7 (d, $^2J_{P\text{-}C}$ = 11.8 Hz, $^{31}P\text{-}C\text{-}C_{arom}$) 125.9, 122.4,

119.5 (d, $^2J_{P\text{-}C}$ = 11.8 Hz, ^{31}P=N-C4/6$_{DBF}$), 109.4. HRMS (EI) *m/z* : Calcd for $C_{48}H_{36}N_2OP_2$: 718.23029. Found 718.23228. (100.00 %) [M^+].

4,6-*bis*-(1,1,1,3,3,3-hexafluoro-2-propylimino)dibenzofuran 32

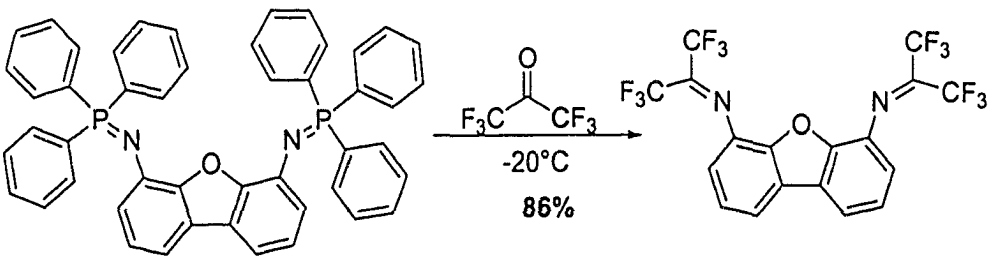

31 **32**

To a solution of 4,6-*bis*(azido)dibenzofuran **24** (0.065 g, 0.3 mmol) in Et_2O (5 mL) at RT under N_2 was added triphenylphosphine (0.236 g, 0.9 mmol, 3 equiv.). This suspension was stirred at RT overnight then cooled to –20 °C. Condensed hexafluoroacetone (2 mL, -20 °C) was then added to the suspension rapidly by canula. The resultant suspension was stirred and allowed to warm to RT gradually overnight. The solvent was evaporated in vacuo and the crude mixture extracted with hexanes (2 x 5 mL). Organic extracts were combined and the solvent evaporated. The crude product was recrystallized from hexanes to yield 4,6-*bis*-(1,1,1,3,3,3-hexafluoro-2-propylimino)dibenzofuran **32** (0.110 g, 0.22 mmol, 86 %) as a pale yellow solid. ^{1}H NMR (300 MHz, $CDCl_3$): δ 7.85 (d, *J* = 7.72, 2H, H1/H9), 7.41 (t, J_{obs} = 7.9 Hz, 2H, H2/H8), 7.04 (d, *J* = 7.8 Hz, 2H, H3/H7). ^{13}C NMR (APT, 125 MHz, $CDCl_3$): 132.5 (d, *J* = 3.1 Hz, 2C, N=C), 132.0 (d, 10.3 Hz, 2C, F_3C1/F_3C1'), 131.0 (C3/C7, 3°), 130.9 (C1/C9, 3°), 125.6 (C2/C8, 3°), 128.6 (d, 12.2 Hz, 2C, F_3C3/F_3C3'), 123.7 (C4A/C5A,4°), 119.5

(C9A/C9B, 4°), 117.1 (C4/C6, 4°). ^{19}F NMR (400 MHz, $CDCl_3$) δ -65.4, -69.8. (HRMS (EI) *m/z* : Calcd for $C_{18}H_6F_{12}N_2O$: 494.02884. Found 494.02787 (100.00 %) [M^+].

4,6-*bis*(1,1,1,3,3,3-hexafluoro-2-methyl-2-propylamino)dibenzofuran 33

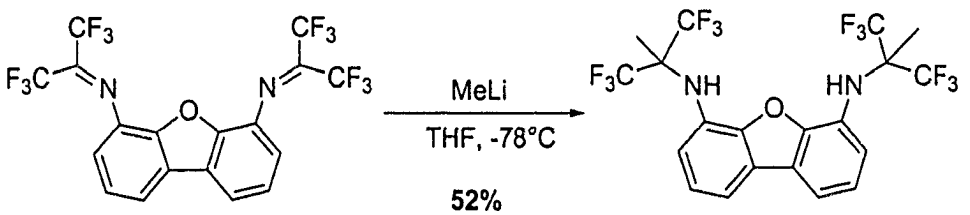

32 **33**

To the yellow suspension of 4,6-*bis*-(1,1,1,3,3,3-hexafluoro-2-propylimino) dibenzofuran **32** (618 mg, 0.5 mmol) in THF (10 mL) at -78 °C was added MeLi (5.21 mL, 7.5 mmol, 1.44 M in Et_2O) by syringe. The stirred mixture was allowed and warm to RT overnight during which time the yellow suspension turned a deep maroon. The reaction was quenched with the addition of H_2O (10 mL). Solvents were partially removed *in vacuo*, Et_2O (20 mL) was added and the organic fraction washed with H_2O (3 x 10 mL), brine (10 mL), dried over powdered Na_2SO_4, and evaporated *in vacuo*. The crude organic product was purified by MPLC (silica, 10 : 1 Hexanes : EtOAc), and recrystallized from cold pentane to yield 4,6-*bis*-(1,1,1,3,3,3-hexafluoro-2-methyl-2-propylamino)dibenzofuran **33** (342 mg, 0.6 mmol, 52%) as pale white crystals. The crystals proved suitable for analysis by X-ray crystallography. (**Appendix A**) R_f = 0.3 (20:1 Hex : EtOAc). IR (CH_2Cl_2, cast) 3366 (w), 3018 (w), 1923 (w), 1633 (w), 1604 (w), 1599 (w), 1491 (w), 1456 (w), 1423 (w), 1406 (w), 1394 (w), 1347 (w), 1300 (s), 1272 (s), 1219 (s), 1203 (s), 1189 (s), 1177 (s), 1161 (s),

1143 (s), 1112 (s), 1080 (s), 1059 (m) cm^{-1}. ^1H NMR (500 MHz, $CDCl_3$): δ 7.66 (dd, J = 7.6, 0.7 Hz, 2H, H1/H9), 7.25 (t, J_{obs} = 7.8 Hz, 2H, H2/H8), 7.14 (d, J = 7.6 Hz, 2H, H3/H5), 4.28 (s, br, 2H, NH), 1.63 (s, 6H, CH_3). ^{19}F NMR (400 MHz, $CDCl_3$): -77.3. HRMS (EI) *m/z* : Calcd for $C_{20}H_{14}F_{12}N_2O$: 526.09143. Found 526.09132 (100.00 %) [M^+].

4,6-*bis*(1,1,1,3,3,3-hexafluoro-2-phenyl-2-propylamino)dibenzofuran 34

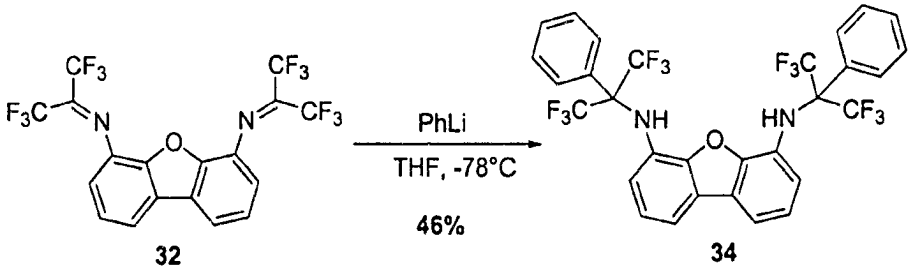

32 **34**

To the yellow suspension of 4,6-*bis*-(1,1,1,3,3,3-hexafluoro-2-propylimino) dibenzofuran **32** (250 mg, 0.5 mmol) in THF (5 mL) at -78°C was added PhLi (1.62 mL, 2.91, 1.8 M in hexanes) by syringe. The stirred mixture was allowed to warm to RT overnight, during which time the yellow suspension turned a deep maroon. The reaction was quenched with the addition of H_2O (10 mL). Solvents were partially removed *in vacuo*, Et_2O (20 mL) was added and the organic phase washed with H_2O (3 x 10 mL), brine (10 mL), dried over powdered Na_2SO_4, and evaporated *in vacuo*. The crude maroon organic fraction was purified by MPLC (silica, 10 : 1 hexanes : EtOAc) and recrystallized from Et_2O : hexanes (10 : 1) to yield 4,6-*bis*-(1,1,1,3,3,3-hexafluoro-2-phenyl-2-propylamino)dibenzofuran **34** (151 mg, 0.23 mmol, 46%) as pale white crystals. The crystals proved suitable

for analysis by X-ray crystallography **(Appendix A)** R_f = 0.2 (10:1 Hex : EtOAc). IR (CH_2Cl_2, cast) 3396 (w), 3068 (w), 1642 (m), 1599 (m), 1542 (m), 1498 (m), 1453 (m), 1429 (m), 1416 (m), 1337 (m), 1260 (s), 1239 (s), 1209 (s), 1189 (s), 1143 (s), 1081 (w), 1060 (m), 1038 (m), 976 (m) cm^{-1}. ^1H NMR (300 MHz, $CDCl_3$): δ 7.80 (d, *J* = 7.9 Hz, 4H, Ph H2/H6), 7.53-7.45 (m, 6H, Ph H3/H4/H5), 7.34 (d, *J* = 6.8 Hz, 2H, H1/H9), 6.87 (t, J_{obs} = 7.87 Hz, 2H, H2/H6), 6.13 (d, *J* = 7.72, 2H, H3/H7), 5.18 (s, br, 2H, NH). ^{13}C NMR (125 MHz, $CDCl_3$): δ 145.3 (C4A/C5A, 2C, 4°), 130.3 (Ph C2/C6, 4C, 3°), 129.1 (Ph C4, 2C, 3°), 128.8 (Ph C3/C5, 4C, 3°), 127.9 (C2/C8, 2C, 3°), 127.7 (C9A/9B, 2C, 4°), 124.7 (C4/C6, 2C, 4°), 123.0 (C1/C9, 2C, 3°), 122.4 (C-CF_3, 2C, 4°), 114.5 (Ph C1, 2C, 4°), 112.5 (C3/C7, 2C, 3°), 70.2-69.6 (m, *J* = 81.9, 4C, CF_3). HRMS (EI) *m/z* : Calcd for $C_{30}H_{18}F_{12}N_2O$: 650.12275. Found 650.12274 (100.00 %) [M^+].

4,6-*bis*(2-hydroxy-3-*tert*-butyl-4-methylbenzylimino)dibenzofuran 30

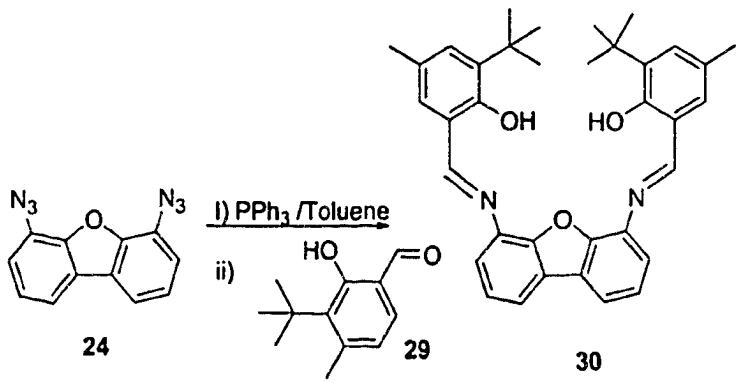

To a solution of 4,6-*bis*(azido)dibenzofuran **24** (1.96 g, 7.9 mmol) in toluene (30 mL) was added triphenylphosphine (4.35 g, 16.6 mmol). The reaction mixture was allowed to stir overnight at room temperature. To this suspension was

added 2-hydroxy-3-*tert*-butyl-4-methyl benzaldehyde[14] **29** (3.8 g, 19.7 mmol). The resultant suspension was stirred and heated to 60 °C for 2 days. The solvents were partially removed and the crude organics were purified by MPLC (silica, 1 : 1 hexanes : EtOAc) and recrystallized from THF : hexanes (10 : 1) to yield 4,6-*bis*(2-hydroxy-3-*tert*-butyl-4-methylbenzylimino)dibenzofuran (2.57 g, 4.7 mmol, 48%) as yellow crystals, spectroscopically identical to the compound **30**.

Notes and References

[1] Curphey, T. *Org. Prep. Proc. Int.* **1981**, *13*, 113-118.

[2] Dzwiniel, T. Ph.D. Dissertation, University of Alberta. 1999.

[3] Kobylinskaya, T.; Dashevskaya, T.; Shalamai, A.; Levitskaya, Z. *J. Gen. Chem. USSR* **1992**, *62*, 913-917.

[4] Chan, D.; Monaco, K.; Wang, R., Winters, M. *Tetrahedron. Lett.* **1998**, *39*, 2933-2936.

[5] Rettig, M.; Maitlis, D.; Cotton, A.; Webb, T. *Inorg. Syn.* **1977**, *17*, 135-137.

[6] Tsang, K.; Diaz, H.; Graciani, N.; Kelly, J. *J. Am. Chem. Soc.* **1994**, 116, 3988-4005.

[7] Jones, L.; Foster, J. *J. Org. Chem.* **1970**, *35*, 1777-1781.

[8] Colle, T.; Lewis, E. *J. Am. Chem. Soc.* **1979**, *101*, 1813-1818.

[9] Yamato, T.; Komine, M.; Nagano, Y. *Org. Prep. Proc. Int.* **1997**, *29*, 301-304.

[10] Vogel's Textbook of Practical Organic Chemistry, 5th edition. London: Longman Scientific and Technical, 1989, pg 1254.

[11] Prasad, J.; Panapoulous, A.; Rubin, J. *Tetrahedron. Lett.* **2000**, *41*, 4065-4068.

[12] Zeller, K-P.; Berger, S. *J. Chem. Soc. Perkin Trans. 2* **1977**, 54-58.

[13] Higginbottom, R.; Suschitzky, R. *J. Chem.Soc.* **1962**, *2*, 2367-2369.

[14] Pospisil, P.; Carsten, D.; Jacobsen, E. *Chem. Eur. J.* **1996**, *2*, 974-980.

[15] Bruson, H.; Kroege, J. *J. Am. Chem. Soc.* **1940**, 36-43.

[16] Diaz, H.; Kelly, J.; *Tet. Lett.* **1991**, *32*, 5725-5728.

[17] Hanawa, H.; Kii, S.; Maruoka, K. *Adv. Synth. Catal.* **2001**, *343*, 57-60.

Appendix

1 - X-ray crystallographic structure report of 1,8-bis(1,1,1,3,3,3-hexafluoro-2-methyl-2-propylamino)dibenzofuran **33**

Figure Legends

Figure 1. Perspective view of the 1,8-bis(1,1,1,3,3,3-hexafluoro-2-methyl-2-propylamino)dibenzofuran molecule showing the atom labelling scheme (primed atoms are related to unprimed ones by the crystallographic rotation axis (0, *y*, 1/4)). Non-hydrogen atoms are represented by Gaussian ellipsoids at the 20% probability level. Hydrogen atoms are shown with arbitrarily small thermal parameters.

Figure 2. Alternate view of the molecule, with the dibenzofuran group oriented 'edge-on.' Hydrogen atoms bound to carbons have been omitted.

Figure 1

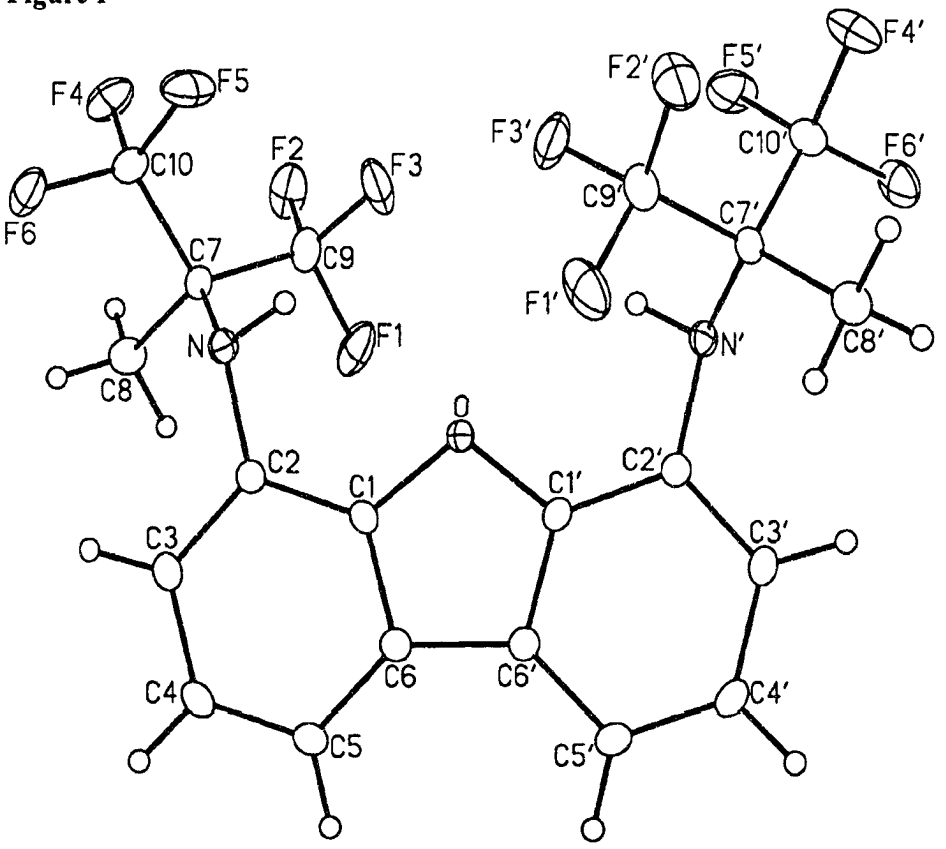

Figure 2

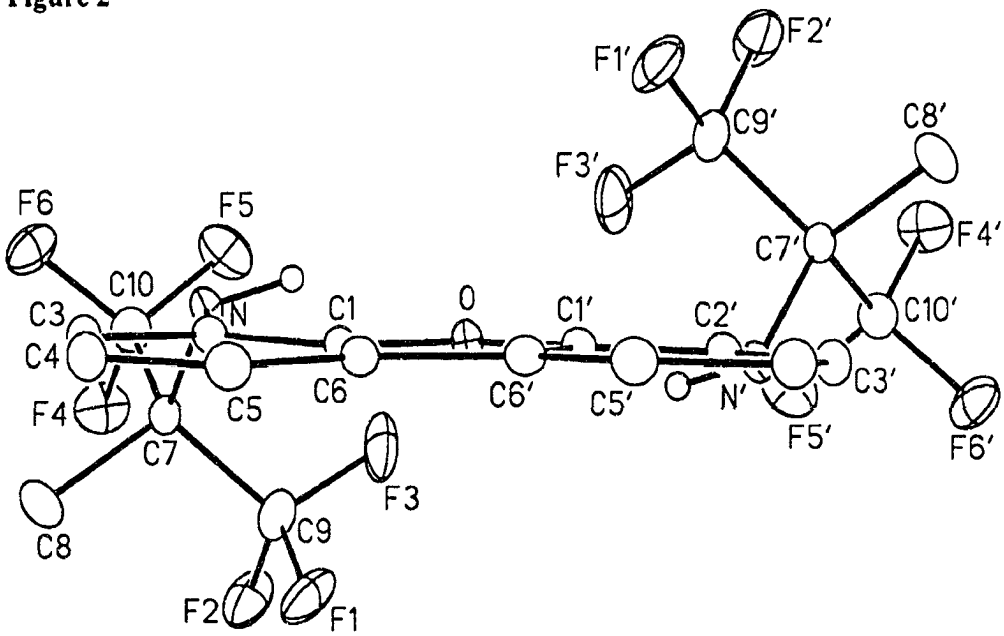

List of Tables

Table 1. Crystallographic Experimental Details

A. Crystal Data	
formula	$C_{20}H_{14}F_{12}N_2O$
formula weight	526.33
crystal dimensions (mm)	0.63 × 0.14 × 0.12
crystal system	monoclinic
space group	*C*2/*c* (No. 15)
unit cell parameters[a]	
a (Å)	19.455 (2)
b (Å)	9.9797 (12)
c (Å)	11.3710 (14)
β (deg)	108.968 (2)
V (Å^3)	2087.8 (4)
Z	4
ρ_{calcd} (g cm^{-3})	1.674
μ (mm^{-1})	0.178
B. Data Collection and Refinement Conditions	
diffractometer	Bruker PLATFORM/SMART 1000 CCD[b]
radiation (λ [Å])	graphite-monochromated Mo Kα (0.71073)
temperature (°C)	−80
scan type	ω scans (0.2°) (25 s exposures)
data collection 2θ limit (deg)	52.80
total data collected	6711 ($-24 \le h \le 23, -12 \le k \le 12, -14 \le l \le 14$)
independent reflections	2136 (R_{int} = 0.0314)
number of observed reflections (*NO*)	1822 [$F_o^2 \ge 2\sigma(F_o^2)$]
structure solution method	direct methods (*SHELXS–86*[c])
refinement method	full-matrix least-squares on F^2 (*SHELXL–93*[d])
absorption correction method	multi-scan (*SADABS*)
range of transmission factors	0.9790–0.8962
data/restraints/parameters	2136 [$F_o^2 \ge -3\sigma(F_o^2)$] / 0 / 159
goodness-of-fit (*S*)[e]	1.025 [$F_o^2 \ge -3\sigma(F_o^2)$]
final *R* indices[f]	
R_1 [$F_o^2 \ge 2\sigma(F_o^2)$]	0.0463
wR_2 [$F_o^2 \ge -3\sigma(F_o^2)$]	0.1191
largest difference peak and hole	0.337 and −0.252 e Å^{-3}

[a]Obtained from least-squares refinement of 3811 reflections with 4.64° < 2θ < 52.80°.

[b]Programs for diffractometer operation, data collection, data reduction and absorption correction were those supplied by Bruker.

(continued)

Table 1. Crystallographic Experimental Details (continued)

[c]Sheldrick, G. M. *Acta Crystallogr.* **1990**, *A46*, 467–473.

[d]Sheldrick, G. M. *SHELXL-93*. Program for crystal structure determination. University of Göttingen, Germany, 1993. Refinement on F_o^2 for all reflections (all of these having $F_o^2 \geq -3\sigma(F_o^2)$). Weighted R-factors wR_2 and all goodnesses of fit S are based on F_o^2; conventional R-factors R_1 are based on F_o, with F_o set to zero for negative F_o^2. The observed criterion of $F_o^2 > 2\sigma(F_o^2)$ is used only for calculating R_1, and is not relevant to the choice of reflections for refinement. R-factors based on F_o^2 are statistically about twice as large as those based on F_o, and R-factors based on ALL data will be even larger.

[e]$S = [\Sigma w(F_o^2 - F_c^2)^2/(n-p)]^{1/2}$ (n = number of data; p = number of parameters varied; $w = [\sigma^2(F_o^2) + (0.0579P)^2 + 2.2852P]^{-1}$ where $P = [\text{Max}(F_o^2, 0) + 2F_c^2]/3$).

[f]$R_1 = \Sigma||F_o| - |F_c||/\Sigma|F_o|$; $wR_2 = [\Sigma w(F_o^2 - F_c^2)^2/\Sigma w(F_o^4)]^{1/2}$.

Table 2. Atomic Coordinates and Equivalent Isotropic Displacement Parameters

Atom	*x*	*y*	*z*	U_{eq}, Å^2
F1	0.16238(9)	0.20445(17)	0.35584(13)	0.0725(5)*
F2	0.20742(9)	0.39501(17)	0.33156(14)	0.0724(5)*
F3	0.09200(9)	0.37120(17)	0.28422(16)	0.0756(5)*
F4	0.19025(8)	0.47549(13)	0.10020(14)	0.0634(4)*
F5	0.07436(8)	0.45050(13)	0.04614(16)	0.0662(4)*
F6	0.13563(8)	0.34691(15)	-0.05135(12)	0.0593(4)*
O	0.0000	0.08388(16)	0.2500	0.0270(4)*
N	0.08199(8)	0.18221(14)	0.09553(14)	0.0302(3)*
C1	0.03717(9)	-0.00074(16)	0.19504(15)	0.0266(4)*
C2	0.07924(9)	0.04404(17)	0.12433(16)	0.0278(4)*
C3	0.11106(10)	-0.05653(18)	0.07397(17)	0.0333(4)*
C4	0.10253(10)	-0.19253(18)	0.09714(18)	0.0356(4)*
C5	0.05945(10)	-0.23437(18)	0.16633(17)	0.0334(4)*
C6	0.02492(9)	-0.13570(17)	0.21424(16)	0.0282(4)*
C7	0.14675(9)	0.26437(18)	0.14887(17)	0.0300(4)*
C8	0.21744(10)	0.1940(2)	0.1551(2)	0.0436(5)*
C9	0.15229(12)	0.3110(2)	0.2807(2)	0.0484(5)*
C10	0.13671(11)	0.38558(19)	0.0603(2)	0.0413(5)*

Anisotropically-refined atoms are marked with an asterisk (*). The form of the anisotropic displacement parameter is: $\exp[-2\pi^2(h^2a^{*2}U_{11} + k^2b^{*2}U_{22} + l^2c^{*2}U_{33} + 2klb^*c^*U_{23} + 2hla^*c^*U_{13} + 2hka^*b^*U_{12})]$.

Table 3. Selected Interatomic Distances (Å)

Atom1	Atom2	Distance	Atom1	Atom2	Distance
F1	C9	1.338(3)	C1	C2	1.394(2)
F2	C9	1.336(2)	C1	C6	1.397(2)
F3	C9	1.330(3)	C2	C3	1.396(2)
F4	C10	1.337(2)	C3	C4	1.403(3)
F5	C10	1.338(2)	C4	C5	1.387(3)
F6	C10	1.320(3)	C5	C6	1.399(2)
O	C1	1.3858(18)	C6	C6'	1.454(3)
O	C1'	1.3858(18)	C7	C8	1.525(2)
N	C2	1.422(2)	C7	C9	1.540(3)
N	C7	1.460(2)	C7	C10	1.546(3)

Table 4. Selected Interatomic Angles (deg)

Atom1	Atom2	Atom3	Angle	Atom1	Atom2	Atom	Angle
C1	O	C1'	104.91(17)	N	C7	C10	105.05(15)
C2	N	C7	122.74(14)	C8	C7	C9	108.52(17)
O	C1	C2	123.70(15)	C8	C7	C10	108.15(15)
O	C1	C6	112.11(14)	C9	C7	C10	110.61(16)
C2	C1	C6	124.13(15)	F1	C9	F2	107.0(2)
N	C2	C1	121.11(15)	F1	C9	F3	106.73(18)
N	C2	C3	123.20(15)	F1	C9	C7	109.29(18)
C1	C2	C3	115.33(15)	F2	C9	F3	107.21(19)
C2	C3	C4	121.55(16)	F2	C9	C7	113.78(16)
C3	C4	C5	121.88(16)	F3	C9	C7	112.48(19)
C4	C5	C6	117.66(16)	F4	C10	F5	106.95(16)
C1	C6	C5	119.34(15)	F4	C10	F6	106.85(16)
C1	C6	C6'	105.43(9)	F4	C10	C7	112.60(17)
C5	C6	C6'	135.24(10)	F5	C10	F6	107.19(18)
N	C7	C8	113.83(15)	F5	C10	C7	112.01(16)
N	C7	C9	110.62(14)	F6	C10	C7	110.92(16)

Primed atoms related to one unprimed ones by the crystallographic 2-fold rotation axis $(0, y, 1/4)$.

Table 5. Torsional Angles (deg)

Atom1	Atom2	Atom3	Atom4	Angle	Atom1	Atom2	Atom3	Atom4	Angle
C1'	O	C1	C2	177.0(2)	C4	C5	C6	C6'	177.8(2)
C1'	O	C1	C6	-0.34(9)	N	C7	C9	F1	65.3(2)
C7	N	C2	C1	110.33(19)	N	C7	C9	F2	-175.26(18)
C7	N	C2	C3	-76.9(2)	N	C7	C9	F3	-53.1(2)
C2	N	C7	C8	41.7(2)	C8	C7	C9	F1	-60.3(2)
C2	N	C7	C9	-80.8(2)	C8	C7	C9	F2	59.2(2)
C2	N	C7	C10	159.79(16)	C8	C7	C9	F3	-178.65(17)
O	C1	C2	N	-5.1(3)	C10	C7	C9	F1	-178.78(16)
O	C1	C2	C3	-178.45(14)	C10	C7	C9	F2	-59.3(2)
C6	C1	C2	N	171.93(16)	C10	C7	C9	F3	62.9(2)
C6	C1	C2	C3	-1.4(3)	N	C7	C10	F4	176.52(16)
O	C1	C6	C5	-179.01(14)	N	C7	C10	F5	55.9(2)
O	C1	C6	C6'	0.8(2)	N	C7	C10	F6	-63.80(19)
C2	C1	C6	C5	3.6(3)	C8	C7	C10	F4	-61.6(2)
C2	C1	C6	C6'	-176.50(17)	C8	C7	C10	F5	177.83(17)
N	C2	C3	C4	-175.07(17)	C8	C7	C10	F6	58.1(2)
C1	C2	C3	C4	-1.9(3)	C9	C7	C10	F4	57.1(2)
C2	C3	C4	C5	3.0(3)	C9	C7	C10	F5	-63.5(2)
C3	C4	C5	C6	-0.7(3)	C9	C7	C10	F6	176.81(16)
C4	C5	C6	C1	-2.4(3)					

a

Primed atoms related to one unprimed ones by the crystallographic 2-fold rotation axis $(0, y, 1/4)$.

Table 6. Anisotropic Displacement Parameters (U_{ij}, Å^2)

Atom	U_{11}	U_{22}	U_{33}	U_{23}	U_{13}	U_{12}
F1	0.0949(11)	0.0899(11)	0.0343(7)	0.0068(7)	0.0231(7)	-.0304(9)
F2	0.0807(10)	0.0889(11)	0.0511(9)	-0.0264(7)	0.0262(8)	-.0457(9)
F3	0.0783(10)	0.0860(11)	0.0857(12)	-0.0368(9)	0.0584(9)	-.0126(8)
F4	0.0678(9)	0.0483(7)	0.0683(10)	0.0087(6)	0.0139(7)	-.0251(7)
F5	0.0574(8)	0.0411(7)	0.0959(12)	0.0129(7)	0.0189(8)	0.0153(6)
F6	0.0791(10)	0.0642(8)	0.0378(7)	0.0099(6)	0.0235(7)	-.0126(7)
O	0.0260(8)	0.0270(8)	0.0318(9)	0.000	0.0147(7)	0.000
N	0.0245(7)	0.0320(8)	0.0362(8)	0.0019(6)	0.0127(6)	0.0020(6)
C1	0.0229(8)	0.0299(8)	0.0268(9)	-0.0028(7)	0.0081(7)	0.0027(6)
C2	0.0240(8)	0.0306(8)	0.0285(9)	-0.0008(7)	0.0081(7)	0.0001(7)
C3	0.0297(9)	0.0397(10)	0.0334(10)	-0.0040(8)	0.0145(7)	0.0007(8)
C4	0.0345(10)	0.0362(9)	0.0373(10)	-0.0074(8)	0.0134(8)	0.0061(8)
C5	0.0343(9)	0.0278(8)	0.0365(10)	-0.0030(7)	0.0093(8)	0.0019(7)
C6	0.0262(8)	0.0295(8)	0.0276(9)	-0.0006(7)	0.0068(7)	0.0003(7)
C7	0.0287(9)	0.0333(9)	0.0310(9)	0.0005(7)	0.0140(7)	-.0020(7)
C8	0.0270(10)	0.0431(11)	0.0611(14)	0.0022(9)	0.0149(9)	-.0009(8)
C9	0.0526(13)	0.0575(13)	0.0422(12)	-0.0100(10)	0.0249(10)	-0189(10)
C10	0.0442(11)	0.0349(10)	0.0462(12)	0.0041(8)	0.0164(9)	-.0045(8)

The form of the anisotropic displacement parameter is:

$\exp[-2\pi^2(h^2a^{*2}U_{11} + k^2b^{*2}U_{22} + l^2c^{*2}U_{33} + 2klb^*c^*U_{23} + 2hla^*c^*U_{13} + 2hka^*b^*U_{12})]$

Table 7. Derived Atomic Coordinates and Displacement Parameters for Hydrogen Atoms

Atom	*x*	*y*	*z*	U_{eq}, Å^2
H1N	0.0449	0.2235	0.1153	0.036
H3	0.1392	-0.0323	0.0228	0.040
H4	0.1269	-0.2578	0.0645	0.043
H5	0.0536	-0.3268	0.1807	0.040
H8A	0.2151	0.1653	0.0714	0.052
H8B	0.2243	0.1156	0.2095	0.052
H8C	0.2583	0.2559	0.1882	0.052

2 - X-ray crystallographic structure report of 4,6-*bis*(1,1,1,3,3,3-hexafluoro-2-phenylpropan-2-amino)dibenzofuran **34**

Figure 1. Perspective view of the 4,6-bis(1,1,1,3,3,3-hexafluoro-2-phenylpropan-2-amino)dibenzo[*b*,*d*]furan molecule showing the atom labelling scheme. Non-hydrogen atoms are represented by Gaussian ellipsoids at the 20% probability level. The hydrogen atoms of the amino groups are shown with arbitrarily small thermal parameters; all other hydrogens are not shown.

Figure 2. Alternate view of the molecule, with the dibenzofuran group oriented 'edge-on.'

Figure 1

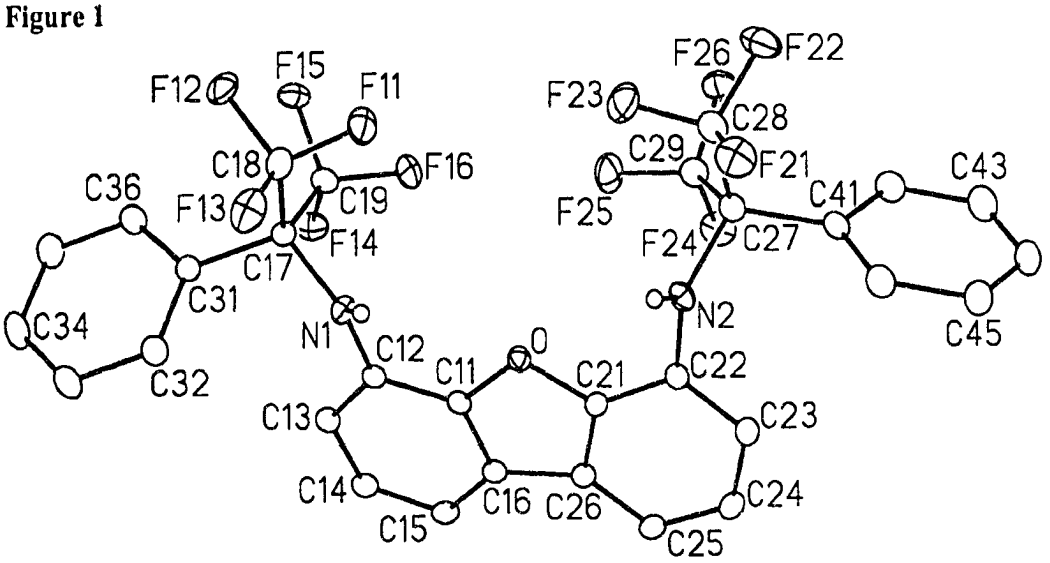

Figure 2

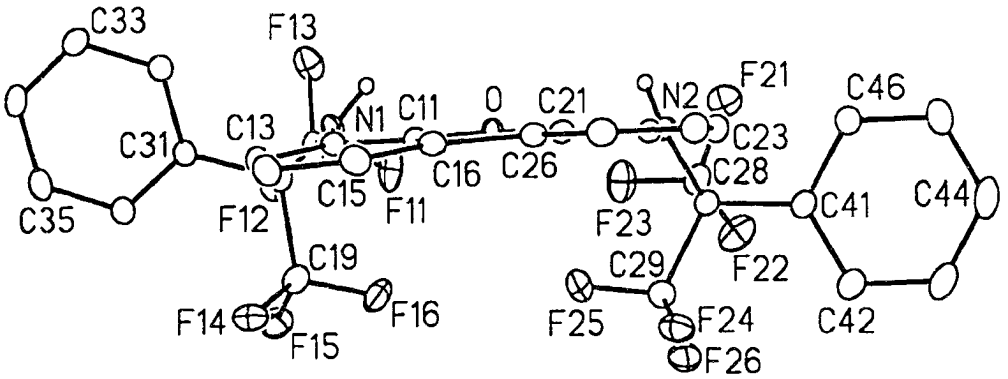

List of Tables

Table 1. Crystallographic Experimental Details

A. Crystal Data	
formula	$C_{30}H_{18}F_{12}N_2O$
formula weight	650.46
crystal dimensions (mm)	0.30 × 0.29 × 0.11
crystal system	monoclinic
space group	$P2_1/n$ (an alternate setting of $P2_1/c$ [No. 14])
unit cell parameters[a]	
a (Å)	12.6766 (6)
b (Å)	14.7986 (7)
c (Å)	14.5099 (7)
β (deg)	91.1128 (9)
V (Å^3)	2721.5 (2)
Z	4
ρ_{calcd} (g cm^{-3})	1.588
μ (mm^{-1})	0.154
B. Data Collection and Refinement Conditions	
diffractometer	Bruker PLATFORM/SMART 1000 CCD[b]
radiation (λ [Å])	graphite-monochromated Mo Kα (0.71073)
temperature (°C)	−80
scan type	ω scans (0.2°) (20 s exposures)
data collection 2θ limit (deg)	52.82
total data collected	16569 ($-15 \le h \le 15$, $-18 \le k \le 18$, $-13 \le l \le 18$)
independent reflections	5580 (R_{int} = 0.0411)
number of observed reflections (*NO*)	3831 [$F_o^2 \ge 2\sigma(F_o^2)$]
structure solution method	direct methods (*SHELXS-86*[c])
refinement method	full-matrix least-squares on F^2 (*SHELXL-93*[d])
absorption correction method	multi-scan (*SADABS*)
range of transmission factors	0.9833–0.9553
data/restraints/parameters	5580 [$F_o^2 \ge -3\sigma(F_o^2)$] / 0 / 406
goodness-of-fit (S)[e]	1.006 [$F_o^2 \ge -3\sigma(F_o^2)$]
final R indices[f]	
R_1 [$F_o^2 \ge 2\sigma(F_o^2)$]	0.0471
wR_2 [$F_o^2 \ge -3\sigma(F_o^2)$]	0.1192
largest difference peak and hole	0.540 and −0.473 e Å^{-3}

[a]Obtained from least-squares refinement of 5603 reflections with $5.04° < 2\theta < 50.96°$.

[b]Programs for diffractometer operation, data collection, data reduction and absorption correction were those supplied by Bruker.

(continued)

Table 1. Crystallographic Experimental Details (continued)

[c]Sheldrick, G. M. *Acta Crystallogr.* **1990**, *A46*, 467–473.

[d]Sheldrick, G. M. *SHELXL-93*. Program for crystal structure determination. University of Göttingen, Germany, 1993. Refinement on F_o^2 for all reflections (all of these having $F_o^2 \geq -3\sigma(F_o^2)$). Weighted R-factors wR_2 and all goodnesses of fit S are based on F_o^2; conventional R-factors R_1 are based on F_o, with F_o set to zero for negative F_o^2. The observed criterion of $F_o^2 > 2\sigma(F_o^2)$ is used only for calculating R_1, and is not relevant to the choice of reflections for refinement. R-factors based on F_o^2 are statistically about twice as large as those based on F_o, and R-factors based on ALL data will be even larger.

w=1/[\s^2^(Fo^2^)+(0.0510P)^2^+1.1001P]

[e]$S = [\Sigma w(F_o^2 - F_c^2)^2/(n-p)]^{1/2}$ (n = number of data; p = number of parameters varied; $w = [\sigma^2(F_o^2) + (0.0510P)^2 + 1.1001P]^{-1}$ where $P = [\text{Max}(F_o^2, 0) + 2F_c^2]/3$).

[f]$R_1 = \Sigma||F_o| - |F_c||/\Sigma|F_o|$; $wR_2 = [\Sigma w(F_o^2 - F_c^2)^2/\Sigma w(F_o^4)]^{1/2}$.

Table 2. Atomic Coordinates and Equivalent Isotropic Displacement Parameters

Atom	*x*	*y*	*z*	U_{eq}, Å^2
F11	0.16708(13)	0.24429(10)	-0.04953(12)	0.0657(5)*
F12	0.13326(12)	0.38339(10)	-0.01959(11)	0.0553(4)*
F13	0.28202(13)	0.34653(10)	-0.07521(10)	0.0577(4)*
F14	0.19800(10)	0.27515(10)	0.23286(10)	0.0492(4)*
F15	0.07618(10)	0.30999(10)	0.13448(11)	0.0542(4)*
F16	0.15359(11)	0.18142(10)	0.12679(12)	0.0586(4)*
F21	0.21296(12)	-0.09931(11)	-0.22020(10)	0.0605(4)*
F22	0.06379(11)	-0.13118(12)	-0.16290(12)	0.0690(5)*
F23	0.13746(14)	-0.00346(11)	-0.13425(12)	0.0691(5)*
F24	0.18585(11)	-0.15465(11)	0.10066(10)	0.0564(4)*
F25	0.15373(12)	-0.02290(10)	0.04712(12)	0.0640(5)*
F26	0.04578(10)	-0.13122(11)	0.01866(12)	0.0603(4)*
O	0.37531(10)	0.05681(9)	0.06135(10)	0.0292(3)*
N1	0.33847(13)	0.24117(12)	0.06985(12)	0.0325(4)*
N2	0.31532(13)	-0.08862(12)	-0.05342(13)	0.0340(4)*
C11	0.41579(15)	0.10791(14)	0.13380(14)	0.0285(5)*
C12	0.39353(15)	0.19904(14)	0.14341(14)	0.0291(5)*
C13	0.43217(16)	0.23899(15)	0.22393(15)	0.0331(5)*
C14	0.49205(16)	0.18864(16)	0.28784(16)	0.0368(5)*
C15	0.51754(16)	0.09889(16)	0.27373(15)	0.0358(5)*
C16	0.47840(15)	0.05732(15)	0.19402(15)	0.0301(5)*
C17	0.25591(16)	0.30801(14)	0.08146(15)	0.0314(5)*
C18	0.2088(2)	0.32109(16)	-0.01649(18)	0.0433(6)*
C19	0.16977(17)	0.26912(16)	0.14449(18)	0.0413(6)*
C21	0.41354(15)	-0.02933(14)	0.07787(15)	0.0295(5)*
C22	0.38487(15)	-0.10285(14)	0.02309(15)	0.0302(5)*
C23	0.43302(17)	-0.18413(15)	0.04791(17)	0.0374(5)*
C24	0.50262(17)	-0.18940(15)	0.12302(17)	0.0395(6)*
C25	0.52663(16)	-0.11601(15)	0.17835(16)	0.0366(5)*
C26	0.47960(15)	-0.03351(14)	0.15510(15)	0.0307(5)*
C27	0.21216(16)	-0.13341(15)	-0.05951(16)	0.0351(5)*
C28	0.15574(19)	-0.09173(17)	-0.14490(19)	0.0462(6)*
C29	0.14813(18)	-0.11051(17)	0.02683(19)	0.0452(6)*
C31	0.29845(16)	0.39992(14)	0.11451(15)	0.0314(5)*
C32	0.40111(18)	0.42351(16)	0.09357(17)	0.0397(5)*
C33	0.4405(2)	0.50755(17)	0.11855(19)	0.0497(7)*
C34	0.3776(2)	0.56847(17)	0.1634(2)	0.0534(7)*
C35	0.2755(2)	0.54539(17)	0.1839(2)	0.0530(7)*
C36	0.23569(18)	0.46188(16)	0.15951(18)	0.0427(6)*
C41	0.22367(16)	-0.23545(15)	-0.07644(16)	0.0360(5)*

Table 2. Atomic Coordinates and Displacement Parameters (continued)

Atom	*x*	*y*	*z*	U_{eq}, Å^2
C42	0.15975(19)	-0.29930(17)	-0.03616(19)	0.0461(6)*
C43	0.1732(2)	-0.39022(18)	-0.0566(2)	0.0583(8)*
C44	0.2481(2)	-0.41762(18)	-0.1168(2)	0.0601(8)*
C45	0.3113(2)	-0.35434(18)	-0.1582(2)	0.0562(7)*
C46	0.29933(19)	-0.26370(17)	-0.13779(18)	0.0454(6)*

Anisotropically-refined atoms are marked with an asterisk (*). The form of the anisotropic displacement parameter is: $\exp[-2\pi^2(h^2a^{*2}U_{11} + k^2b^{*2}U_{22} + l^2c^{*2}U_{33} + 2klb^*c^*U_{23} + 2hla^*c^*U_{13} + 2hka^*b^*U_{12})]$.

Table 3. Selected Interatomic Distances (Å)

Atom1	Atom2	Distance
F11	C18	1.339(3)
F12	C18	1.330(3)
F13	C18	1.326(3)
F14	C19	1.328(3)
F15	C19	1.337(3)
F16	C19	1.338(3)
F21	C28	1.328(3)
F22	C28	1.325(3)
F23	C28	1.336(3)
F24	C29	1.335(3)
F25	C29	1.331(3)
F26	C29	1.336(3)
O	C11	1.385(2)
O	C21	1.383(2)
N1	C12	1.409(3)
N1	C17	1.452(3)
N2	C22	1.420(3)
N2	C27	1.467(3)
C11	C12	1.385(3)
C11	C16	1.388(3)
C12	C13	1.390(3)
C13	C14	1.401(3)
C14	C15	1.383(3)
C15	C16	1.393(3)
C16	C26	1.458(3)
C17	C18	1.543(3)
C17	C19	1.549(3)
C17	C31	1.536(3)
C21	C22	1.392(3)
C21	C26	1.387(3)
C22	C23	1.393(3)
C23	C24	1.391(3)
C24	C25	1.381(3)
C25	C26	1.397(3)
C27	C28	1.547(3)
C27	C29	1.544(3)
C27	C41	1.537(3)
C31	C32	1.387(3)
C31	C36	1.386(3)
C32	C33	1.386(3)
C33	C34	1.376(4)
C34	C35	1.376(4)
C35	C36	1.378(3)
C41	C42	1.382(3)
C41	C46	1.386(3)
C42	C43	1.389(4)
C43	C44	1.364(4)
C44	C45	1.378(4)
C45	C46	1.383(3)

Table 4. Selected Interatomic Angles (deg)

Atom1	Atom2	Atom3	Angle	Atom1	Atom2	Atom3	Angle
C11	O	C21	104.37(15)	C22	C23	C24	121.3(2)
C12	N1	C17	107.28(19)	C23	C24	C25	122.7(2)
C22	N2	C27	121.28(17)	C24	C25	C26	117.3(2)
O	C11	C12	122.32(18)	C16	C26	C21	105.13(18)
O	C11	C16	112.46(18)	C16	C26	C25	136.0(2)
C12	C11	C16	125.22(19)	C21	C26	C25	118.8(2)
N1	C12	C11	116.95(18)	N2	C27	C28	105.41(18)
N1	C12	C13	127.6(2)	N2	C27	C29	109.52(18)
C11	C12	C13	115.44(19)	N2	C27	C41	111.47(17)
C12	C13	C14	120.5(2)	C28	C27	C29	108.68(19)
C13	C14	C15	122.5(2)	C28	C27	C41	107.91(19)
C14	C15	C16	117.8(2)	C29	C27	C41	113.48(19)
C11	C16	C15	118.3(2)	F21	C28	F22	107.0(2)
C11	C16	C26	105.28(18)	F21	C28	F23	106.0(2)
C15	C16	C26	136.3(2)	F21	C28	C27	112.0(2)
N1	C17	C18	104.20(17)	F22	C28	F23	107.4(2)
N1	C17	C19	109.48(17)	F22	C28	C27	111.9(2)
N1	C17	C31	112.94(16)	F23	C28	C27	112.1(2)
C18	C17	C19	109.03(18)	F24	C29	F25	106.4(2)
C18	C17	C31	107.67(17)	F24	C29	F26	106.9(2)
C19	C17	C31	106.7(2)	F24	C29	C27	110.97(19)
F11	C18	F12	113.07(18)	F25	C29	F26	106.9(2)
F11	C18	F13	124.12(17)	F25	C29	C27	111.5(2)
				F26	C29	C27	113.7(2)
F11	C18	C17	111.50(19)	C17	C31	C32	118.67(19)
F12	C18	F13	107.1(2)	C17	C31	C36	122.11(19)
F12	C18	C17	112.6(2)	C32	C31	C36	119.1(2)
F13	C18	C17	111.38(19)	C31	C32	C33	120.2(2)
F14	C19	F15	107.3(2)	C32	C33	C34	120.2(2)
F14	C19	F16	106.7(2)	C33	C34	C35	119.7(2)
F14	C19	C17	111.43(17)	C34	C35	C36	120.5(2)
F15	C19	F16	106.59(17)	C31	C36	C35	120.2(2)
F15	C19	C17	113.70(19)	C27	C41	C42	123.1(2)
F16	C19	C17	110.7(2)	C27	C41	C46	117.9(2)
O	C21	C22	122.34(19)	C42	C41	C46	119.0(2)
O	C21	C26	112.65(18)	C41	C42	C43	119.8(3)
C22	C21	C26	124.99(19)	C42	C43	C44	121.0(3)
N2	C22	C21	118.82(19)	C43	C44	C45	119.7(3)
N2	C22	C23	126.3(2)	C44	C45	C46	119.9(3)
C21	C22	C23	114.8(2)	C41	C46	C45	120.7(2)

Table 5. Torsional Angles (deg)

Atom1	Atom2	Atom3	Atom4	Angle	Atom1	Atom2	Atom3	Atom4	Angle
C21	O	C11	C12	-78.67(18)	C31	C17	C18	F12	-57.6(2)
C21	O	C11	C16	0.6(2)	C31	C17	C18	F13	62.7(2)
C11	O	C21	C22	175.74(19)	N1	C17	C19	F14	80.5(2)
C11	O	C21	C26	-2.6(2)	N1	C17	C19	F15	-158.18(18)
C17	N1	C12	C11	140.5(2)	N1	C17	C19	F16	-38.2(2)
C17	N1	C12	C13	-42.2(3)	C18	C17	C19	F14	-166.14(18)
C12	N1	C17	C18	-70.92(19)	C18	C17	C19	F15	-44.8(3)
C12	N1	C17	C19	-54.4(2)	C18	C17	C19	F16	75.2(2)
C12	N1	C17	C31	72.5(3)	C31	C17	C19	F14	-46.4(2)
C27	N2	C22	C21	-118.7(2)	C31	C17	C19	F15	74.9(2)
C27	N2	C22	C23	64.5(3)	C31	C17	C19	F16	-165.06(17)
C22	N2	C27	C28	173.04(19)	N1	C17	C31	C32	26.6(3)
C22	N2	C27	C29	56.3(3)	N1	C17	C31	C36	-157.3(2)
C22	N2	C27	C41	-70.1(3)	C18	C17	C31	C32	-87.9(2)
O	C11	C12	N1	-7.9(3)	C18	C17	C31	C36	88.2(3)
O	C11	C12	C13	174.43(18)	C19	C17	C31	C32	151.6(2)
C16	C11	C12	N1	172.89(19)	C19	C17	C31	C36	-32.3(3)
C16	C11	C12	C13	-4.8(3)	O	C21	C22	N2	1.1(3)
O	C11	C16	C15	-75.18(18)	O	C21	C22	C23	178.26(18)
O	C11	C16	C26	1.4(2)	C26	C21	C22	N2	179.20(19)
C12	C11	C16	C15	4.1(3)	C26	C21	C22	C23	-3.7(3)
C12	C11	C16	C26	-79.37(19)	O	C21	C26	C16	3.4(2)
N1	C12	C13	C14	-175.5(2)	O	C21	C26	C25	-78.02(17)
C11	C12	C13	C14	1.9(3)	C22	C21	C26	C16	-74.87(19)
C12	C13	C14	C15	1.5(3)	C22	C21	C26	C25	3.7(3)
C13	C14	C15	C16	-2.2(3)	N2	C22	C23	C24	178.0(2)
C14	C15	C16	C11	-0.4(3)	C21	C22	C23	C24	1.1(3)
C14	C15	C16	C26	-175.6(2)	C22	C23	C24	C25	1.4(3)
C11	C16	C26	C21	-2.8(2)	C23	C24	C25	C26	-1.4(3)
C11	C16	C26	C25	179.0(2)	C24	C25	C26	C16	177.0(2)
C15	C16	C26	C21	172.8(2)	C24	C25	C26	C21	-1.0(3)
C15	C16	C26	C25	-5.4(4)	N2	C27	C28	F21	55.0(2)
N1	C17	C18	F11	61.6(2)	N2	C27	C28	F22	175.2(2)
N1	C17	C18	F12	-177.77(19)	N2	C27	C28	F23	-64.0(2)
N1	C17	C18	F13	-57.5(2)	C29	C27	C28	F21	172.38(19)
C19	C17	C18	F11	-55.2(3)	C29	C27	C28	F22	-67.4(3)
C19	C17	C18	F12	65.4(2)	C29	C27	C28	F23	53.4(3)
C19	C17	C18	F13	-174.29(18)	C41	C27	C28	F21	-64.2(2)
C31	C17	C18	F11	-178.23(19)	C41	C27	C28	F22	56.0(3)

C41	C27	C28	F23	176.81(19)
N2	C27	C29	F24	-73.4(2)

Table 5. Torsional Angles (continued)

Atom1	Atom2	Atom3	Atom4	Angle	Atom1	Atom2	Atom3	Atom4	Angle
	Angle								
N2	C27	C29	F25	45.1(3)	C36	C31	C32	C33	0.9(4)
N2	C27	C29	F26	166.03(19)	C17	C31	C36	C35	-176.7(2)
C28	C27	C29	F24	171.94(19)	C32	C31	C36	C35	-0.7(4)
C28	C27	C29	F25	-69.6(2)	C31	C32	C33	C34	-0.7(4)
C28	C27	C29	F26	51.3(3)	C32	C33	C34	C35	0.4(4)
C41	C27	C29	F24	51.9(3)	C33	C34	C35	C36	-0.3(4)
C41	C27	C29	F25	170.32(19)	C34	C35	C36	C31	0.4(4)
C41	C27	C29	F26	-68.7(3)	C27	C41	C42	C43	178.4(2)
N2	C27	C41	C42	141.8(2)	C46	C41	C42	C43	0.9(4)
N2	C27	C41	C46	-40.7(3)	C27	C41	C46	C45	-177.9(2)
C28	C27	C41	C42	-102.9(3)	C42	C41	C46	C45	-0.3(4)
C28	C27	C41	C46	74.6(3)	C41	C42	C43	C44	-0.7(4)
C29	C27	C41	C42	17.6(3)	C42	C43	C44	C45	-0.1(4)
C29	C27	C41	C46	-164.9(2)	C43	C44	C45	C46	0.7(4)
C17	C31	C32	C33	177.0(2)	C44	C45	C46	C41	-0.5(4)

Table 6. Anisotropic Displacement Parameters (U_{ij}, Å^2)

Atom	U_{11}	U_{22}	U_{33}	U_{23}	U_{13}	U_{12}
F11	0.0893(11)	0.0435(9)	0.0623(11)	-0.0074(7)	-0.0464(9)	0.0013(8)
F12	0.0637(9)	0.0463(8)	0.0549(10)	0.0023(7)	-0.0237(7)	0.0161(7)
F13	0.0860(11)	0.0563(9)	0.0307(8)	0.0052(7)	-0.0009(8)	0.0128(8)
F14	0.0398(7)	0.0664(10)	0.0415(9)	0.0104(7)	0.0046(6)	-.0025(7)
F15	0.0282(7)	0.0627(10)	0.0718(11)	0.0032(8)	-0.0033(6)	0.0003(6)
F16	0.0524(9)	0.0408(8)	0.0827(12)	0.0034(8)	0.0026(8)	-.0149(7)
F21	0.0682(10)	0.0739(11)	0.0393(9)	0.0096(8)	-0.0029(7)	-.0037(8)
F22	0.0483(9)	0.0806(12)	0.0772(12)	0.0164(9)	-0.0241(8)	-.0169(8)
F23	0.0830(12)	0.0477(9)	0.0757(12)	0.0048(8)	-0.0199(9)	0.0133(8)
F24	0.0535(9)	0.0779(11)	0.0380(9)	0.0003(8)	0.0092(7)	-.0055(8)
F25	0.0650(10)	0.0528(10)	0.0749(12)	-0.0216(8)	0.0216(8)	-.0005(8)
F26	0.0344(8)	0.0722(10)	0.0747(11)	-0.0043(9)	0.0124(7)	-.0019(7)
O	0.0314(7)	0.0285(8)	0.0276(8)	-0.0019(6)	-0.0021(6)	-.0009(6)
N1	0.0400(10)	0.0334(10)	0.0240(10)	-0.0034(8)	-0.0019(8)	0.0061(8)
N2	0.0349(10)	0.0353(10)	0.0320(10)	0.0036(8)	0.0029(8)	-.0095(8)
C11	0.0252(10)	0.0346(11)	0.0255(11)	-0.0027(9)	-0.0001(8)	-.0037(8)
C12	0.0254(10)	0.0334(11)	0.0286(12)	-0.0002(9)	0.0011(8)	-.0015(8)
C13	0.0319(11)	0.0345(12)	0.0329(13)	-0.0066(10)	-0.0014(9)	-.0016(9)
C14	0.0315(11)	0.0485(14)	0.0301(12)	-0.0075(11)	-0.0052(9)	-0002(10)
C15	0.0287(11)	0.0474(14)	0.0310(12)	0.0017(10)	-0.0050(9)	-0.0042(10)
C16	0.0236(10)	0.0376(12)	0.0292(12)	0.0014(9)	0.0018(8)	0.0000(9)
C17	0.0310(11)	0.0308(11)	0.0322(12)	-0.0002(9)	-0.0055(9)	0.0022(9)
C18	0.0565(15)	0.0341(13)	0.0386(14)	-0.0021(11)	-0.0150(12)	-0.0041(11)
C19	0.0310(12)	0.0419(14)	0.0507(16)	0.0020(12)	-0.0050(11)	-0.0031(10)
C21	0.0256(10)	0.0292(11)	0.0340(12)	0.0030(9)	0.0055(9)	0.0006(8)
C22	0.0280(10)	0.0312(11)	0.0316(12)	-0.0005(9)	0.0047(9)	-0.0030(9)
C23	0.0358(12)	0.0314(12)	0.0452(14)	-0.0025(10)	0.0054(10)	-0.0015(9)
C24	0.0364(12)	0.0311(12)	0.0514(16)	0.0056(11)	0.0056(11)	-0.0058(9)
C25	0.0301(11)	0.0403(13)	0.0393(14)	0.0064(11)	0.0023(9)	0.0033(9)
C26	0.0260(10)	0.0346(12)	0.0316(12)	0.0025(9)	0.0041(9)	-0.0001(9)
C27	0.0326(11)	0.0357(12)	0.0369(13)	0.0001(10)	0.0015(10)	-0.0036(9)
C28	0.0447(14)	0.0423(14)	0.0513(17)	0.0033(12)	-0.0068(12)	-0.0063(11)
C29	0.0368(13)	0.0489(15)	0.0500(16)	-0.0039(13)	0.0056(11)	-0.0031(11)
C31	0.0337(11)	0.0320(11)	0.0283(12)	-0.0030(9)	-0.0024(9)	0.0010(9)
C32	0.0389(12)	0.0374(13)	0.0429(14)	-0.0057(11)	0.0070(10)	-0.0024(10)
C33	0.0448(14)	0.0458(15)	0.0587(18)	-0.0059(13)	0.0088(12)	-0.0146(12)
C34	0.0626(17)	0.0375(14)	0.0602(18)	-0.0153(13)	0.0070(14)	-0.0131(12)
C35	0.0549(16)	0.0433(15)	0.0613(18)	-0.0202(13)	0.0118(13)	-0.0011(12)
C36	0.0370(12)	0.0441(14)	0.0472(15)	-0.0104(12)	0.0043(11)	-0.0017(10)
C41	0.0349(12)	0.0343(12)	0.0387(14)	-0.0001(10)	-0.0045(10)	-0.0060(9)

Table 6. Anisotropic Displacement Parameters (continued)

Atom	U_{11}	U_{22}	U_{33}	U_{23}	U_{13}	U_{12}
C42	0.0427(13)	0.0426(14)	0.0531(16)	0.0019(12)	-0.0001(11)	-0.0069(11)
C43	0.0582(17)	0.0397(15)	0.077(2)	0.0068(14)	-0.0064(15)	-0.0127(13)
C44	0.0597(17)	0.0350(14)	0.085(2)	-0.0094(14)	-0.0162(16)	-0.0010(13)
C45	0.0518(15)	0.0485(16)	0.068(2)	-0.0185(14)	-0.0011(14)	0.0028(13)
C46	0.0429(13)	0.0437(14)	0.0499(16)	-0.0102(12)	0.0057(11)	-0.0060(11)

The form of the anisotropic displacement parameter is:

$\exp[-2\pi^2(h^2a^{*2}U_{11} + k^2b^{*2}U_{22} + l^2c^{*2}U_{33} + 2klb^*c^*U_{23} + 2hla^*c^*U_{13} + 2hka^*b^*U_{12})]$

Table 7. Derived Atomic Coordinates and Displacement Parameters for Hydrogen Atoms

Atom	*x*	*y*	*z*	U_{eq}, Å^2
H1N	0.3552	0.2260	0.0133	0.039
H2N	0.3345	-0.0522	-0.0981	0.041
H13	0.4179	0.3009	0.2357	0.040
H14	0.5161	0.2173	0.3430	0.044
H15	0.5603	0.0667	0.3170	0.043
H23	0.4180	-0.2370	0.0129	0.045
H24	0.5350	-0.2458	0.1368	0.047
H25	0.5732	-0.1214	0.2301	0.044
H32	0.4446	0.3819	0.0620	0.048
H33	0.5111	0.5231	0.1047	0.060
H34	0.4044	0.6262	0.1801	0.064
H35	0.2321	0.5873	0.2151	0.064
H36	0.1650	0.4467	0.1736	0.051
H42	0.1068	-0.2811	0.0054	0.055
H43	0.1297	-0.4340	-0.0282	0.070
H44	0.2566	-0.4800	-0.1301	0.072
H45	0.3630	-0.3730	-0.2008	0.067
H46	0.3434	-0.2203	-0.1661	0.054